

HYDROTH
METROLOGY

STABLE
ISOTOPES

GEYSER
STERNFELD '81

J. HULEN

UNIVERSITY OF CALIFORNIA
RIVERSIDE

The Hydrothermal Petrology and Stable Isotope Geochemistry of
Two Wells in The Geysers Geothermal Field, Sonoma County, California

A Thesis submitted in partial satisfaction
of the requirements for the degree of

Master of Science

in

Geological Sciences

by

Jeffrey Neal Sternfeld

December, 1981

Thesis Committee:

Dr. Wilfred A. Elders, Chairman, U. C. Riverside

Dr. Alan E. Williams, U. C. Riverside

Dr. Peter Schiffman, U. C. Riverside

APPROVAL PAGE

The thesis of Jeffrey Neal Sternfeld is approved:

Peter Schiffman

Alan F. Wilkins

Wilfred A. Oles
Committee Chairman

University of California, Riverside
December, 1981

ACKNOWLEDGEMENTS

The completion of this mega-thesis would not have been possible without the support and encouragement of a great multitude of individuals. Firstly, I would like to thank the members of my committee: Dr. Wilfred Elders for his intellectual, spiritual and financial support during my long career at UCR; Dr. Alan Williams for his instruction in the operation of the isotope lab and assistance in the development of "The Model"; and Dr. Peter ("Hey, that looks like pumpellyite") Schiffman for his expertise on the Franciscan Formation. I would like to express my thanks to Dick Dondanville of Union Geothermal in Santa Rosa, who initiated this project and was instrumental in the procurement of samples and limited funding, and also to Alex Schriener, who acted as my Union liason and tour guide at The Geysers. Special mention goes to Dr. Alfred Truesdell for sending preprints of selected papers on Geysers isotope research; Dr. Bob McLaughlin for his introduction to Geysers petrography; and Dr. Won Park for his instruction in ore microscopy.

I extend my gratitude to a host of UCR/IGPP staffies, students and hangers-on, without whose efforts this thesis would NEVER have reached its final form: Linda Jankov, illustrator par excellance, who drafted the figures; Lori Paustell, who typed this manuscript (and all its assorted editions); Rich Coffman, who prepared thin sections and polished sections; my assistant "bubble bakers" (fluid inclusionists) Carol Mount and Carter Hull; and the many subterranean dwellers in the Geology Building sub-basement who offered friendship, empathy and (non-)intellectual discussion - Keith Miller, Dan Seamount, Steve Sanford, Jim Hoagland, Claudia Garner,

Mike McKibben and Paul Johnson. And lastly (so he gets his own personalized acknowledgement) my deepest appreciation to my beer drinkin', beer makin' buddy and bestest friend Pete Collier for his assistance in XRD analysis, thin section and polished section preparation, and most of all (im-)moral support.

ABSTRACT OF THE THESIS

The Hydrothermal Petrology and Stable Isotope Geochemistry of
Two Wells in The Geysers Geothermal Field, Sonoma County, California

by

Jeffrey Neal Sternfeld

Master of Science, Graduate Program in Geological Sciences

University of California, Riverside, December 1981

Professor Wilfred A. Elders, Chairman

This report is a comprehensive study of the drill cuttings from two wells in The Geysers Geothermal Field, Sonoma County, California. The Geysers Geothermal Field is a large vapor-dominated geothermal field with reservoir temperatures of up to 240°C. It currently supplies steam to the largest geothermal electric installation in the world, with an installed capacity in excess of 1,000 MWe. Geysers 1, a production well, penetrated 1646 m of strata and encountered two major and five minor steam entries. Geysers 2, a non-producing well, penetrated 2835 m of strata and encountered a single uneconomic steam entry.

The strata penetrated by these wells are a melange of imbricated Franciscan Formation fault blocks consisting of interbedded greywacke and argillite, greenstone, and minor serpentinite that were subjected to low grade regional metamorphism during emplacement. The reservoir rock is a stack of juxtaposed greywacke slabs that vary in textural grade.

The strata are crosscut pervasively by a highly communicative, interconnected network of fractures. Mineralogical, textural and stable isotope data indicate that semi-permeable brecciated zones, 50 to 100 m wide, are situated adjacent to the thrust-fault contacts and act as the primary conduits for convective fluid flow in the reservoir.

Based on mineralogical and stable isotope characteristics in both wells, two generations of hydrothermal activity can be recognized, which are here designated the Franciscan Event and Big Geysers Reservoir Events. The Franciscan Event is associated with the Late Cretaceous-Early Tertiary regional metamorphism. The later Big Geysers Events are related to Pliocene to Recent volcanism of the Clear Lake volcanic group and to the present steam field.

The Franciscan Event mineralization consists of quartz, calcite, chlorite, ankerite and ferrierite. The Big Geysers mineralization is subdivided into two successive assemblages. The earlier mineral assemblage was deposited during a water-dominated phase of the geothermal system: it consists of quartz, calcite, adularia, sphene, epidote, andradite, celadonite, micaceous illite, tremolite, diopside, pyrite, marcasite, sphalerite, chalcopryrite, galena, rutile, hematite and bornite. The later mineral assemblage, associated with the transition to the present steam-dominated conditions, consists of calcite, quartz, adularia, pyrrhotite, marcasite, sphalerite, chalcopryrite, galena, fahlore and gersdorffite. The mineral assemblages are distributed in prograde metamorphic mineral zones that progress from greenschist to hornfels facies. The maximum temperature during mineralization was approximately 350°C based on fluid inclusion temperatures and co-existing mineral phases.

Salinity measurements for both quartz and calcite fluid inclusions ranged from .5 to 2.2 wt % NaCl equivalent with an averaged value of about 1%.

The transition from a water-dominated to a vapor-dominated reservoir occurred in three stages. The first was the Meteoric Stage, which is characterized by low $\delta^{18}\text{O}$ values indicative of abundant meteoric water at the inception of the geothermal system. The second stage was the Sealed Circulation Stage, which is characterized by high $\delta^{18}\text{O}$ values, indicative of a low water to rock ratio and a more limited influx of meteoric waters. This was presumably due to a reduction in permeability due to self-sealing by mineral precipitation. During this stage the hydrothermal fluids were superheated and geopressed with respect to hydrostatic boiling, as evidenced by fluid inclusion temperature data.

The third stage was the Stepped Boiling Stage, which is characterized by the occurrence of pyrrhotite as the principal iron sulfide phase, calcite fluid inclusion temperatures corresponding to vapor-static boiling, and calcite $\delta^{13}\text{C}$ values which indicate that the water present was steam condensate. A steam-water interface descended through the reservoir in steps, affecting each successive thrust fault block individually. Decompression of the geopressed fluids caused boiling, which in turn formed mineralized barriers in the high permeability zones. Residual waters trapped above each of these barriers or incrustation seals were subject to steam-static vaporization and the fluids below the seals maintained their high temperatures and pressures. The factors which promoted the pressure drop which caused vaporization of the reservoir were increased permeability in the discharge system due to hydraulic fracturing caused by geopressing and tectonic activity, and insufficient permeability in the recharge system due to sealing of fractures.

TABLE OF CONTENTS

	<u>Page</u>
ACKNOWLEDGEMENTS	iii
ABSTRACT OF THE THESIS	v
LIST OF TABLES	x
LIST OF FIGURES	xii
INTRODUCTION	1
REGIONAL STRUCTURE AND GEOLOGY	5
GEOPHYSICS	8
HYDROTHERMAL GEOLOGY	9
Surface Features	9
Previous Work	9
THE STEAM RESERVOIR	12
PETROLOGICAL METHODOLOGY	17
Problems Inherent to the Study of Well Cuttings	17
Analytical Techniques	19
Sample Preparation	19
Petrography and Microprobe	20
X-ray Diffraction	21
WELL-BORE LITHOLOGY	26
Geysers 1	26
Introduction	26
Rock Descriptions	26
Wackes	26
Shale	28
Definition of Lithologic Units	28
XRD Analysis	32
Geysers 2	40
Introduction	40
Rock Descriptions	43
Sedimentary Strata	43
XRD Analysis	45
Ultramafic Strata	50
Greenstone Strata	51
HYDROTHERMAL MINERALIZATION	57
Introduction	57
Descriptive Mineralogy of Silicates and Carbonates	59
Distribution of Silicates and Carbonates	64
Geysers 1	64
Geysers 2	68
Descriptive Mineralogy of Opaque Minerals	71

TABLE OF CONTENTS (continued)

	<u>Page</u>
HYDROTHERMAL MINERALIZATION (continued)	
Distribution of Opaque Minerals	81
Geysers 1	81
Geysers 2	87
Sources of the Ionic Species	91
FLUID INCLUSION GEOTHERMOMETRY	94
Introduction	94
Methodology	94
Sample Preparation	95
Results for Geysers 1	96
Calcite	96
Quartz	102
Results for Geysers 2	105
STABLE ISOTOPE GEOCHEMISTRY	109
Introduction	109
Previous Work	111
Sample Preparation	113
Results of Present Study	113
Calcite	113
Geysers 1	119
Geysers 2	124
Quartz	132
Isotope Temperature and Water Calculations	135
Interpretation of Isotope Data	138
INTERPRETATION AND ASSIMILATION OF DATA	147
Synthesis of Hydrothermal Processes	147
Presentation of a Reservoir Model	156
REFERENCES	166
APPENDIX	175

LIST OF TABLES

<u>Table</u>		<u>Page</u>
1	XRD mineral identification, detection limits and standard errors	23
2	XRD mineralogy of Geysers 1 greenstones	39
3	XRD mineralogy of Geysers 2 greenstones	54
4	Fluid inclusion salinities from Geysers 1	100
5	Calculated ¹⁸ O water compositions from Geysers 1	137

TABLES IN THE APPENDIX

A-1	XRD index of Franciscan Formation rock samples	176
A-2	XRD mineralogy of Geysers 1 sandstones	177
A-3	XRD mineralogy of Geysers 1 shales	178
A-4	XRD mineralogy of Geysers 1 air drilled cuttings	179
A-5	XRD mineralogy of Geysers 2 sandstones	180
A-6	XRD mineralogy of Geysers 2 shales	181
A-7	Plagioclase compositions	182
A-8	White mica compositions	183
A-9	Pumpellyite compositions	184
A-10	Green epidote compositions	185
A-11	Yellow green epidote compositions	186
A-12	Andradite compositions	187
A-13	Ferrierite compositions	188
A-14	Pyrrhotite compositions	189
A-15	Chalcopyrite compositions	190
A-16	Sphalerite compositions	191

LIST OF TABLES (continued)

<u>Table</u>		<u>Page</u>
A-17	Geysers 1 carbonate isotope data	192
A-18	Geysers 1 silicate isotope data	193
A-19	Geysers 2 carbonate isotope data	194
A-20	Geysers 2 silicate isotope data	196

LIST OF FIGURES

<u>Figure</u>		<u>Page</u>
1	Regional map of northern California	3
2	Well location map, The Geysers	10
3	Structural model of The Geysers	14
4	Lithologic column of Geysers 1	25
5	XRD spindle diagram of mud drilled sandstone cuttings from Geysers 1	34
6	XRD spindle diagram of mud drilled shale cuttings from Geysers 1	36
7	XRD spindle diagram of air drilled cuttings from Geysers 1	38
8	Lithologic column of Geysers 2	42
9	XRD spindle diagram of sandstone cuttings from Geysers 2	47
10	XRD spindle diagram of shale cuttings from Geysers 2	49
11	Mineral zonation in Geysers 1	66
12	Mineral zonation in Geysers 2	70
13	Distribution of opaque minerals versus depth in Geysers 1	78
14	Distribution of opaque minerals versus depth in Geysers 2	83
15	Plot of sphalerite compositions from Geysers 1 versus temperature	89
16	Calcite fluid inclusion homogenization temperatures versus depth from Geysers 1	98
17	Quartz fluid inclusion homogenization temperatures versus depth from Geysers 1	104
18	Calcite fluid inclusion homogenization temperatures versus depth from Geysers 2	107

LIST OF FIGURES (continued)

<u>Figure</u>		<u>Page</u>
19	^{13}C versus depth of calcites from Geysers 1	115
20	^{13}C versus depth of calcites from Geysers 2	117
21	^{18}O versus depth of calcites from Geysers 1	121
22	^{18}O versus depth of calcite and quartz from Geysers 1	123
23	^{13}C versus ^{18}O of calcites from Geysers 1	127
24	^{13}C versus ^{18}O of calcites from Geysers 2	129
25	Composite ^{13}C versus ^{18}O	131
26	^{18}O versus depth of quartz from Geysers 1	134
27	Composite of ^{18}O trends versus depth of the Big Geysers Event, Geysers 1	143
28	Schematic diagram of reservoir model	163

FIGURES IN THE APPENDIX

A-1	Calcite fluid inclusion homogenization temperatures from Geysers 1	198
A-2	Quartz fluid inclusion homogenization temperatures from Geysers 1	200
A-3	Calcite fluid inclusion homogenization tempera- tures from Geysers 2	202

INTRODUCTION

The Geysers Geothermal Field is located approximately 110 km north-northwest of San Francisco. It is situated in the Mayacmas Mountains and incorporates portions of Sonoma and Lake Counties in northern California, U.S.A. (see Figure 1). The boundaries of the steam field are undetermined as recent exploration and production are continuously extending the field toward the north and southeast. An overall area of 60 to 120 km² and a reservoir volume of 1160 km³ have been estimated (U.S. Geological Survey Circ. 790, 1978).

The first attempt to exploit the steam potential in The Geysers began in the early 1920's by J. D. Grant and The Geysers Development Company. The eight successful wells were abandoned for lack of a market (Allen and Day, 1927). Today The Geysers is the worlds' largest producing geothermal field with an expected generating capacity of 1800 MWe of electricity by the mid-1980's (Lipman et al., 1978).

Unlike the other major geothermal fields in the world that were developed by governmental agencies (such as Wairakei, Larderello, and Cerro Prieto), The Geysers was explored and drilled by private energy resource companies. The proprietary nature of their efforts in an area open to leasing of government land has precluded the release of information into the public domain. By 1978 the leasing process was concluded. The Geothermal Division of Union Oil Company of California, the largest operating company in The Geysers, offered Dr. Elders and the Institute of Geophysics and Planetary Physics at the University of California, Riverside (UCR) the opportunity to conduct the first detailed petrological study of subsurface samples. This study is the result of that arrangement.

Figure 1. Regional map of northern California showing the location of The Geysers (modified from Weres et al., 1977).

This study is an analysis of drilled cuttings from two boreholes which in this report will be referred to as Geysers 1 and 2 at the request of Union Geothermal. Geysers 1 is a good producing well located in the primary production region of the Big Geysers. Geysers 2 is an abandoned non-producing well. Since this is a pioneering study, every appropriate analytic technique developed by the staff and graduate students of the Institute of Geophysics and Planetary Physics over the last ten years was utilized during two years of data collection. The techniques include thin section petrography, ore mineral reflected microscopy, X-ray diffractometry, fluid inclusion geothermometry, stable isotope geochemistry of carbonates and silicates, and electron microprobe analysis.

The objectives of this report are (1) to characterize and evaluate the authigenic hydrothermal mineralization; (2) to use these data to determine paleo-thermal and paleo-barometric conditions in the system; and (3) to suggest the causes and mechanisms involved in the evolution of the present vapor-dominated reservoir.

REGIONAL STRUCTURE AND GEOLOGY

The Geysers Geothermal Resource Area is located on the northwestern flank of the Mayacmas antiform, a southeastern plunging structure which is the northern extension of the regional Diablo antiform (Garrison, 1972). The Franciscan rocks which comprise the antiform are completely dissected by northwest trending imbricate thrust faults and en-echelon northwest trending high angle and strike-slip faults (McNitt, 1968). The imbricate thrust faults delineate tectonic wedges of eugeosynclinal material accreted to the hanging wall of a subduction zone during the late Mesozoic and early Tertiary. A regional warping, which formed the Mayacmas antiform and initiated the strike slip and high angle faulting, is associated with the late Tertiary development of the San Andreas fault system (McLaughlin, 1975, 1977). Fault movement continues into the present along the major strike slip and reactivated thrust faults (McLaughlin, 1975; Hamilton and Muffler, 1972).

The local stratigraphy can be divided into three components, the predominant Franciscan assemblage, dating from the late Jurassic to early Late Cretaceous (McLaughlin, 1977), the Quaternary volcanics of the Clear Lake area, and the Quaternary alluvial deposits and landslides. The Franciscan rocks and alluvial sands and gravels are described in detail by McLaughlin (1976, 1977) and the Clear Lake volcanics by Hearn, Donnelly and Goff (1976a, 1976b, 1977) and Anderson (1936). The Franciscan and volcanic rocks will be briefly described in the following section.

The Franciscan assemblage is a melange of sedimentary and igneous rocks deposited or tectonically emplaced in an ocean basin in an

arc-trench gap environment; these rocks have been differentially subjected to high pressure (blue schist) metamorphism. The sedimentary rocks are flysch-type wackes, argillites, and conglomerates, derived primarily from andesitic sources, and also subordinate volumes of chert. The igneous group can be divided into basaltic greenstones, composed of pillow flows, pillow breccias, gabbros, diabases and basaltic tuffs, and ultramafic constituents, including antigoritic serpentinites, amphibolites and eclogites. In a few scattered localities coherent ophiolite complexes are observed (McLaughlin, 1976). More commonly, however, the ultramafic members are present as lens-like masses tectonically emplaced into sedimentary blocks along fault zones.

Within the Franciscan, in the Geysers-Clear Lake area, McLaughlin (1976) designated three structural units. These units are based on two criteria; the gross lithology and the textural grade of metamorphic deformation and reconstitution, as established by Blake *et al.* (1970). Units 1 and 3, representing the least and most extensive metamorphic grades, respectively, are not observed in the "Big Geysers", the main production area of the Geysers Field. Unit 1 is a feebly folded and metamorphosed sequence of sandstones and argillites containing authigenic albite, phengite and incipient pumpellyite found southwest of the steam field. Unit 3 is a thoroughly reconstituted sequence of metawackes and subordinate meta-cherts and meta-greenstones which characteristically contain lawsonite, jaditic pyroxene and sodic amphibole. Unit 3 is encountered in the southern portion of the steam field in the Little Geysers and Castle Rock production areas.

Structural unit 2 outcrops in the main steam field and acts as the reservoir rock at depth. It consists of tectonically emplaced slabs of

well-bedded wacke with minor shale interbeds and cherty basaltic greenstones. These slabs are separated by lenticular masses of shaley melange, containing shattered, sheared masses of wacke, chert, greenstone, and sporadically, blueshist and eclogite. The wackes exhibit mineral assemblages common to textural zones 1 and 2 of Blake et al. These are quartz+albite±phengite±lawsonite±pumpellyite.

The Clear Lake volcanics are concentrated in the Clear Lake topographic basin, 15 km north of The Geysers steam field. The bulk of the volcanics are silicic extrusives ranging from andesite to rhyolite, distributed as domes, flows and pyroclastic deposits (Hearn, Donelly and Goff, 1976). Minor volumes of basalt, characterized by phreatomagmatic eruptions, are the most recent additions to the volcanic pile. The eruptions have been dated by K-Ar analysis to be Late Pliocene to Recent.

The oldest volcanic flows are found within or at the boundary of the currently delineated production area. These are the Caldwell Pines olivine basalt flow, dated at 1.69 my, the Ford Flat olivine andesite flows, dated at 1.64 my, and the Cobb Mountain biotite rhyolite dome, dated at 1.4 my with minor dacitic flank and summit eruptions at 1.05 my (Hearn, Goff and Donelly, 1977). Union Oil Company geologists have recently discovered subsurface felsitic intrusive rocks in several wells south of the Cobb Mountain volcanic center. Although extensively hydrothermally altered, the sanidine K-Ar age for the biotite-rich felsite is 1.6 my, which correlates with the local extrusive volcanics (Schriener and Suemnicht, 1980).

GEOPHYSICS

Geophysical studies in the Clear Lake and Geysers areas have added to the abundant volcanic and hot spring evidence that an active magma chamber underlies the Clear Lake basin. Residual Bouguer gravity surveys by Chapman (1966) and Isherwood and Chapman (1975), exhibit a circular major gravity low centered under Mount Hannah and a secondary low under the steam production area. Corroborative evidence can be found in electrical resistivity studies by Stanley et al., 1973 (resistivity lows correspond to gravity lows) and teleseismic studies by Iyer et al., 1979 (1.0 second P-wave delay found under Mount Hannah, .5 second delay under steam field). The consensus interpretation infers the existence of a magma chamber with a diameter of 10-20 km centered under Mount Hannah with a cupola of partial molten material extending southward beneath the steam field.

HYDROTHERMAL GEOLOGY

Surface Features

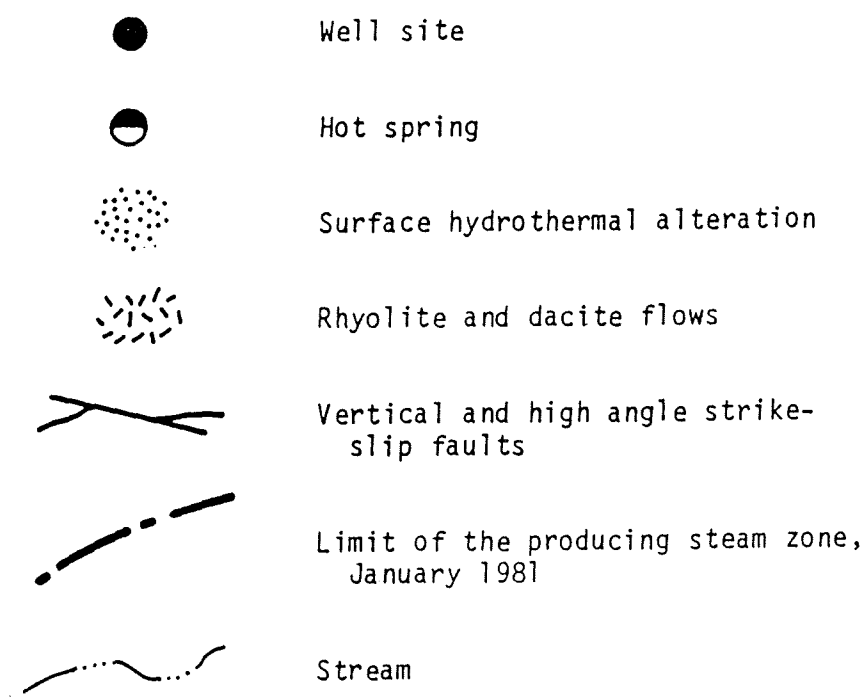
Surface manifestations of hydrothermal activity are restricted to a narrow belt, 10 km in length, of fault-controlled hot springs, fumaroles, sinter deposits and acid leaching (Baily, 1946). The Big Sulphur Creek strike-slip fault zone serves as the primary conduit for ascending hydrothermal fluids and gases which affect only the northern bank of Big Sulphur Creek. This hydrothermal belt corresponds directly with the long axis of the subsurface steam reservoir which is bounded on the north by the Sulphur Bank fumarole area and on the south by Castle Rock Hot Springs (see Figure 2).

The most active thermal area, "The Geysers," is restricted to a small amphitheatre in Geysers Canyon covering a mere 20 hectares. Hydrothermal features include steam vents, mud pots, hot springs ranging from 50 to 100°C and sinter deposits. Water chemistries range from acid sulfate to sodium bicarbonate types (White et al., 1971). Although present natural discharge is almost non-existent since steam production from wells began, spring discharge was historically low. Allen and Day (1927) reported the total measured outflow of the major springs to range from 6700 to 10500 liter/hour depending on seasonal variation. Today, the sole remaining thermal area characterized by sinter deposits and mud pots is Little Geysers, an amphitheatre approximately 8 km southeast of the Geysers.

Previous Work

The most obvious surficial hydrothermal alteration is the surface bleaching of greywacke due to intense acid leaching attributable to the high sulfuric acid content of the mineral springs and fumaroles. Rock

Figure 2. Location map of The Geysers showing well sites.



Taken from McLaughlin, 1974, 1978; Ehni, 1981.

textures are destroyed and replaced by a porous mass of kaolinite, alunite, opal, residual quartz and native sulfur (McNitt, 1961; White, 1968). Volsen (1946) identified a multitude of sulphates of magnesia, ammonia, alumina and iron. In the alteration products, other hydrothermal minerals which have been reported from outcrop, road cut and shallow steam well drill cuttings and ejecta include trace amounts of cinnabar in the Sulphur Banks area (Bailey, 1946), pyrite and marcasite (White, 1968), wairakite (Steiner, 1958), potassium feldspar replacing labradorite, chlorite replacing augite, leucoxene replacing titaniferous magnetite, sericitization of plagioclase and veins of calcite, quartz, and siderite (McNitt, 1961).

Moore (1980) described hydrothermal minerals and mineral assemblages from five pieces of core representing four wells. She reported vein occurrences of pyrite, adularia, quartz, calcite, prehnite, epidote, amphibole and tourmaline. The well, Thermal 10, located approximately 1 km southeast of Geysers 1, contained at 100 m, veins of quartz, chlorite, pyrite, prehnite and extensive replacement of greywacke fabric by adularia. Greenstone core from well HSI (1478 m), located approximately 2 km northwest of Geysers 2, contained veins of calcite and pyrite. An assemblage of prehnite+epidote+calcic amphibole (green actinolite?) + tourmaline was described from wellbore DVI located in the Little Geysers area.

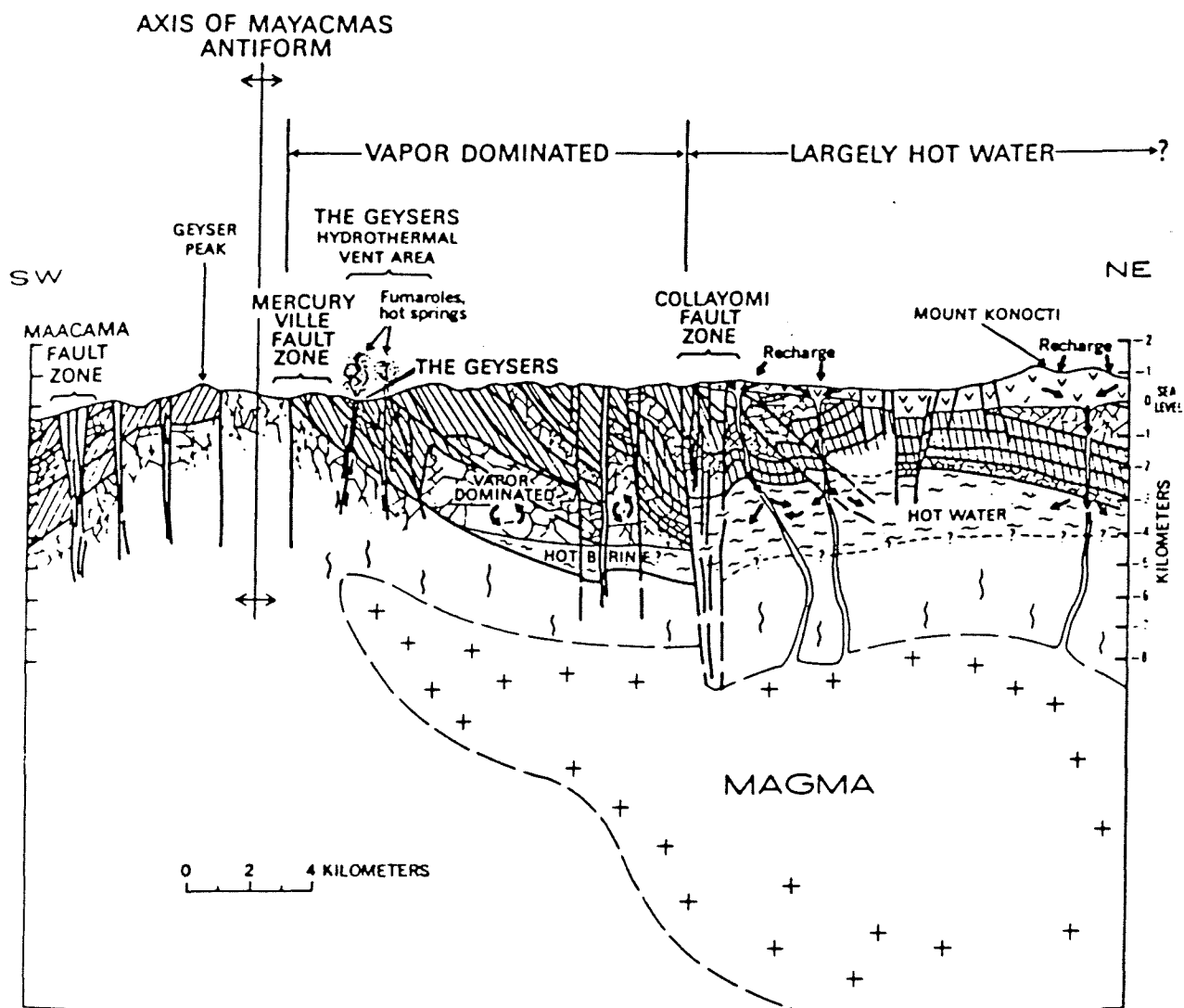
THE STEAM RESERVOIR


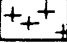



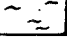
The Geysers-Clear Lake Geothermal Area can be divided into vapor-dominated and hot water-dominated regions. The vapor-dominated reservoir is bounded on the south by the Mercuryville Fault Zone and on the north by the Collayomi Fault Zone. Figure 3 is a cross-section illustrating the structural constraints on the steam reservoir, fault controlled thermal surface manifestations and the geometry of the assumed magmatic heat source.

The steam reservoir has a disparate distribution across the steam field. Steam entries in the Little Geysers and Castle Rock Springs areas are encountered, at depths greater than 1000 m, beneath a thick serpentinite cap rock (McLaughlin and Stanley, 1976). In the Sulphur Banks and Thermal areas there exists a shallow steam anomaly above 640 m and a deeper regional fracture system at depths greater than 1000 m (Lipman et al., 1978; Garrison, 1972). All portions of the steam reservoir are capped by a zone of steam condensate.

The reservoir rock in The Geysers is a massive tectonic block of relatively homogeneous meta-greywacke, locally capped by greenstone or serpentinite. The wacke itself is dense and impermeable, lacking inherent porosity, due to its argillaceous nature and subsequent greenschist metamorphism. Lipman et al. (1978) reports core analyses indicating an interstitial porosity of 3-7% and air permeabilities less than 1 millidarcy. The reservoir rock is intensely fractured and shattered along thrust faults and vertical shear zones, creating narrow sheet-like reservoirs. The steam is therefore restricted to open fractures that are isolated laterally and vertically by unfractured impermeable rocks (Garrison, 1972; Weres et al., 1977; Lipman et al., 1978).

Figure 3. Cross-section model of The Geysers developed by McLaughlin (1977) showing major structural features and the relationship of the steam reservoir to the magma body suggested by geophysical data.



- | | |
|---|--|
|  Impermeable cap rocks (Serpentine, greenstone, melange, metagraywacke) |  Partially crystallized magma body inferred to be at depth, with center below 10 kilometers |
|  Fracture networks in graywacke reservoir rocks |  Water vapor in steam reservoir above boiling water table |
|  Clear Lake Volcanics and associated vents providing recharge to geothermal system |  Hot water |

The steam recovered at The Geysers is dry and superheated by 12°C. Steam in the deep regional fracture system maintains uniform reservoir temperatures (236-240°C) and pressures (32-35 kg/cm²) which are less than hydrostatic. Temperatures recorded in the shallow steam anomaly plot along the reference boiling point curve for water until a maximum of 240°C is achieved.

The enthalpy of the steam encountered in the deep production zones has remained relatively constant at 667-669 cal/g. These temperatures, pressures and enthalpies are significant as they represent the maximum enthalpy of saturated steam (White et al., 1971; Truesdell and White, 1973).

The previously published model for The Geysers suggests that a water-dominated hydrothermal system existed initially which was converted to steam-dominated due to inadequate recharge of meteoric waters and a potent heat source (McLaughlin and Stanley, 1978). The influx of cool recharge water was thought to have been impeded by the limited fracture system and self-sealing due to carbonate and silica mineralization (Facca and Tonani, 1965). The present steam reservoir was believed to be generated from vaporization at the interface of a deep water table with a salinity of 25% wt % NaCl (White et al., 1971).

The controlling vaporization pressures of a 25% NaCl brine solution (underpressured with respect to hydrostatic boiling pressures) was thought to account for the superheated steam temperatures, the uniformity of the reservoir pressures and the trends of measured downhole temperature and pressure of the steam (White et al., 1971; Truesdell and White, 1973).

The deepest wells to date (greater than 3100 m) have not been reported as penetrating either the postulated deep seated brine or the base of the

steam reservoir (Lipman et al., 1978). Deep water entries were reported in the Castle Rock area but the liquid proved to be steam condensate (Truesdell and Frye, 1978).

PETROLOGICAL METHODOLOGY

Problems Inherent to the Study of Well Cuttings

The rock material studied in this investigation consists entirely of drill cuttings, as core was not available from these two wells. The cuttings were produced by drilling either with mud or with air acting as the lubrication medium. There are many problems inherent to the study of cuttings.

The most obvious problem is the small size of the individual cutting chips. Mud drilled cuttings are measured in millimeters and size decreases as a function of depth. Chips originating at depths less than 2000 ft (600 m) are 5-10 mm in length, while cuttings from below 5000 ft (1700 m) are less than 2 mm. Air drilled samples are especially minute. An average sample consists of silt to fine grained sized rock fragments (usually 20 to 50% of sample) and rock flour, dust and grit. In the case of wacke, the rock grains are the framework grains and the rock flour the chloritized matrix material. Therefore only microstructures can be studied utilizing mud cuttings and only bulk mineralogies using air drilled material. Cross cutting relationships between different generations of hydrothermal veins are essentially impossible to determine from drill cuttings.

At The Geysers, Union Geothermal staff collected five random samples per 100 ft (30 m) of drilled depth. Therefore, a sample is a composite representing 20 ft (6 m) of stratigraphy. The exact correlation between the cuttings and the labeled depth is imprecise due to three conditions. Firstly, uncertainties arise from variable (unknown and therefore uncompensated) lag times between contact with the drill bit and collection at the surface. Secondly, wells are not drilled vertically. Several wells

are drilled from an individual pad and each is drilled at inclined angles of up to 20° (Were et al., 1977). Union Geothermal did not submit down-hole geometries with the cuttings. Thirdly, because of the dense, highly indurated nature of the Franciscan complex and the steep regional dip, the bit tends to follow paths of least resistance and will deflect along fractures, fault planes and bedding planes (Were et al., 1977; Glass, 1977).

The effect of the first condition is that the labeled depth is greater than the absolute depth and the effects of the latter two are that the labeled depth is greater than the true vertical depth. For simplicity, samples will be identified by the minimum depth of the labeled interval, and labeled depth will be treated as true depth.

Another problem of drill cuttings involves contamination. The Franciscan rocks are well indurated, therefore contamination by the ingredients and additives in the muds are minimal. However, the sample can be contaminated by the mixing of cuttings during the slow ascent of the mud or by sloughing of wall rock from above.

Air drilled material is subject to severe chemical and physical contamination. While the upward travel is relatively instantaneous, the sample can be contaminated above ground. Caking and subsequent sloughing of rock material onto the surfaces in discharge lines and mixing of cuttings during the centrifugal steam separation process within the vertical muffler is common. In addition to this mixing problem, evidence for chemical contamination is abundant. The drilling process utilizes a high-pressured mist of water and chemical additives in air. Therefore, the contact between the fine grained cuttings, iron drill bit fragments and water at high temperature, albeit brief, results in surficial oxidation coatings.

Analytical Techniques

Sample Preparation

Cuttings splits were supplied by Union Geothermal Division at Santa Rosa. The sampling interval supplied for Geysers 1 was two samples per 100 ft (30 m) and the interval for Geysers 2 was one per 100 ft (30 m).

Mud drilled cuttings were washed in distilled water to remove drilling mud contaminants and dried overnight in a 60°C oven. The samples were examined and described with the aid of a binocular microscope. Cuttings were subsequently selected for specific petrographic and geochemical analyses. Representative bulk cuttings were selected for X-ray diffraction and thin-section preparation; cuttings enriched with ore minerals were set aside for polished section preparation; and lastly, chips and fragments of obvious calcite and quartz vein material were separated for fluid inclusion and stable isotope studies.

Air drilled cuttings required specialized treatment. First, unbiased admixtures of rock flour and sand-sized particles were collected for bulk X-ray diffraction analyses. The cuttings were then sieved with a 170 mesh (.088 mm) screen to remove the powdered component and iron filings were extracted with a magnet. The sand-sized grains were washed and dried as were the mud drilled cuttings.

The cleansed air drilled cuttings were examined and described with the aid of a binocular microscope. A random sample of cuttings was separated for thin section preparation. The remaining material was sieved a second time with a 120 mesh (.124 mm) screen and the coarser fraction was put through a Frantz Isodynamic magnetic separator. The material was separated twice. The first run concentrated the strongly magnetic base metal sulfides and residual iron filings from which polished sections were

prepared. The second run separated the paramagnetic calc-silicates (epidote, tremolite, diopside) from the non-magnetic quartz, plagioclase and lithic fragments. Thin sections were prepared from the concentrated calc-silicate material.

Petrography and Microprobe

Hand picked mud drilled cuttings were impregnated in a 20 mm diameter epoxide plug. Cuttings designated for petrographic evaluation were mounted on a 1 inch diameter glass slide and ground to standard thin section thickness on a dry carbide lap. A select group of thin section slides were polished with diamond paste for microprobe analysis. Epoxide plugs designated for reflected-light ore microscopy were ground on a wet carbide lap to expose the ore minerals and the surface was polished with diamond paste.

A thin coating of air drilled cuttings was sprinkled on the surface of epoxide puddles which were poured onto a teflon plate. A glass slide was set over the air drilled cuttings and the epoxy was allowed to dry. The slides were appropriately ground to thin section thickness or polished for reflected-light microscopy.

A total of 108 thin sections and 71 polished sections were prepared from the mud-drilled and air drilled cuttings from Geysers 1. Seventy-three thin sections and 24 polished sections were prepared from Geysers 2 material.

The thin sections and polished sections were studied under a Zeiss petrographic microscope equipped with transmitted and reflected light sources. The sulfide microprobe analyses were performed by Todd Solberg at the Virginia Polytechnic Institute, Blacksburg, Virginia. The silicate microprobe analyses were conducted at the California Institute

of Technology, Pasadena, California, with the assistance of Art Chodos. The computerized microprobe data at each institution was reduced by the method of Bence and Albee.

X-ray Diffraction

Hand-picked bulk rock samples from selected depths were ground using a steel mortar, an agate mortar and Fisher automatic grinders. The powdered samples were analyzed on an automated Picker X-ray Diffractometer using $\text{CuK}\alpha$ radiation, a graphite crystal monochromator, and a scanning speed of $2^\circ/2\theta$ per minute. The X-ray peak intensities were processed and mineralogical modal compositions calculated by a computer interface utilizing a pattern matching technique (Johnson *et al.*, 1977). The data were displayed, reviewed and modified on a computer terminal. Each sample was subsequently glycolated and reanalyzed to aid in the identification of clay minerals.

The automated X-ray diffraction system employs a reference file of standard mineral diffraction peak locations and intensities. A special library of 25 minerals was created to cope with the expected Franciscan and hydrothermal mineral assemblages based on previous hydrothermal studies of the Imperial Valley and Cerro Prieto (Elders *et al.*, 1978) and Franciscan rock studies (Ernst, 1971; Bailey *et al.*, 1964; McLaughlin and Stanley, 1977). A suite of Franciscan Formation metagreywackes and greenstone from Panoche Pass, California (UCR collection) and a suite of surface samples from the vicinity of The Geysers (collected by Union Geothermal) were X-rayed to establish the peak locations and approximate intensities for lawsonite, pumpellyite, jadeitic pyroxene and glaucophane (see Table A-1). Peak locations for ferrierite were established by Wise *et al.*

(1969). The mineral name abbreviation, detection limits and standard deviations are listed on Table 1.

In this study, 64 samples from Geysers 1 and 88 samples from Geysers 2 were analyzed. The results are presented in tables and on "spindle" diagrams.

TABLE 1

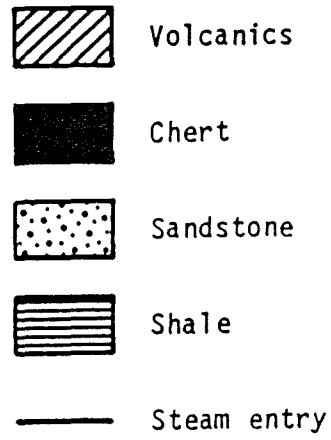
X-ray Diffraction Mineral and Detection Limits and Standard Errors

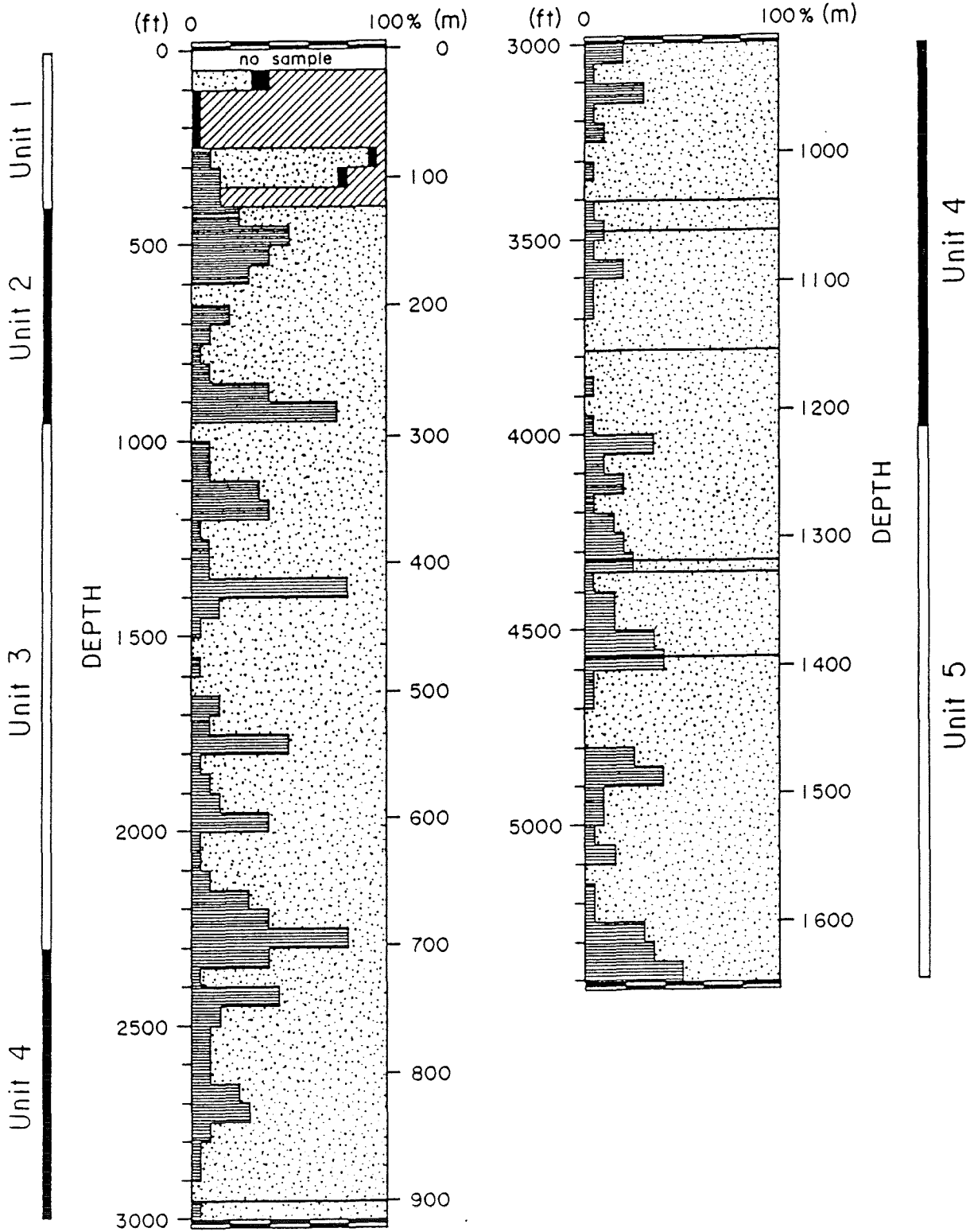
<u>Symbol</u>	<u>Mineral</u>	<u>True Value</u>	<u>Standard Error (1 S.D.)</u>	<u>Detection Limit</u>
QUAR	Quartz	60%	±3.1	<1
PLAG	Plagioclase (Albite)	10	±2.7	<2
ALKA	Alkali Feldspar	10	±2.6	<3
MICA	Muscovite and/or Biotite	5	±2.6	>2
ILLI	Illite	5	±1.0	>2
TMIX	Illite/Montmorillonite mixed layer clay 25% expandables	--	--	>5
MONT	2-H ₂ O Montmorillonite	--	--	>5
CHLO	Chlorite	10	±1.5	>1
VERM	Vermiculite	--	--	--
CALC	Calcite	10	±1.9	>1
WAIR	Wairakite and/or Analcite	5	±2.7	<1
LAUM	Laumontite	--	--	--
PUMP	Pumpellyite	--	--	--
LWSO	Lawsonite	--	--	--
PYRI	Pyrite	5	±3.7	>4
HEMA	Hematite	--	--	--
ILME	Ilmenite	--	--	--
MAGN	Magnetite	--	--	--
EPID	Epidote	5	±1.0	>4
PREH	Prehnite	5	±1.0	>4
AMPH	Hornblende	5	1.0	<1
AUGI	Augite	--	--	--
JADE	Jadeite	--	--	--
GLAU	Glaucophane	--	--	--

-- Not Determined

The detection limits etc., are from Elders *et al.*, 1978.

Figure 4. Lithologic column of Geysers 1. Unit 1 lithologic units (see text).





WELL-BORE LITHOLOGY

Geysers 1

Introduction

Geysers 1 is located in the Sulphur Banks tract of the Big Geysers production area (see Figure 2). The well was mud drilled to a depth of 2945 ft (898 m) where a steam entry was encountered. It was then air drilled to a total depth of 5400 ft (1646 m). Seven additional steam entries, irregularly spaced between 3400 ft (1036 m) and 4600 ft (1402 m), were encountered before the well was put into production. Steam temperatures were recorded as 376°F (191°C). The lithology as determined in this study is shown in Figure 4.

The lithology of Geysers 1 is simple, consisting of interbedded fine to medium-grained wackes and microwacke/shales capped by a block of cherty basaltic greenstones (see Figure 4). The well can be divided into five lithologic blocks based on lithologic criteria and hydrothermal mineralization. These blocks are bounded by major shale partings that are either demarcations between transitions in sediment sources or are thrust faults (McLaughlin, 1977).

Rock Descriptions

Wackes

The term wacke will be used in this report to describe sediments that are predominantly composed of framework grains of silt to sand-sized grains.

The principal stable framework grains in the wackes are quartz, albite and lithic (volcanic, metamorphic, chert) clasts. Common accessory detrital grains are reddish brown biotite, zircon, sphene, epidote, hornblende and, more rarely, detrital chlorite. Opaque grains of ferric

oxide and vitrinite (detrital plant material) are ubiquitous throughout the sequence. Vitrinite reflectivity increases with depth (indicative of increased thermal metamorphism) and approaches the reflection behavior of anthracite (Ramdohr, 1969) below 670 m. All vitrinite grains are angular to subangular.

Quartz grains do not exhibit signs of strain (undulatory extinction) or authigenic overgrowths and contain abundant fluid inclusions. The albite grains are blocky angular clasts commonly displaying well-developed albite and pericline twinning. Zonation is absent. The feldspars are almost pure albite in composition (see Table A-7). Sericitization is common at all depths. The severity of alteration, and the number of affected grains increase with depth. Replacement minerals include chlorite, pumpellyite, smectite, illite, micas, and minute apatite grains.

The interstitial material is a fine-grained matrix of chlorite, chloritoids, clay, and micaceous minerals of highly variable textures and colors. Since it is beyond the scope of this report to systematically analyze these minerals, the term phyllosilicates will be employed in subsequent sections in reference to this material. Coarser grained aggregates and fibrous mats of pennine and celadonite are identifiable due to their diagnostic crystal habits and anomalous birefringence.

The wackes contain trace amounts of lawsonite, pumpellyite and phengite. The mineralogy and fabrics are typical of metamorphic textures 1' to 1.5 (Ernst, 1971). Phengite is the most common of the three, occurring as wispy, fibrous mats and aggregates replacing interstitial phyllosilicates, vermicular growths replacing biotite and chlorite and occasionally as subhedral to euhedral grains (<.05 mm) in the matrix.

Lawsonite is ubiquitous at all depths but never exceeds 1% of the total rock and, in most instances, is present only as sporadic porphyroblasts. Lawsonite grains occur as minute (<.02 mm) euhedral tablets and blocks in plagioclase grains, euhedral equant to elongate rectangular grains (<.23 mm) and rarely vermicular intergrowths in fibrous phengite aggregates. Pumpellyite is uncommon. With the exception of lithologic Unit 4 (described in a subsequent section) pumpellyite occurs as isolated radiating needles (<.01 mm) in plagioclase usually forming doublets or triplets. Well-developed examples form dense radiating splays of needles and acicular interwoven mats.

Shale

Shale will be employed to describe two types of fine-grained materials. The first group consists of medium to dark grey microwackes that are fine silt to clay-sized compositional equivalents of the local wackes. Quartz, micas, albite and lithic clasts are identifiable. The second group of shales are typically dense and extremely fine-grained. In hand samples these shale cuttings are jet black to reddish brown and are characterized by conchoidal fracture and a vitreous luster. They are composed of quartz grains, phyllosilicates and up to 50% reddish brown opaques. The opaque material consists of fine-grained organic debris and amorphous iron oxide. Bands of framboidal to idiomorphic pyrite (less than .01 mm) of diagenetic character are occasionally observed. Pyrite is absent in the microwackes except for hydrothermal veining.

Definition of Lithologic Units

Unit 1 - Unit 1, 0-122 m, consists of basaltic greenstone and cherts interrupted by a lens of wacke and shale. The cherts exhibit a wide

variety of colors (red, grey, white and green) and often contain inclusions of idiomorphic pyrites (<.025 mm). Cherts occur as veinlets, pockets, and massive interbeds within the basalt. The wackes are very poorly sorted volcanic wackes. Framework grains are fine and coarse-grained chert fragments, microlitic and vitrophyric volcanic clasts, shale, quartz, albite and detrital biotite (up to 10%). The interstitial material is an inhomogeneous orthomatrix paste of phyllosilicates, iron oxides, and silt. Quartz and calcite veining is locally well-developed and pervasive (calcite > quartz). Feldspars are extensively, or often completely, replaced by phyllosilicates.

The greenstone is a medium-grained hypocrystalline (intersertal) panidiomorphic-granular amygdaloidal diabase. Three types of primary minerals are present. Anhedra to subhedral pale brown clinopyroxene occurs as disseminated granules and columns which are partially replaced by brown chlorite, sphene and iron oxide. Euhedral laths of plagioclase have been completely replaced by a cloudy, grey matrix of clays, micas and albite and are intergrown with irregular veins and masses of chlorite and pumpellyite, and euhedral (partially embayed) grains and dendritic needles of iron. Primary titanomagnetite has been replaced by magnetite and leucoxene, and are speckled by late stage pyrite and hematite grains (<.01 mm). The original glassy groundmass has been devitrified into chlorite, pumpellyite, and celadonite and the amygdules are filled by a mosaic of radial chlorite aggregates, or less commonly, chert. Subordinate cuttings of holohyaline and vitrophyric plagioclase-rich basalts are found mixed with the sedimentary rocks.

Unit 2 - Unit 2, 122-262 m, is composed of interbedded fine to medium-grained lithic wackes and shales. Lithic clasts compose 5-50% of the framework grains and include fine and coarse-grained cherts, micro-litic and vitrophyric volcanics, quartzite, and shale (often with quartz veinlets). The wacke textures vary from well-sorted, with a phyllosilicate cement, to poorly-sorted with an orthomatrix of phyllosilicates and silt. Feldspar alteration is minor or absent. Phengite and lawsonite are present in trace amounts (<1%) and pumpellyite is negligible. Unit 2 can be classified as textural grade 1.

Unit 3 - Unit 3, 262-670 m, consists of interbedded very fine to medium-grained quartz wackes and shales. Quartz and feldspar predominate. Lithic clasts are rare (<1%). The wackes are poorly to very poorly sorted and the interstitial material is a mixture of silt-sized quartz (and albite?) and phyllosilicates. The wacke fabric grades downward from framework grain-supported matrix, set in a pseudomatrix (15-20% interstitial material), to a coarse siltstone/very fine-grained chloritic siltstone with 20-30% "floating" stable grains.

Feldspar sericitization is more common than in Unit 2. Individual grains exhibit minor to partial replacement. The rocks in this block belong to textural grade 1. Lawsonite occurrences remain sporadic. Isolated needles of pumpellyite are present in trace amounts. Phengite is relatively abundant and approaches 2% of the total rock.

Unit 4 - Unit 4, 670-1220 m, is composed of interbedded lithic wackes and shales. The wacke contains up to 25% lithic fragments. Lithic clasts are primarily metastable siltstones and mudstones (deformation

progressively grades into pseudomatrix material) and minor well-indurated shales and vitric volcanics. The rock is dense and well compacted framework grain supported wacke and locally displays weak schistosity. Interstitial phyllosilicate material is subordinate, consisting of pseudomatrix and thin bands of cement. Feldspar alteration ranges from partial to extensive. Ninety percent of all albite grains exhibit phyllosilicate replacement or pumpellyite intergrowths. Quartz and calcite veins are common (quartz >> calcite). Calcite appearances are sporadic and disappears completely by 975 m.

The textural grade of Unit 4 ranges from 1 to 1.5. Phengite is similar in habit and abundance to Unit 3. It commonly occurs as fibrous aggregates and subhedral grains less than .1 mm. Lawsonite and pumpellyite are abundant, collectively constituting approximately 3% of the total rock. Euhedral porphyroblasts of lawsonite (<.2 mm) are common. Pumpellyite occurs as isolated needles, acicular radiating fans and massive blocky intergrowths confined to albite twins in plagioclase (see Table A-9) and as acicular mats in the matrix intergrown with chlorite and phengite (see Table A-9).

Unit 5 - The nature of the air drilled cuttings does not preserve the wacke fabric -- only the major detrital grains are observable. Therefore, the last lithologic block, Unit 5, is delineated in the air drilled cuttings based on three criteria. One, it is a zone of interbedded wacke and shales in contrast to the upper 305 m of air drilled strata that is argillite poor. Two, lawsonite and pumpellyite are present in the air drilled portion of Unit 4, but they are absent or extremely rare in Unit 5. And three, trace amounts of glaucophane frag-

ments (<1%) are present at 1220 m. According to McLaughlin (1976) blueschist minerals in The Geysers area occur only as exotic blocks in thrust fault melange.

XRD Analysis

The X-ray analyses of the bulk compositions of selected wacke material (mud drilled cuttings) are displayed in Figure 5 and Table A-2, selected shale material (mud drilled cuttings) in Figure 6 and Table A-3, air drilled material in Figure 7 and Table A-4 and volcanics in Table 2. It should be noted that the mineral abundances are approximate, especially for those minerals with weight percentages less than 5%. These analyses are useful to identify minerals and to estimate relative abundances.

The reported XRD abundance of alkali feldspar is highly erroneous. The major peak is masked by a plagioclase peak and the adularia identification is based on secondary peaks. The listed percentages are two to three times greater than thin section observation confirms but the general trend of adularia enrichment with depth is valid.

The modal lithology of the wackes and air drilled cuttings remains relatively constant. The ratio of quartz to plagioclase is approximately 2:1 throughout the well. The percentages of illite and chlorite are also uniform, each comprising about 10% of the total. The sole exception is the wacke sample at 210 ft (64 m) which is relatively low in quartz and high in feldspar. The composition of the shallow sample, which is derived from the wacke interbedded in the greenstone block, has equal proportions of quartz and plagioclase and twice the chlorite content of the main block of sediments. These values reflect the volcanoclastic components in the material. It can be inferred that the reservoir greywacke is a relatively

Figure 5. XRD spindle diagram showing the relative mineral abundances vs depth of the mud drilled sandstones from Geysers 1.

GREYWACKE

DEPTH SAMPLE QUAR PLAG ALKA NICA ILLI INIX ZNIX MONT CHLO CALC DOLO ARAG WAIR LAUM PUMP LUSO PYRI HERA ILME MAGN EPID PREH AMPH AUGI
(ft)

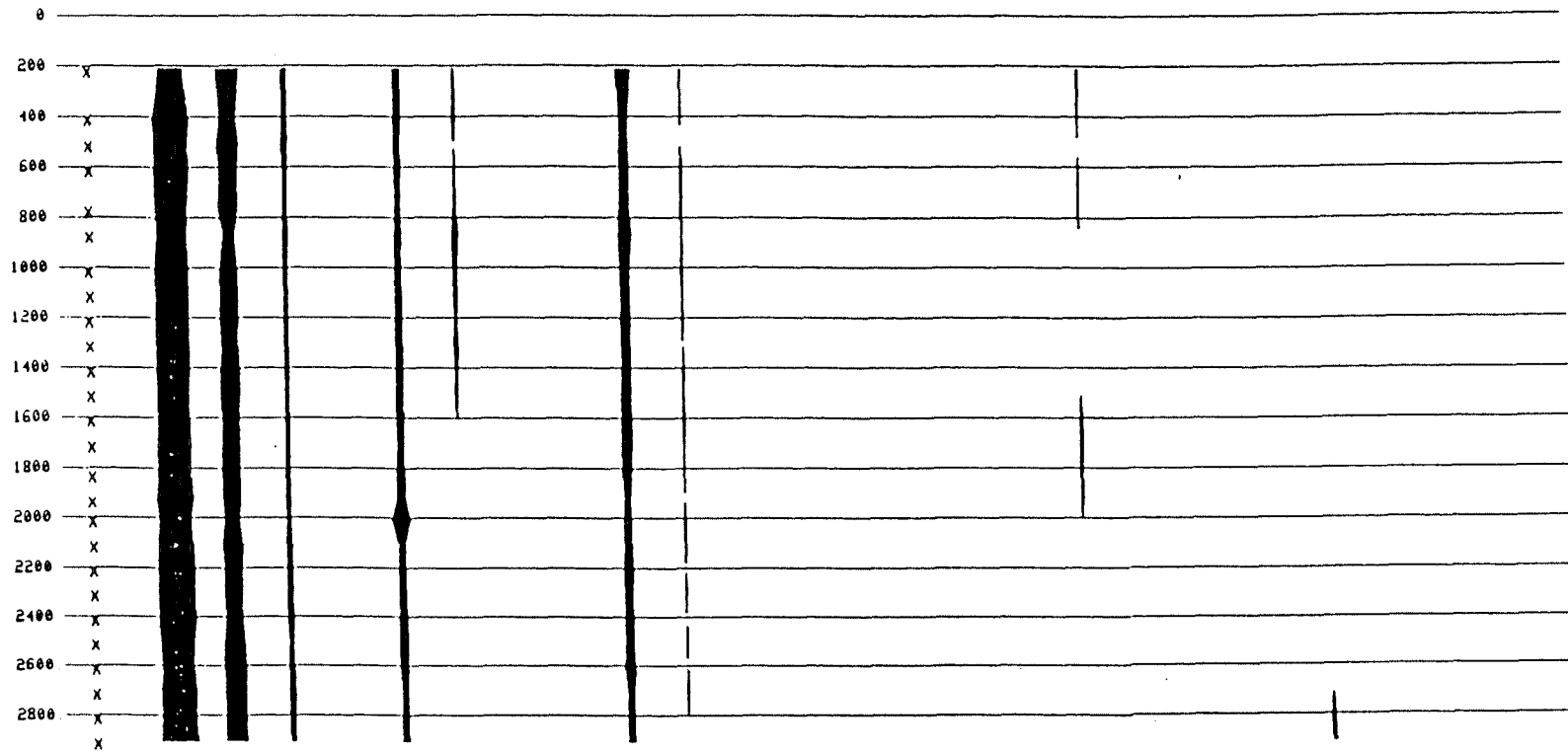


Figure 5

Figure 6. XRD spindle diagram showing the relative mineral abundances vs depth of mud drilled shales from Geysers 1.

SHALES

DEPTH SAMPLE QUAR PLAG ALKA MICA ILLI IMIX 2MIX MONT CHLO CALC DOLO ARAG WAIR LAUR PUMP LUSO PYRI HEMA ILAE MAGN EPID PREH AMPH AUGI
(ft)

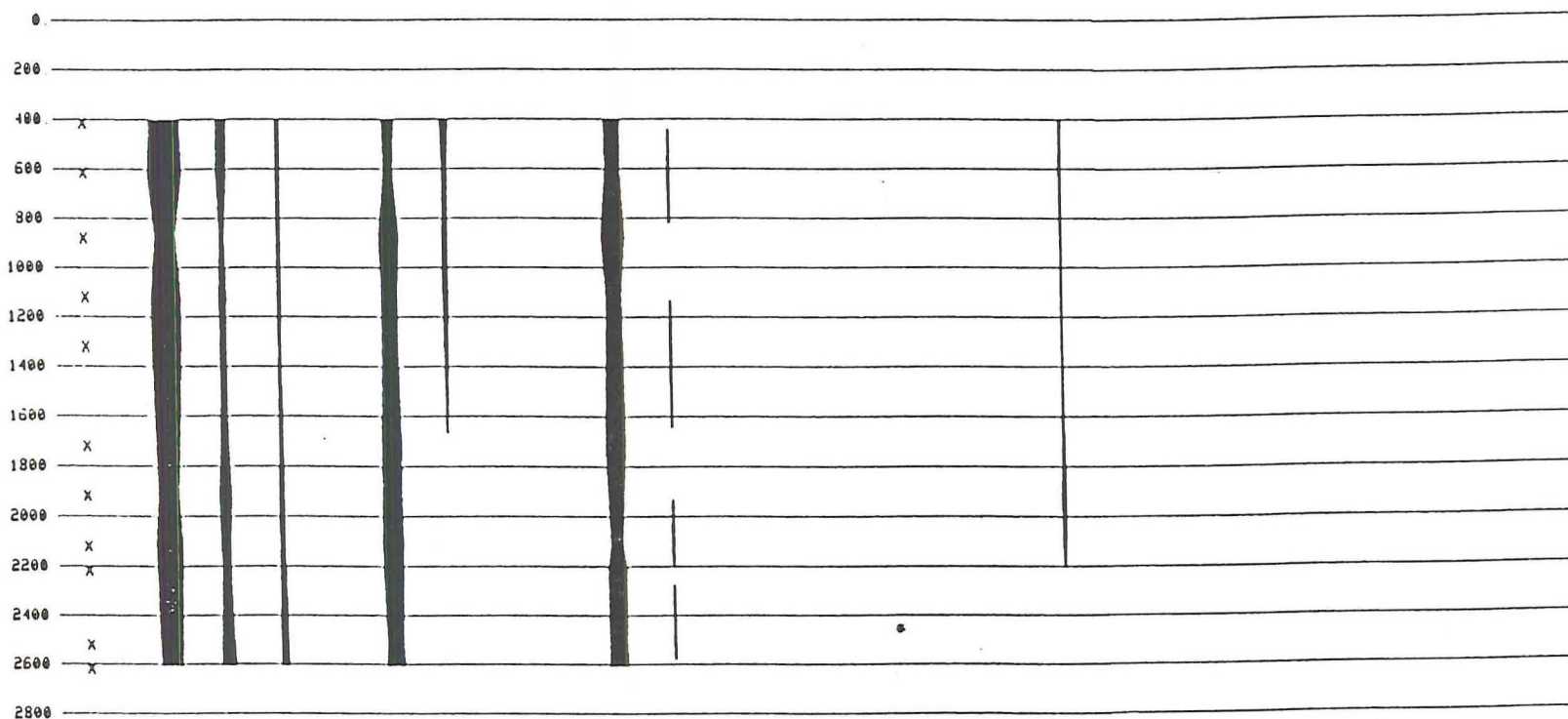


Figure 5

Figure 7. XRD spindle diagram showing the relative mineral abundances vs depth of air drilled bulk samples from Geysers 1.

AIR DRILLED

DEPTH SAMPLE QUAR PLAG ALKA MICA ILLI IMIX SMIX MONT CHLO CALC DOLO ARAG UAIR LAUM PLUM LUSO PYRI HEHA ILNE MAGN EPID PREH AMPH AUGI
(ft)

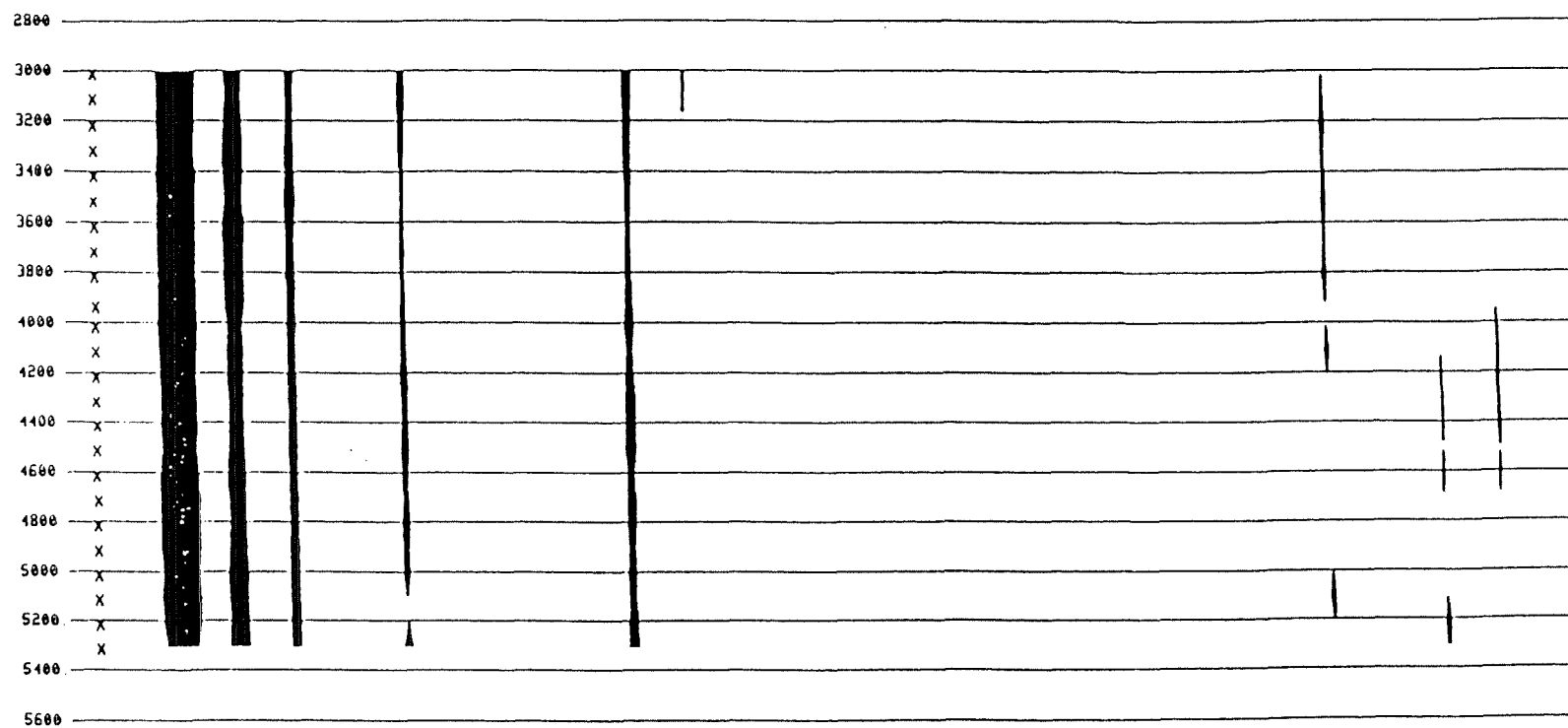


Figure 7

TABLE 2

Geysers 1 Volcanics

<u>DEPTH</u> <u>(ft)</u>	<u>QUAR</u>	<u>PLAG</u>	<u>MICA</u>	<u>ILLI</u>	<u>TMIX</u>	<u>CHLO</u>	<u>CALC</u>	<u>ARAG</u>	<u>PUMP</u>	<u>HEMA</u>	<u>AUGI</u>	<u>PREH</u>	<u>AMPH</u>	<u>ANALYSIS</u>
110	1.7	29.2		5.9	.9	42.1					20.2			1 - 1
150	1.0	37.4		4.9		37.4	2.4				16.8			1 - 2
300	8.2	33.5		12.2	2.1	31.7	12.4							1 - 3

homogeneous block of sediments despite the apparent variations in metamorphic grades observed in thin section.

The shale compositions are more variable. The quartz to plagioclase ratios range from 6:1 to 2:1. These samples are composites of black and dark grey shale cuttings and the higher the proportion of black shale (discussed earlier) in the sample, the greater the ratio of quartz to feldspar. The overall composition of the shales is similar to the wacke compositions, with the exception of higher potassium feldspar content. In both the wackes and shales, the interlayered montmorillonite/illite clays disappear by about 1500 ft (457 m) just as pyrite becomes abundant.

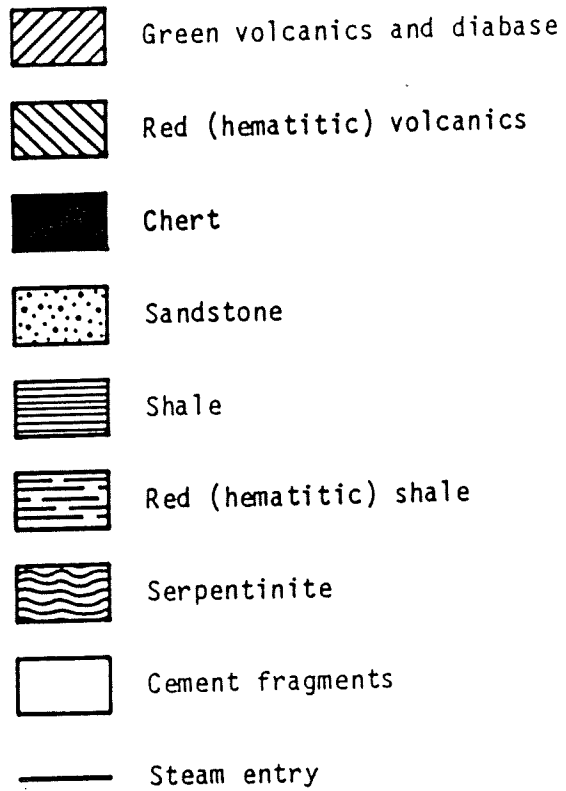
Geysers 2

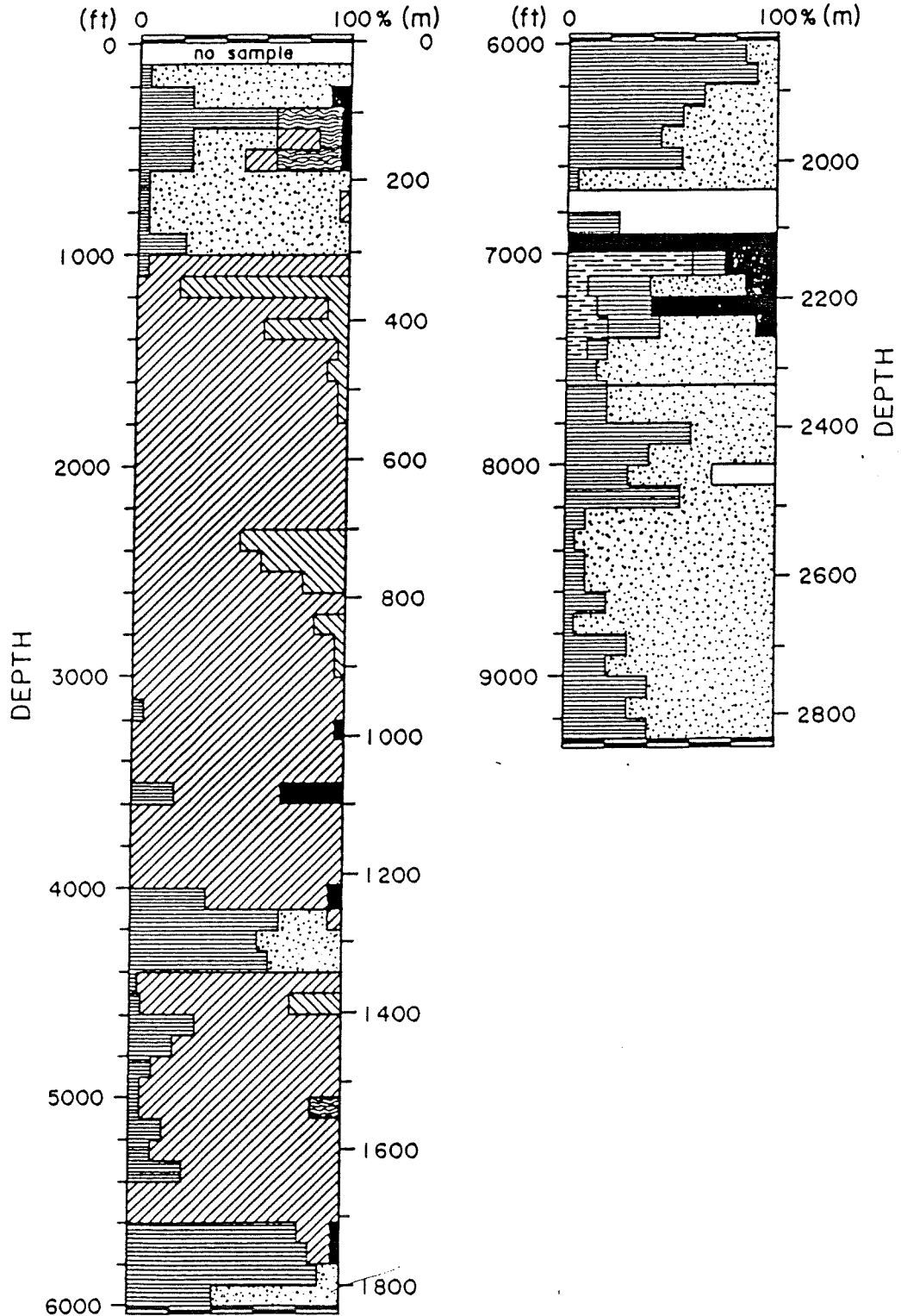
Introduction

Geysers 2 is located near the western edge of the Cobb Mountain rhyolite flow (see Figure 2). The well was mud-drilled to a depth of 9264 ft (2824 m) before it was sealed and abandoned. A single steam entry was encountered at 7620 ft (2323 m). There are no local surface manifestations of hydrothermal activity and, as shown on the location map, the site lies outside the known producing field. The lithology of the well (see Figure 8) is more complex than Geysers 1. The strata are dominated by a 1500 m block of greenstones and the wacke and shale blocks contain interbeds of serpentine, chert and cherty-shales.

In comparison to the other well, the sedimentary units of Geysers 2 are characterized by a higher proportion of shales and the wackes are finer-grained. The sandstones are commonly "dirty" -- predominated by orthomatrix -- and are imbued with a reddish brown tint. The hydrothermal mineralization is sparse (<1%) and does not appear to be strongly influenced by lithologic blocks.

Figure 8. Lithologic column of Geysers 2.





Rock Descriptions

Sedimentary Strata

The greywacke and interbedded shales in Geysers 2 can be divided into four distinct compositional and metamorphic textural blocks. Three of these blocks are separated by the tectonic emplacement of the two major blocks of greenstone strata. The fourth wacke unit is characterized by a sudden change in detrital components and the appearance of hydrothermal minerals similar to the wacke-wacke thrust contacts observed in Geysers 1. An associated change in metamorphic textural grade, however, is not observed.

The block of sediments above the volcanics (0-305 m) is characterized by micaceous illite, lawsonite, pumpellyite and prehnite. Vermiculite is found in the shallowest wackes and vermiculite and montmorillonite in the shales. These are probably weathering by-products (Bailey et al., 1963). The fabric of the wackes is weakly to strongly shistose (textural grade 2) with biotite a dominant interstitial mineral. Lithic clasts (chert, slate and vitrophyic volcanics) make up about 25% of the framework grains. Minor to partial replacement of the plagioclase by fibrous pumpellyite is common, similar in habit to the first well. Felty pumpellyite mats and aggregates of fibrous phengite are also present. Lawsonite is uncommon and occurs primarily as inclusions in plagioclase or as grain boundary overgrowths on plagioclase grains.

The wackes below the serpentinite body (182-189) contain veins of massive ankerite and ferrierite (a magnesium-bearing zeolite). Both minerals were identified by XRD analysis and in thin section. The ferrierite forms as isolated spherulites radiating aggregates of bladed

white crystals up to 1.27 mm in length and as massive crusts of intergrown fibrous sheaves and aggregates. The chemical composition (see Table A-13) indicates it is rare barium ferrierite and a composition of a reported barium ferrierite is given for comparison (Wise and Tschernich, 1976). This zeolite was probably deposited during ocean-floor or subsequent Franciscan metamorphism. Another barium-rich zeolite, harmatome, has been described from low-grade Franciscan greenstone in Marin County which has not been exposed to recent geothermal activity (Swanson and Schiffman, 1979).

The block of sediments that interrupts the volcanic strata (1220-1340 m) is composed of siltstones and microwackes. The proportion of lithic frameworks grains is high, 25 to 35%, and the clasts include shales, volcanics and cherts. Carbonaceous material is common and is concentrated along selected bedding planes.

The wackes below 1700 m share strong compositional and textural similarities. The rocks are quartz wackes as the distribution of lithic clasts (shale and chert only) drops below 2%. The orthomatrix is silty and contains traces of vitrinite. The wacke cuttings commonly exhibit well-developed bedding planes and orientated grains. Shistosity is very weak or absent but the grains show signs of stress -- quartz grains display undulatory extinction and albite twins are offset.

These wackes can be classified as textural grade 1 to 1.5. Lawsonite, phengite and pumpellyite are ubiquitous but scarce (<1%). When these minerals do appear, they are fine-grained, less than .15 mm, and poorly crystalline. Lawsonite is restricted to plagioclase hosts and

minor xenoblastic grains in the interstitial phyllosilicates. Pumpellyite occurs as isolated needles, splays and, very rarely, as acicular mats.

At 2100 m the continuous sequence of fine-grained wackes, siltstone and shale is broken by interbeds of multi-colored cherts (red, green, white, blue) and hematitic cherty-shales (see Figure 8 - 7000 ft). The wackes below the chert layer are clay rich (see Figure 9 - 7500 ft) but the overall detrital character of the sediments between 1700 and 2100 m and between 2256 and 2500 m are identical.

The fourth wacke unit begins at 2500 m (8200 ft) and is characterized by the increase in the granularity of the wackes and a rapid decrease in the volume of interstitial material to 20% or less (note the behavior of illite on Figure 9). This transition to a medium-grained, framework-supported wacke is also characterized by the reappearance of biotite and detrital chlorite. The metamorphic textures and occurrences of lawsonite and pumpellyite are identical to the wackes between 1700 m and 2500 m, and the wacke material is similarly poor in lithic clasts. It is questionable whether this boundary represents a tectonic thrust contact or a facies change in the original depositional environment. This boundary does mark the first appearance of hydrothermal minerals such as adularia and epidote and the disappearance of calcite and mixed-layer clays.

XRD Analysis

The X-ray analyses of Geysers 2 wackes are displayed on Figure 9 and Table A-5, shale on Figure 10 and Table A-6.

Figure 9. XRD spindle diagram showing the relative mineral abundances vs depth of sandstones from Geysers 2.

SANDSTONE

DEPTH SAMPLE QUAR PLAG ALKA MICA ILLI IMIX ZHIX MONT CHLO UERM CALC WAIR LAUM PUMP LUSO PYRI HEMA ILNE MAGN EPID PREH AMPH AUGI JADE GLAU
(ft)

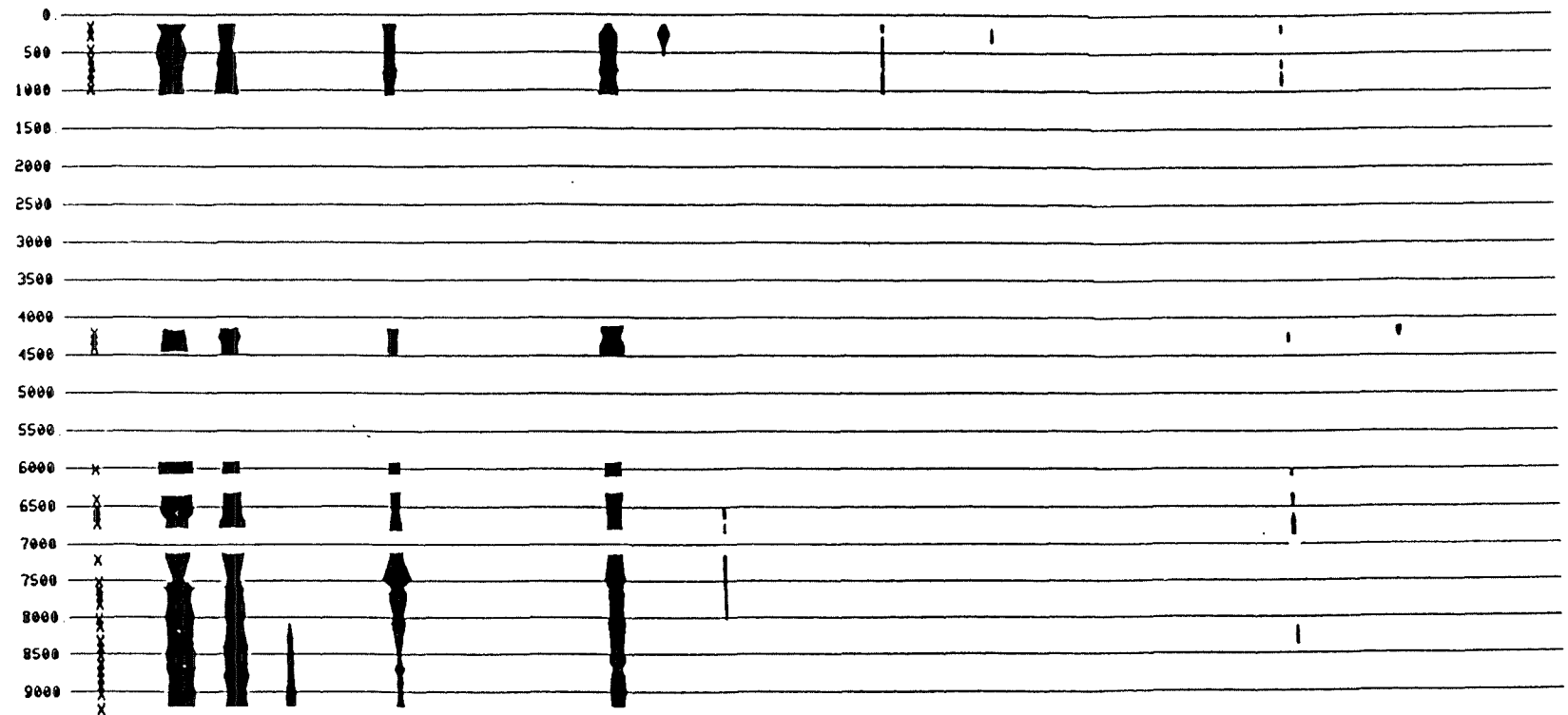


Figure 3

Figure 10. XRD spindle diagram showing the relative mineral abundances of shales from Geysers 2.

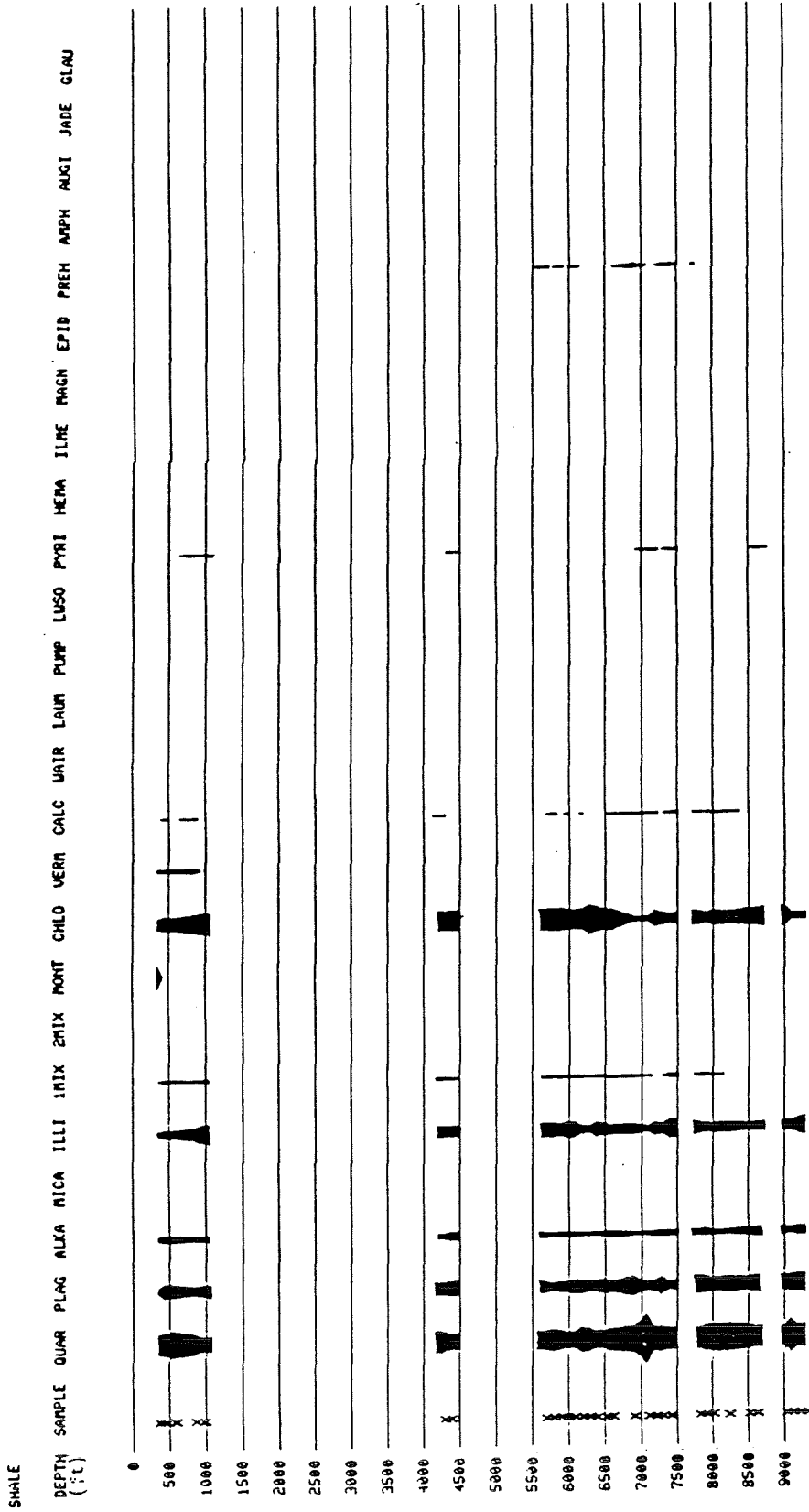


Figure 10

It is evident from the X-ray data that the sediments of the well Geysers 2 differ radically from those of Geysers 1. Firstly, the relative abundances of the phyllosilicates are appreciably greater -- particularly chlorite. The percentages of chlorite + illite are two to three times higher for the wackes of Geysers 2. Secondly, the chlorite is more enriched in magnesium. Thirdly, the ratios of quartz to plagioclase are lower, ranging from 1.5:1 to 1:1. Fourthly, the wackes and shales do not exhibit the relative homogeneity observed in the first well.

The prehnite is problematic. It has been identified by X-ray sporadically throughout the well, especially in the upper wacke block (0-305 m) but it has not been verified in thin section. A platy, highly birefringent micaceous mineral occurs in this block, commonly replacing either plagioclase or matrix phyllosilicates. This particular habit is dissimilar to phengite or lawsonite occurrences, but the classification of this mineral as prehnite requires microprobe analysis. Moore (1980) describes geothermal prehnite in The Geysers forming mono-mineralic veins or co-existing with epidote. The occurrences of prehnite and the unknown mineral in Geysers 2 are probably due to Franciscan regional metamorphism. Prehnite + pumpellyite + lawsonite assemblages in metagreywackes are described in the literature (Miyashiro, 1973) under the term "prehnite-pumpellyite facies." This assemblage has not been identified in the Franciscan terrains in the vicinity of The Geysers.

Ultramafic Strata

The serpentinite-ultramafic assemblage, 91-182 m, consists of three distinct lithologies. The most abundant of these lithologies appears greasy and dark green in cuttings and in thin section is composed of

massive mesh-structured "serpentine" veined with dolomite, calcite and quartz. Elliptical to sinuous pockets of chlorite, talc, fibrous tremolite and garnet are also present. XRD analysis shows that the "serpentine" has been replaced by interlayered chlorite/montmorillonite and chlorite/vermiculite. The second type, also dark green in hand sample, is composed of foliated fibrous to prismatic crystals of tremolite (<.03 mm) set in a matrix of fine-grained serpentine. Small disseminated clots (<.01 mm) of green epidote replace tremolite. The third type is cream to yellow in hand sample and, in thin section, is seen to be composed of the mesh-structured altered serpentine which has been extensively replaced (70 to 85%) by magnesite (-siderite) and minor dolomite. The magnesite was identified by XRD analysis.

Greenstone Strata

The sequence of greenstones in Geysers 2 spans 1400 m and consists of interbedded cherty volcanic rocks interrupted by a major (faulted?) wacke-shale parting between 1220 and 1340 m (see Figure 8). The greenstone block is abruptly bounded by greywacke strata of dissimilar lithologies. These contacts are inferred to be thrust faults. The greenstones can be divided into spilitic pillow basalts, micro-gabbros and pyroclastic. All are basaltic in composition and are metamorphosed to prehnite-pumpellyite facies assemblages. Minor (<1%) cross-cutting veins of calcite, chlorite, sulfides and quartz are ubiquitous secondary hydrothermal features at all depths. Systematic textural or mineralogical changes due to geothermal activity are absent.

The greatest proportion (95%) of volcanic material is amygduloidal vitrophyric basalt. Hand samples range from pale yellowish green to

grayish green, although a minor volume of red material is also present (see Figure 8). Amygdules containing chlorite and calcite and phenocrysts of plagioclase and pyroxene can be megascopically identified. A complete gradation of textural relationships from intersertal to holohyaline is observed in thin section. These textures represent core to rim transitions within pillow basalt suites (Bailey, 1964; Bamba, 1974; Swanson and Schiffman, 1979).

The primary phenocrysts are limited to plagioclase, clinopyroxene and titanomagnetite. Plagioclase is the dominant phenocryst constituting 65 to 100% of the crystalline mode. Crystals are typically euhedral. Albite twinning is common and zonation is absent. All grains are partially to extensively replaced by phyllosilicate minerals. Most feldspars are cloudy, dusty pseudomorphs consisting of fine grained albite, chlorite-group minerals, pumpellyite, sphene and minor iron oxides.

The predominant pyroxene is pale brown titaniferous augite which occurs as anhedral grains and as prismatic crystals. The grains are partially to extensively replaced by chlorite, sphene and iron oxides. A second pyroxene phase, a pleochroic green aegirine-augite (?) was observed at two depths. These pyroxenes are fresh, unzoned and appear primary in origin. The iron oxides occurs as euhedral crystals and dendritic growths of titanomagnetite in diabasic basalts and as microlites and crystallites in holohyaline basalts.

A common feature of the pillow basalts is amygdules of diverse shapes, dimensions and mineralogies which often contain various phases and textures. The majority of amygdules are rounded or oblate but

angular and arcuate cavities are not uncommon. The sizes range from less than .10 mm to over 2 mm in length. The three most common minerals are calcite, chlorite and pumpellyite. Locally abundant minerals and accessory minerals are silica, talc, zeolite (analcite?), actinolite and aragonite.

The basalts can be grouped into three classes based on phenocryst abundance. Diabasic basalts are the most common type and correspond to the greyish green cuttings. Textures range from intersertal to intergranular. Hyalopilitic basalts form pale green to yellowish green cuttings and typically have variolitic textures in thin section. XRD analyses of the diabases (analyses 2-16 to 2-22 on Table 3) and hyalopilitic basalts (analyses 2-9 to 2-14 on Table 3) are strikingly similar. Diabasic material tends to have higher percentages of chlorite and augite. Holohyaline material corresponds to glassy moderate green to dusky green cuttings. It is composed primarily of an opaque or cloudy granular chlorite matrix characterized by patches of fibrous pumpellyite and fresh chlorite in swirled and arcuate concentrations. Talc veins and microcrystalline quartz filled amydules occur only in holohyaline basalts.

A minor proportion of cuttings exhibit a dark dusky red coloration. These cuttings are concentrated at discrete depths (see Figure 8). These samples contain a high percentage of hematite at the expense of chlorite (see analyses 2-4 to 2-8 on Table 3). All pillow basalt textural varieties are observed in thin section but a bias toward holohyaline and hyalopilitic textures exists.

TABLE 3

Geysers 2 Volcanics

DEPTH (ft)	QUAR	PLAG	MICA	ILLI	IMIX	CHLO	CALC	ARAG	PUMP	HEMA	AUGI	PREH	AMPH	ANALYSIS
3000	1.9	17.9	14.2			28.7			14.6		22.6			2 - 1
5200	1.4	24.2	8.9			34.4			3.6		27.4			2 - 2
4500	9.1	49.1	31.9			.5						7.3	2.1	2 - 3
1110	3.5	28.3		12.5	2.9	4.9			9.0	27.4	11.5			2 - 4
1500	3.1	32.8		6.7	.6	11.0	17.7			28.2				2 - 5
2300	4.6	30.3		9.5		21.7		2.0	4.2	15.4	14.5			2 - 6
2300	4.6	28.9		11.1		16.1			6.0	17.7	15.6			2 - 7
4500	68.8	1.4		11.5		11.4				5.4	1.5			2 - 8
1900	2.0	35.3		5.8	.3	25.7	7.3		3.9		19.8			2 - 9
2300	2.2	42.7		9.0	1.8	21.3	3.3		3.6		16.1			2 - 10
2900	3.0	38.1		5.1		27.6			2.6		23.6			2 - 11
3600	5.6	43.4		4.0		23.5	4.9		1.5		17.1			2 - 12
3900	8.7	29.6		2.6		28.6			7.1		23.4			2 - 13
5000	6.9	41.8		2.0		25.1	4.3		4.5		15.4			2 - 14
2300	7.4	33.8		5.7		17.3			21.9		13.9			2 - 15
1000	7.5	42.9		4.9		17.3			4.8		22.5			2 - 16
1500	1.0	30.1		4.4		35.6	2.8		6.0		20.0			2 - 17
1900	5.5	32.3		1.8		36.0	5.9		4.2		14.3			2 - 18
2300	4.9	38.1		7.6		27.1			7.8		14.5			2 - 19
3600	14.1	26.7		3.0		39.7	2.0		2.5		12.0			2 - 20
3900	8.7	29.6		2.6		28.6			7.1		23.4			2 - 21
5000	6.3	25.2		3.7		34.8			7.2		22.8			2 - 22

Analysis: 2 - 1 and 2 - 2 = 2 pyroxene micro-gabbro; 2 - 3 = hornblende micro-gabbro; 2 - 4 to 2 - 8 = red volcanics (2 - 6 is vesicular); 2 - 9 to 2 - 14 = light green/yellowish green volcanics; 2 - 15 = pillow glass; 2 - 16 to 2 - 22 = dark green volcanics.

Two types of medium grained holocrystalline micro-gabbros are present. The sericitization of the plagioclase grains, in each type, is so pervasive that it is difficult to identify the laths in plane light while the mafic and opaque phases are relatively fresh and unaltered. The first variety of micro-gabbro is a two pyroxene ophitic gabbro (see analyses 2-1 and 2-2 on Table 3). Oikocrysts of colorless orthopyroxene (enstatite?) and pleochroic green clinopyroxene (Fe-rich augite?) range from 1.25 to 2.6 mm in diameter. Accessory titanomagnetite occurs as euhedral grains, skeletal polygons and dendrites. These grains have been altered to magnetite with perpendicular sets of rutile exsolution lamellae and rims of leucoxene. The second variety of micro-gabbro is a hornblende gabbro (see analysis 2-3 on Table 3). The basaltic hornblende forms stubby prisms ranging up to .14 mm and comprises up to 5% of the total rock. The plagioclase laths have been replaced by a matrix of albite and fine-grained prehnite and muscovite.

Minor amounts of tuffaceous material are interspersed throughout the volcanic sequence. The dominant type is composed of spherical globules of brown glass, less than .075 mm in diameter, which are either isolated in groundmass, or pale green chlorite and pumpellyite or partially accumulated into boytroidal aggregates. Less commonly, the tuff consists of angular blocks of devitrified dark green glass and equigranular angular fragments of seritized plagioclase (<.15 mm) set in a groundmass of silt, hematitic clays, granules of brown augite (<.05 mm), pale green chlorite and pumpellyite.

One cutting (1097 m) resembled a welded (andesitic) vitric tuff. The arcuate shards are compacted and flattened into a eutaxitic fabric.

Y-shaped and U-shaped shards were recognized. The shards are partially to extensively devitrified. Partially altered shards have a core of brown glass and an outer rim of fine-grained radiating fibrous material which may be chlorite. Completely devitrified shards have an axiolitic structure. Inclusions of plagioclase laths (up to .96 mm), fragments of hyalopilitic basalt, and intersertal plates of pale green chlorite are also present.

HYDROTHERMAL MINERALIZATION

Introduction

The differentiation of recent hydrothermal (low to high temperature - low pressure) minerals from Franciscan regional metamorphic (low to high temperature - high pressure) minerals from detrital material was often difficult. Authigenic minerals were distinguished from detrital clasts by their subhedral to euhedral morphologies. The recognition of authigenic minerals was facilitated by the dominance of fracture fill deposition in The Geysers. The identification of recent authigenic ("geothermal") mineralization deposited by the present geothermal system, which is the primary purpose of this report, was contingent upon subjective textural and mineral assemblage criteria.

The greywacke units encountered in Geysers 1 and 2, which were described in an earlier section, are basically non-shistose and are typical of low grade Franciscan metamorphism (textural zones 1 to 1.5 of Blake et al., 1967, and Ernst, 1971). Therefore, the expected regional metamorphic mineral assemblage is quartz, calcite, albite, chlorite, phengite, pumpellyite and lawsonite. Calc-silicates and alumino-silicates such as garnets, epidote, actinolite and sphene are restricted to high grade regional metamorphosed wackes and meta-basalts, whereas sulfides and potassium feldspar are absent (Blake et al., 1967; Ernst, 1971; Moore, 1980). Since these two minerals were identified in the wells studied, they must represent recent hydrothermal activity.

A major problem is to distinguish between the recent hydrothermal quartz, calcite, chlorite and white mica and their regional metamorphic equivalents. Some recent quartz and calcite veins were identified by the

presence of iron sulfide or adularia inclusions in thin section or by their unique stable isotope signatures. Significant transitions in clay crystallinity (disappearance of mixed layer illite and the appearance of micaceous illite) were observed in XRD analysis and can be attributed to recent hydrothermal activity. Chlorite, however, could not be differentiated by the analytical methods used in this study.

Celadonite occurring as fine-grained matrix patches and chlorite inclusions in quartz veins of a possible recent origin were recognized in the thin sections from lithologic unit 4 of Geysers 1. This unit, however, is of a higher regional metamorphic grade and may be of Franciscan origin. "Geothermal" chlorite was observed in fluid inclusion calcite chips (discussed in a later chapter) and by Moore (1980) in quartz veins. A systematic study of chlorite was not attempted as other easily discernable, very abundant minerals were present. Chlorite is not included in the detailed mineral descriptions or in the geothermal mineral assemblages, because of the problem of distinguishing hydrothermal from metamorphic chlorite.

The discussion of geothermal authigenic minerals will be divided into five sections. Section one is a compilation of the descriptive mineralogy of the silicates and carbonates. Section two describes the distribution of these minerals in Geysers 1 and 2. Section three is a compilation of the descriptive mineralogy of opaque ("ore") minerals. Section four describes the distribution of opaque minerals in the two wells. Section five is a discussion of the possible sources of the ionic species.

The bulk of the recognizable hydrothermal minerals in greywackes and greenstones from Geysers 1 and 2 were deposited in open fractures.

Porphyroblastic mineral growths are subordinant and grain overgrowths and replacement fabrics are minor or absent. Therefore, authigenic minerals are not observed in the majority of cuttings at any given depth. Where present, the minerals are locally concentrated and usually display sub-hedral to euhedral morphologies. Secondary mineralization is preferentially developed in wackes rather than shales. Less than 1%, by volume, of the shale cuttings are comprised of authigenic minerals whereas up to 20% of the wacke cuttings contain authigenic minerals.

Descriptive Mineralogy of Silicates and Carbonates

Quartz - Secondary quartz is the most abundant hydrothermal mineral in volume and number of occurrences. It is ubiquitous at all depths in both wells. Three varieties of authigenic quartz are recognized. Type 1 consists of massive cryptocrystalline veins and veinlets which are translucent grey or milky white. Type 2 is made up of blocky (some with drusy overgrowths) to coarsely granular vein material which is colorless to bluish white. Type 3, a very minor component primarily observed in Geysers 1, occurs as clear, euhedral quartz crystals sporadically throughout the wells. These vug-deposited crystals are concentrated between 805 m and 860 m in Geysers 1 and below 2440 m in Geysers 2. The largest whole crystal measured 8 mm in length (found at 457 m, Geysers 1) but the majority of crystals and crystal fragments are less than 2.5 mm. The fracture-fill quartz forms massive veins and veinlets and zoned veins, ranging in cross-section width from .01 mm to 3 mm.

In thin section, the veins are composed of densely-packed, equant, polygonal, mosaic grains. The larger veins are symmetrically zoned. Smaller grains line the fracture walls and coarser-sized grains protrude

irregularly toward the center of the fissures. Commonly, open spaces in the vein centers have been subsequently infilled by coarse grained, optically continuous plates of calcite. Cross cutting veins are common. Quartz cuts quartz, calcite cuts quartz, but quartz was never observed cross-cutting calcite.

Calcite - Calcite is subordinate only to vein quartz in abundance but locally may be more voluminous, especially in the greenstone strata. Calcite is present in the upper sections of the well but disappears by 940 m in Geysers 1 and 2650 m in Geysers 2. As with quartz vein material, calcite occurs in a variety of colors and crystalline habits that reflect crystallization conditions and pore space availability. Massive, fine-grained material is pure white to bluish white but may be tinted orange by iron oxide. Blocky rhomboidal calcite and bladed aggregates are greyish white to colorless.

In thin section, the veins are composed of large, optically-discontinuous, mosaic plates up to .35 mm across. Cleavage planes are locally well-developed. Finer-grained crystals are equant, interlocking, scalloped grains. Calcite veins postdate quartz veins but are generally orientated parallel or subparallel to them. Composite and crustified calcite/quartz veins are well-developed between 500 and 670 m. Calcite veins exhibit injection and replacement textures. Pinch and swell, and chambered veins are also common in this depth range.

Adularia - Potassium feldspar is recognized by X-ray analysis but it is impossible to identify in thin section unless stained. Adularia occurs as minute, spherical to barrel-shaped beads less than .01 mm. A few grains grow to .01 mm and are rhomb-shaped. It is found as disseminated grains

in chlorite plates, as linear veinlets in calcite and quartz veins sub-parallel to the wall rock, and as isolated stringers and aggregates in silty matrix material. The adularia crystallizes in large aggregates up to .15 mm but the individual feldspar granules retain their characteristic bead-like morphologies. Adularia is present at all depths of Geysers 1 but is restricted to strata below 2380 m in Geysers 2.

Sphene - Sphene occurs as spherical nodules and elongate rods less than .01 mm in length. Sphene crystallizes in the phyllosilicate matrix, particularly the felty pumpellyite-phyllosilicate mats. It is commonly intergrown with or attached to pyrite grains and carbonaceous material. In Geysers 1, sphene first appears at 580 m associated with pyrite aggregates and as isolated matrix porphyroblasts at 680 m. It is present as a minor but persistent accessory mineral in the air drilled cuttings. In Geysers 2, it first occurs under similar conditions at 2285 m.

Green Epidote - Green epidote forms porphyroblastic crystals in the phyllosilicate matrix and never as veins. This weakly pleochroic green calc-silicate primarily replaces the felty pumpellyite mats in the wacke matrix and, in a few isolated examples, the pumpellyite intergrowths in plagioclase grains. Pockets and mats of clay-rich phyllosilicates are also affected. The green epidote crystallizes as small spherical granules less than .5 mm and as massive angular xenoblastic plates and aggregates of sub-hedral prismatic crystals, up to .15 mm. Although it resembles clinozoisite in thin section, microprobe analyses (see Table A-10) indicate that it is a magnesium bearing epidote (magnesium replaces calcium) with a pistacite composition of 20-25%. The average composition is $\text{Ca}_{1.89}\text{Mg}_{.06}\text{Fe}_{1.0}\text{Al}_{2.30}\text{OH}[\text{Si}_{3.03}\text{O}_{11}]$. Green epidote is the dominant or only epidote

between 713 m and 860 m in Geysers 1 and persists in trace amounts (<1%) in the air drilled cuttings down to a depth of 1200 m.

Yellow Green Epidote - This epidote differs from the green epidote by its color, mode of occurrence and composition. The yellow green epidote occurs only as a fracture-fill vein mineral and is always associated with quartz. It is the dominant calc-silicate in Geysers 1 below 880 m and is the sole epidote mineral in Geysers 2. The crystalline habits range from blocky anhedral mosaic aggregates to aggregates composed of intergrown euhedral (often zoned) prismatic crystals. Prismatic crystals are less than .2 mm and the aggregates are less than .45 mm.

The yellow green epidotes of Geysers 1 (see Table A-11) have a composition that is calcium rich and have a pistacite component ranging from 16 to 22%. The average composition is $\text{Ca}_{1.98}\text{Fe}_{.59}\text{Al}_{2.45}\text{O OH}[\text{Si}_{2.96}\text{O}_{11}]$. The first appearance is at 854 m. The yellow green epidotes of Geysers 2 have a very similar composition but has a higher pistacite component (see Table A-11). The average composition is $\text{Ca}_{1.99}\text{Fe}_{.67}\text{Al}_{2.39}\text{O OH}[\text{Si}_{2.98}\text{O}_{11}]$. The first appearance is at 2440 m.

Garnet - Garnet is encountered in three cuttings in Geysers 2 at 2774 m and 2835 m. It occurs as rounded yellow to pale yellow brown nodules, less than .015 mm, enveloped in massive epidote. The chemical composition (see Table A-12) is pure andradite. Angular, pale yellow isotopic grain fragments are observed in Geysers 1 between 975 m and 1220 m that are assumed to be equivalent in composition to the andradite in Geysers 2.

Diopside - Diopside is present only in the air drilled cuttings of Geysers 1 between 1220 m and 1440 m as strongly pleochroic green crystals

and crystalline fragments. Similar to the crystalline habits of the yellow-green epidote, the diopside forms blocky anhedral mosaic aggregates, and rarely euhedral columnar grains. X-ray analysis and optical properties indicate that it is diopsidic in composition, but this mineral has not been microprobed. Diopside comprises between 1 and 5% of the cuttings when present.

Tremolite-Actinolite - Colorless, isolated columnar crystal fragments and fibrous bladed aggregates of amphibole are present in the air drilled material of Geysers 1 below 1250 m. Optical properties ($2V = 88-90$) distinguish this mineral as tremolite. X-ray analysis cannot differentiate its composition which has not been verified by microprobe analysis. This amphibole is present in trace amounts comprising less than 2% of the cuttings.

"Pumpellyite" - An authigenic bladed aggregate of an unknown blue green mineral occurs once at 762 m in Geysers 1. The aggregate is 1.5 x .8 mm in diameter and appears to be composed of a single homogeneous phase. The crystal habit and optical properties are typical for pumpellyite but the chemical composition (analyses 4 to 6 on Table A9) and corresponding structural formula does not resemble those reported for pumpellyite (Deer, Howie and Zussman, 1965; Schiffman and Liou, 1979).

The unknown is richer in magnesium and more deficient in calcium than any other pumpellyite analysis. The deficiency in calcium in the W-site could theoretically be compensated by the substitution of magnesium (Schiffman and Liou, 1979). Thus, it is possible that the unknown is pumpellyite.

Distribution of Silicates and Carbonates

Geysers 1

The vertical distribution of hydrothermal minerals in Geysers 1 is partially controlled by the previously described lithologic units. Figure 11 exhibits the distribution of geothermal minerals. The first appearances of several minerals coincides with the contact between lithologic blocks. The relative abundances of the major hydrothermal minerals are recorded in the XRD data tables (Tables A-2, A-3, and A-4) with the exception of quartz which is masked by detrital quartz. The calcite can be interpreted as being geothermal in origin as stable isotope data (discussed subsequently) does not indicate the preservation of Franciscan calcite.

The three most common vein minerals are quartz, calcite and adularia. Authigenic quartz is the most abundant in number of occurrences and in volume and it comprises 2-10% of the total rock at any given depth. Calcite is a very common vein mineral, especially at shallow depths (0-200 m). A decrease in vein size and occurrence is noted below 640 m and calcite disappears by 975 m. Adularia is found in trace amounts in wackes at all depths but there exists a gap between 180 m to 396 m where adularia deposition is extremely sparse. The percentages of adularia increases with depth achieving concentrations of 5-10% of total rock in lithologic unit 5.

Calcite (3%), quartz (2%), and adularia (~1%) veining is prevalent throughout lithologic units 1 and 2 (0-300 m). Calcite and adularia occurrences decrease drastically in the upper strata of lithologic unit 3 and quartz veining is also reduced to approximately 1%. Beginning at

Figure 13. Plot of sphalerite compositions from Geysers 1 vs temperature compared with composition curves for sphalerite in equilibrium with pyrite or pyrrhotite.

Scott and Kissin Experimentally determined composition curve.

Browne Curve generated from microprobe data from Broadlands Geothermal Field, New Zealand.
 Averaged composition of analyses 1, 2, 3 from Table A-16.
 Analysis 4 from Table A-16.
 Averaged compositions of two grains:
 analyses 5 and 6; analyses 7 and 8;
 from Table A-16.

Temperatures are based on fluid inclusion data (Figures 16 and 17). Modified from Scott and Kissin (1973); Browne and Lovering (1973).

The disseminated grains are idiomorphic to subidiomorphic cubes ranging from .01 mm to .33 mm with an average size of .05 to .1 mm. Grains in shale clasts and matrix are commonly porous with minor inclusions of rutile, sphene, clays and organic matter. Pyrite idiomorphs associated with quartz veins, deposited either as localized well rock alteration or free-floating inclusions, tend to be non-porous and non-corroded, indicating equilibrium with the fluid. The general distribution of disseminated grains in microwackes and wackes are random and unorientated.

The aggregates are botryoidal, to massive, oblate aggregates characterized by polygonal outer margins. Intergranular mosaic contacts are usually not distinguishable. The axial length of these concentrations range from .2 mm to 1 mm, the largest aggregate being 1.2 x 0.4 mm.

Two types of monomineralic pyrite veins can be recognized. The first type are fissure-fill veins, that, in rare instances, grade into lenticular chambers. The vein geometries are prominent tabular or sheeted bands, generally less than .5 mm across, characterized by sharp subparallel margins. Stratiform (parallel to bedding planes) examples are observed, but most randomly dissect the wacke fabric. The individual grains are well-defined polygonal interlocking mosaic plates. The fissure-fill veins occur in wacke and shale lithologies. In most cases, fissure-fill veins are the only occurrence of sulfides in shales.

Fissure-fill veins with significantly larger dimensions, 1 to 3.45 mm, are observed in impermeable strata -- particularly the greenstones of Geysers 2. They are also observed in the shales of Geysers 1 and 2. These veins are commonly brecciated by randomly orientated fractures (less than

The primary marcasite is invariably intergrown with pyrite and comprises between 30-35% of the iron sulfide in the upper volcanic host rocks. It forms late stage growths within, and/or, enclosing subidiomorphic pyrite porphyroblasts that have precipitated vugs or open fractures. The marcasite is observed as polygonal or rectangular plates (less than .05 mm) concentrated on the outer margins of the pyrite host. More commonly it occurs as subidiomorphic columnar overgrowths radiating outwards from the pyrite core. These grains grow up to .15 mm in length and are characterized by well-developed lamellar twinning. Gangue is rarely present and is exclusively quartz.

In the lower zone, marcasite is present as minor encrustations on the boundaries and along fractures of pyrrhotite. This marcasite morphotype forms massive extremely fine-grained (less than .01 mm) unoriented aggregates. This replacement reaction product is rare, affecting less than 1% of the pyrrhotite population and usually occurs in environments where pyrite is present. In one instance, fine-grained marcasite developed as a buffer between type 1 pyrrhotite and pyrite.

Galena - Galena exhibits a dual morphology that mimics sphalerite. Galena occurs as rounded granular mosaic grains (<.15 mm) associated with type 2 pyrrhotite. Galena platelets are disseminated within the pyrrhotite aggregates as opposed to the lateral segregation pattern of chalcopyrite and sphalerite.

Galena within the iron sulfide poor zone (800-880 m) occurs as massive monomineralic veins, <.175 mm, and as plates and exsolved blebs intergrown with sphalerite. Boundaries with sphalerite are simple curvilinear, interlocking contacts.

gular and prismatic grains and also linear chains of interlocking grains. Both types are situated either in the center of the vein or pushed against the fracture walls. Individual grains are less than .22 mm in length and vein types are less than .25 mm wide.

The pyrrhotite species are often difficult to identify due to natural variations in reflectance and anisotropy caused by random crystallographic orientation. Type 1 exhibits a dark pink reflectance in plane light and an average reflectivity of 34% in air. Anisotropism is moderate, with a reflectance transition from lavender grey to dark grey. Individual grains may display simple twinning and aggregates tend to be optically continuous. Type 1 pyrrhotite occurs in a wide variety of morphologies: pyrite replacement products, veins, and matrix-supported aggregates, and it is associated with calcite gangue.

Type 2 pyrrhotite has a lighter creamy pink reflectance and a slightly higher reflectivity of 37%. Anisotropism is strong, changing from light grey to lavender. It occurs almost exclusively in fracture-fill veins that are monomineralic or as linear chains in quartz gangue. These veins are characteristically composed of granular mosaic interlocking grains which are equant to lobate in shape.

The chemistries of the two pyrrhotite species are nearly identical (see Table A-14). The probe data of type 1 pyrrhotite are from a pyrrhotite+chalcopyrite aggregate set in calcite gangue which originated at 610 m. The type 2 pyrrhotite analyses are from a pyrrhotite+sphalerite vein (no gangue) also occurring at 610 m. Iron and sulfur percentages coupled with fluid inclusion geothermometric data (discussed in following sections) indicate that both pyrrhotite types have hexagonal crystal structures (Scott and Kissen, 1973). X-ray data is unavailable.

irregular in shape - the largest grain being .05 x .02 mm. Hematite needles (less than .015 mm), with random orientations, are intergrown with the bornite.

Rutile - Inclusions of rutile and sphene are commonly observed in pyrite grains in both wells. At certain depths in Geysers 1, isolated cubic grains of rutile less than .20 mm are present. The grains occur as idiomorphs in the matrix phyllosilicates and incorporated in both calcite and quartz.

Distribution of Opaque Minerals

Geysers 1

The opaque minerals in Geysers 1 consist primarily of sulfide minerals with a minor component of rutile, a titanium oxide. Iron oxides such as hematite and magnetite are not present. The distribution of the opaque minerals is displayed on Figure 14. The sulfides can be divided into two groups based on zoned distributions, mineral compositions and associated gangue minerals. Group I sulfides (see Figure 11) are sulfides deposited by fluids which can be characterized by relatively high sulfur fugacities. The primary species are pyrite, sphalerite and galena. Group II sulfides (see Figure 11) are sulfides which were deposited by fluids with low sulfur fugacities or low pH. The primary forms are pyrrhotite and marcasite.

The group I minerals are the dominant sulfide group and can be divided into two assemblages: pyrite±quartz±rutile±sphene and sphalerite+galena+chalcopyrite±quartz crystals. The pyrite assemblage is effectively bracketed by the major shale partings at 400 m and 670 m. The pyrite initially occurs in trace amounts as idiomorphic randomly

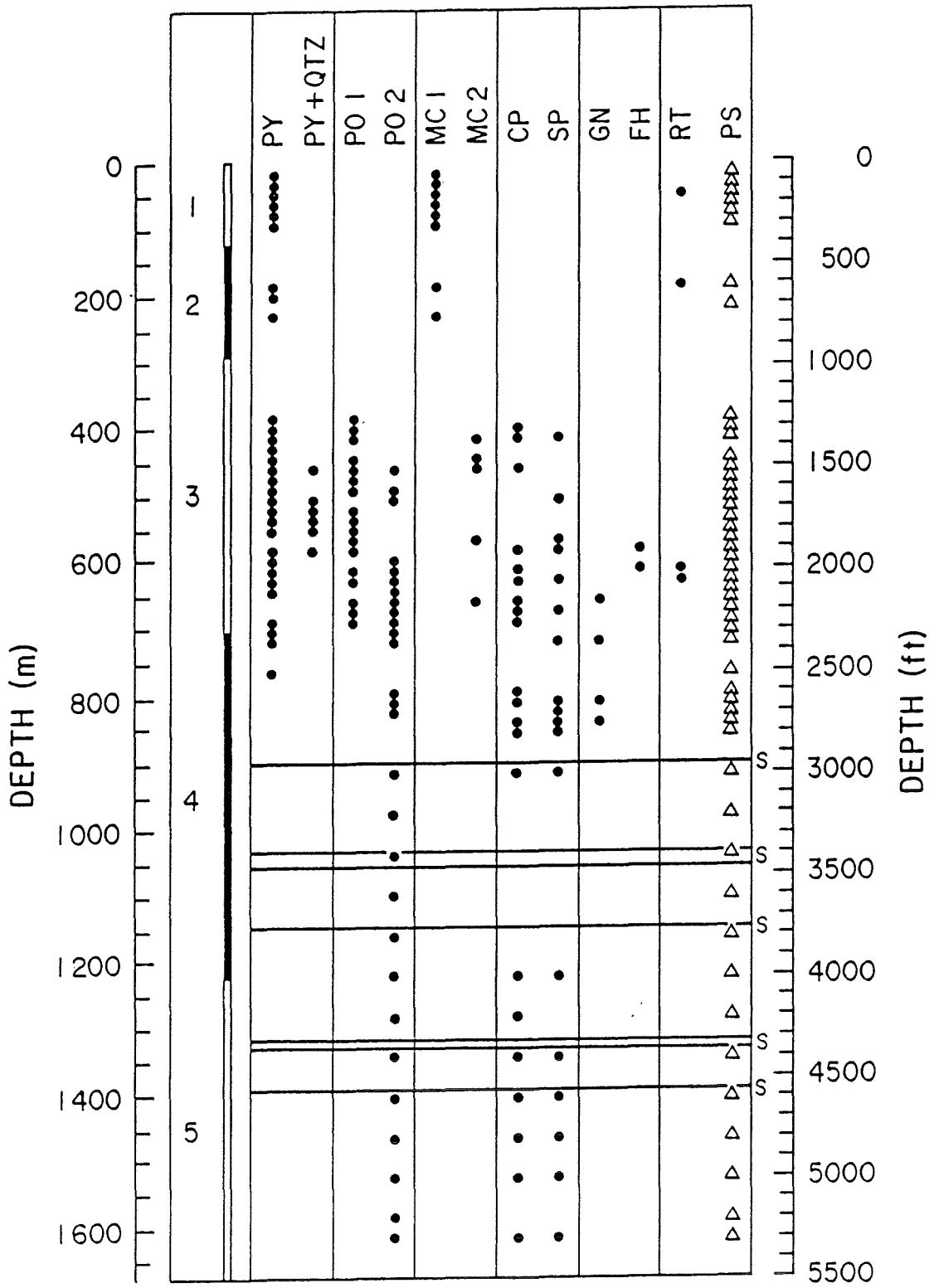
.4 mm from a large pyrrhotite aggregate (see analyses 1-3 on Table A-14). Analysis 4 is from a sphalerite grain occurring in a type 2 pyrrhotite vein (see analyses 4 to 7 on Table A-14). Analyses 5 and 6 are from a sphalerite grain originating at 825 m containing 15% exsolved chalcopyrite blebs and analyses 7 and 8 are from a sphalerite grain at 825 m characterized by 3% exsolved chalcopyrite.

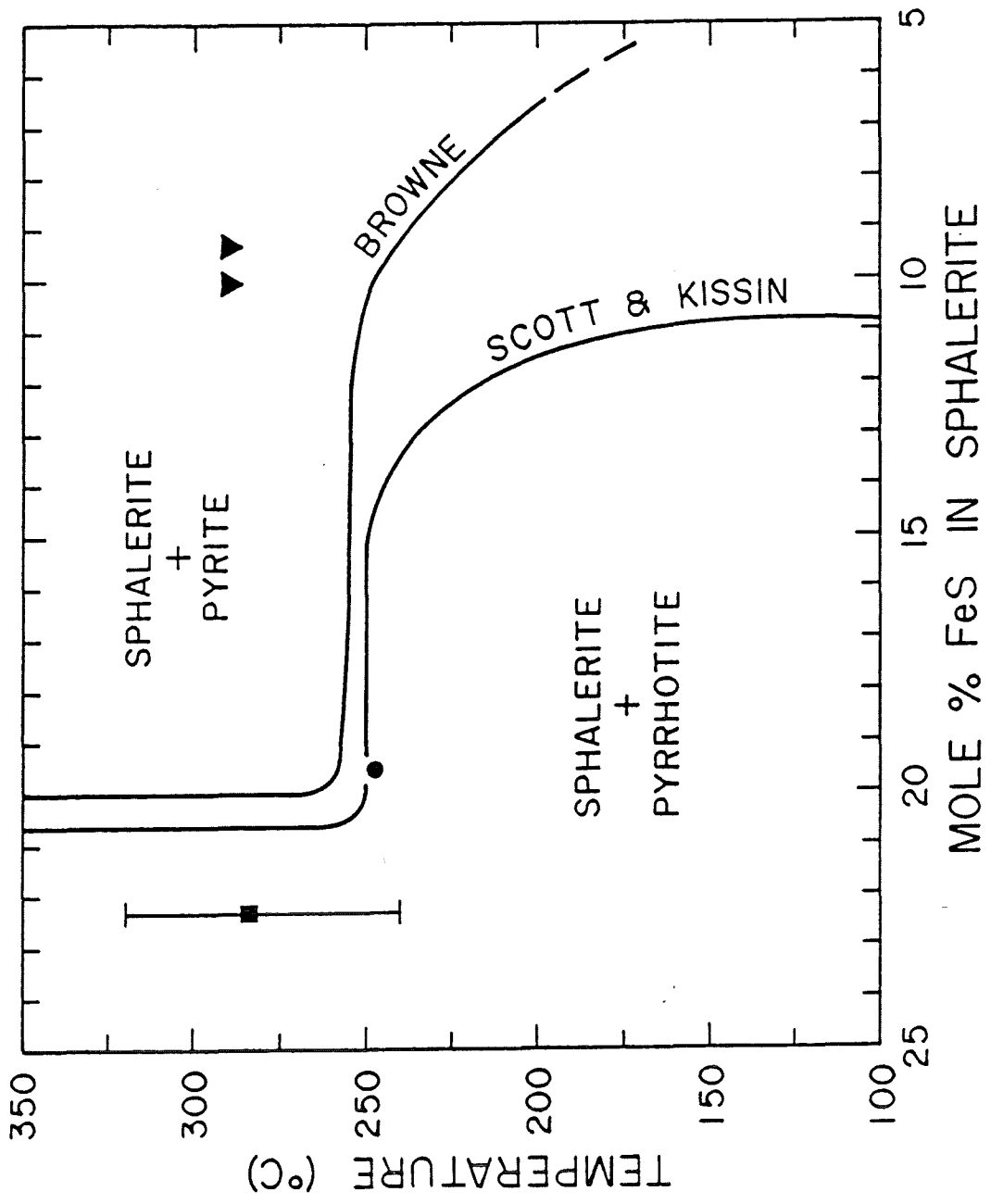
It is evident that these sphalerites represent at least two (possibly three) periods of sulfide deposition. The sphalerites from 825 m have half the iron and greater cadmium contents than these associated with pyrrhotite but are otherwise closely related. Gross similarities exist between the sphalerites from 598 m. The grain associated with the type 2 pyrrhotite is relatively enriched in copper and iron and deficient in zinc.

Figure 13 is a graph of the Fe/Zn ratios of these sphalerites plotted on a TX diagram. The temperatures are inferred from averaged fluid inclusion homogenization data collected at the appropriate depths and from gangue minerals (calcite vein, quartz vein, and quartz crystal) associated with the sphalerite grains. It is clear that the upper sphalerites are in equilibrium with pyrrhotite while the lower sphalerites are in equilibrium with pyrite.

Analyses 1 and 2 on Table A-15 are the compositions of two chalcopyrite grains that flank the sphalerite grain analyzed in analyses 1-3 on Table A-16. It exhibits a minor contamination by zinc.

Marcasite - Marcasite is observed as a primary phase and as a secondary replacement mineral. The primary marcasite is restricted in distribution to the shallow depths of Geysers 1 and the greenstones of Geysers 2. The secondary marcasite is observed in Geysers 1 between 400 and 700 m.





The sphalerite assemblage occurs in localized concentrations between 805 and 860 m, 1340 and 1400 m, and at 1615 m. The absolute abundances of sphalerite+galena+chalcopryrite are less than 1% of the total rock at these levels but only trace amounts or single isolated grains are observed at other depths. It should be noted that galena, while prevalent between 805 and 860 m, was not identified in the air drilled material due to its strong resemblance to stray fragments of drill iron. The crystal textures and the presence of quartz crystals infers these minerals formed in open fractures.

The sphalerite compositions (see Figure 13 and associated discussion) indicate this assemblage was probably cogenetic with the pyrite, although a co-existing iron sulfide is not observed. A strong thermal gradient may account for the observed zonation. The peculiar sphalerite habit (ex-solved chalcopryrite blebs), the co-existing quartz crystals and the micro-probe compositions are identical to sphalerite crystallization in the Broadlands geothermal field (Browne, 1969; Browne and Lovering, 1973). In Broadlands, base metals sulfides without a corresponding iron sulfide phase are observed at depth under the measured conditions of 270°C and 120 bars pressure (Browne and Lovering, 1973).

The Group II sulfides can be divided into three assemblages. These are: (1) pyrite+marcasite±rutile+quartz±calcite±adularia; (2) type 1 pyrrhotite+chalcopryrite+sphalerite(±gersdorffite)+calcite and (3) type 2 pyrrhotite+sphalerite+chalcopryrite+galena+quartz. Each assemblage is restricted to characteristic zones.

The pyrite+marcasite assemblage is found in the shallowest portion of the well (0-230 m) and is primarily restricted to lithologic unit 1.

Minor Sulfides and Oxides - Fahlore (tetrahedrite-tennantite solid solution) occurs as monomineralic veins. It was observed twice in Geysers 1. The largest occurrence has an overall rectangular distribution of .43 x .07 mm. The reflectance is a light olive grey, inferring that the mineral is dominantly tetrahedrite. Scattered pyrite grains (<.01 mm) incorporated in the lattice display framboidal (bacterial) structures indicative of localized dissolution. It can be assumed that the fahlore is contemporaneous with the pyrrhotite deposition.

Gersdorffite is found in only one cutting originating at a depth of 640 m in Geysers 1. While the chemistry of this rare white mineral has not been verified, its identification is based on reflectivity, hardness and characteristic parallel cleavage planes. The gersdorffite occurs as blocky to irregular shaped grains less than .07 mm in length which are orientated in discontinuous linear bands in calcite gangue. Sphalerite and pyrrhotite are also present as isolated grains and as intergrown aggregates with the gersdorffite.

Hematite is encountered at three depths in Geysers 2. Two occurrences of veined hematite at 945 and 1097 m are incorporated in quartz gangue. The hematite forms massive blocky aggregates and stringers of columnar subhedral to euhedral grains. The largest aggregate is 1.3 x 1.6 mm and is composed of mosaic interlocked plates averaging .1 x .06 mm. Twinning lamellae are common. Minor disseminated exsolution blebs (less than .05 mm) of magnetite (?) are observed. The third occurrence at 183 m is a small cluster of bornite grains and hematite needles replacing a spinel grain. The bornite grains are rounded to

encountered as monomineralic pyrrhotite veins, veinlets and fracture-fill replacing matrix material and less commonly occurs as pyrrhotite+base metal aggregates in quartz gangue. The relative abundances of the sulfide phases are type 2 pyrrhotite 98%, sphalerite 1%, galena <1%, chalcopyrite <<1% and fahlore <<1%. The fahlore has been included with this assemblage because it forms monomineralic veins similar to type 2 pyrrhotite. It also, like other occurrences of type 2 pyrrhotite, resulted in the intensive localized destruction of pre-existing pyrite grains.

The type 2 pyrrhotite assemblage is ubiquitous in trace amounts at all depths below 900 m (the air drilled segment). The occurrences are sparse between 800 and 1400 m, but become more abundant between 1200 and 1460 m and again at 1615 m. It is especially abundant, comprising almost 1% of the total rock, at 1340 m and 1402 m. This behavior parallels the localized concentrations of group I sulfides in lithologic unit 5, except that pyrrhotite is more common and more evenly distributed throughout this zone.

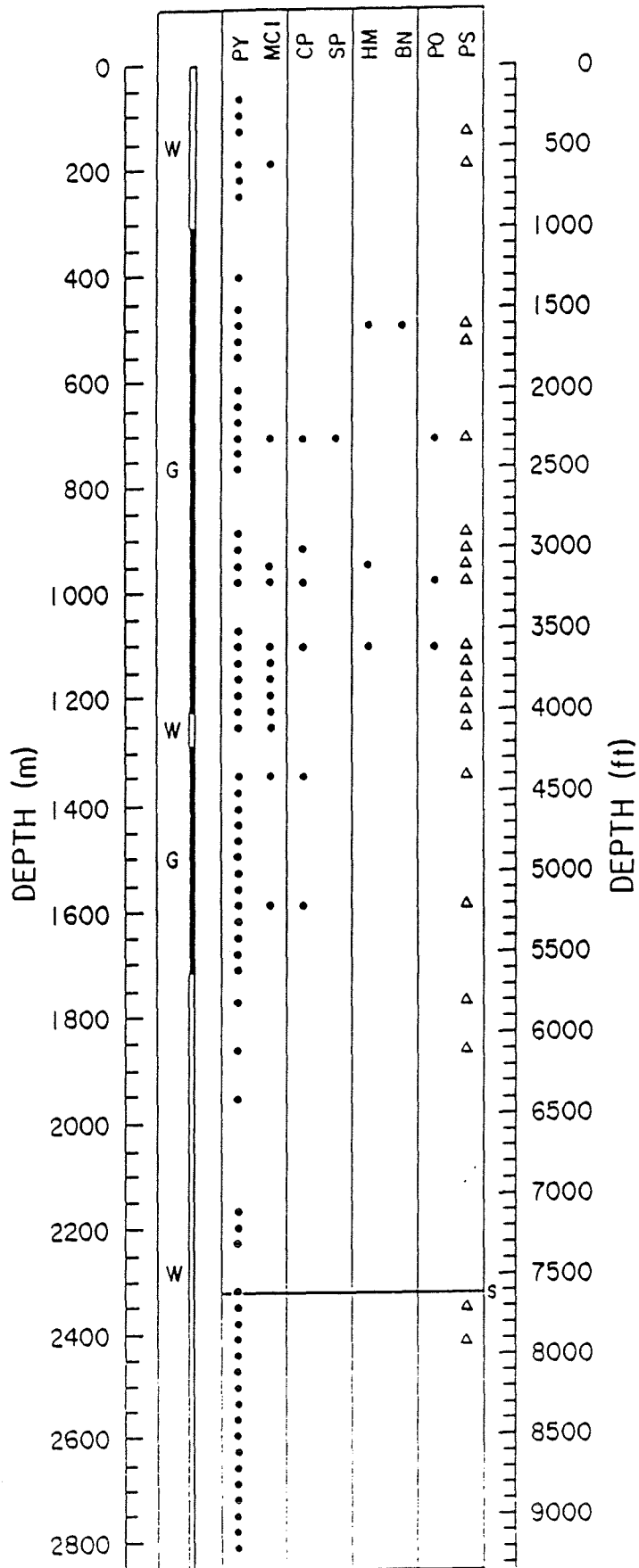
Geysers 2

The opaque mineral deposition in Geysers 2 lacks the pyrrhotite development observed in Geysers 1. Pyrite is the dominant iron sulfide phase and is common throughout the well (see Figure 15). The sulfide and oxide mineral phases are present in the following percentages: pyrite 90%, marcasite 10%, chalcopyrite <<1%, hematite <<1%, bornite <<1%, pyrrhotite <<1% and sphalerite <<1%.

All sulfides are hydrothermal in origin as the primary opaque minerals incorporated in the greenstones are titanomagnetite and spinel, and pyrite has not been recognized in the Franciscan metasediments as

Figure 14. Distribution of opaque minerals vs depth in Geysers 1.

PY	Pyrite
P01	Type 1 pyrrhotite (calcite gangue)
P02	Type 2 pyrrhotite (quartz gangue)
MC1	Primary marcasite
MC2	Secondary marcasite
CP	Chalcopyrite
SP	Sphalerite
GN	Galena
FH	Fahlore (tetrahedrite-tennantite)
RT	Rutile
PS	Polished section



disseminated cubes in meta-stable shale clasts. With increasing depth, pyrite develops in the orthomatrix, forming subidiomorphic to irregular crystals due to the variable matrix partitioning between framework grains. With increasing depth the abundance of pyrite steadily increases until pyrite constitutes 3-4% of the total rock between 550 and 640 m. At these depths, disseminated idiomorphic grains are pervasively distributed in shales, as well as wackes, and there is minor replacement of stable framework grains (particularly feldspars) by idiomorphic pyrite. Also, localized botryoidal aggregates of pyrite extensively to completely replace shaly clasts; orthomatrix gaps and fracture-fill veins are common. fracture-fill veins are common and there is minor replacement of stable framework grains (particularly feldspars) by idiomorphic pyrite.

The lower boundary of pyrite occurrence is distinguished by a rapid transition into a zone of pyrite destruction that coincides with the maximal pyrrhotite deposition. Individual grains are altered by desulfurization and dissolution into framboidal or bacterial aggregates. Replacement by pyrrhotite (type 1) is observed but is uncommon. At 550 m the destruction process is minor and localized to calcite veins or pyrrhotite contacts. By 640 m the framboidal alteration is extensive and pervasive. Framboidal pyrite, in trace amounts, occurs down to a maximum depth of 790 m.

The sphalerite assemblage begins abruptly at 800 m and persists throughout the lower interval of the well (see Figure 14). The assemblage consists of sphalerite (characterized by chalcopyrite blebs)+galena±chalcopyrite±quartz crystals. The sulfides occur as monomineralic veins and as intergrown multi-phase aggregates.

(0-300 m), pyrite (and trace marcasite) is restricted to sporadic veined occurrences always enveloped in quartz gangue. In the lower wacke strata (1700 m to total depth) all occurrences of sulfides consists of disseminated idiomorphic cubes of pyrite with localized aggregated clusters identical to Assemblage I in Geysers 1. Massive mosaic veins are extremely rare. Pyrite is most common in depths corresponding to calcite and calc-silicate authigenic mineralization (2200 m to total depth). Pyrite, however, is present only in trace amounts (<1/2%).

Sources of the Ionic Species

The primary mode of crystallization of the authigenic minerals is precipitation in open fractures - veins and veinlets. These minerals include quartz, calcite, adularia, yellow-green epidote, andradite, tremolite, diopside, base metal sulfides and pyrrhotite. Minor porphyroblastic mineral growth is observed in the silty, fine-grained phyllosilicate orthomatrix in the greywacke. These minerals are pyrite, sphene, adularia and green epidote. The carbonate and calc-silicate assemblages observed in vein occurrences are rich in calcium and magnesium and are iron deficient. The authigenic mineralogies of some well-studied geothermal systems (Salton Sea and Cerro Prieto) are generally enriched in iron. The epidotes in these areas have higher pistacite values, amphiboles are actinolitic and the pyroxenes are diopside-hedenbergite (Elders *et al.*, 1978; McDowell and Elders, 1980). Authigenic minerals in The Geysers correspond better with metamorphic mineral assemblages derived from limestone terrains (Winkler, 1979; Miyashiro, 1973).

All major ions which are found in observed authigenic minerals in The Geysers - Mg, Ca, Si, Fe, K, Al, S, Zn, Cu, and Pb - are available

These minerals constitute less than 1% of the total rock. The sulfides are found as veins, veinlets, and disseminated idiomorphic grains. Gangue is not commonly present and is most commonly quartz. Marcasite makes up approximately 30% of the assemblage and, as described in the mineralogy section, occurs as secondary overgrowths on earlier precipitated pyrite. Marcasite is never observed without pyrite, although pyrite grains frequently do not contain traces of marcasite. All occurrences at 200 m are large brecciated veins and aggregated vug fillings.

The assemblages containing the two pyrrhotites and associated base metal sulfides were deposited during a later event or period of activity which is in chemical and thermal disequilibrium with the pre-existing pyrite grains. This is evidenced by the localized destruction and replacement of pyrite grains that were either enveloped by the intruding ore-bearing fluids or are within a thermal aureole, a few tenths of millimeters wide, surrounding veins and mineral aggregates.

The type 1 pyrrhotite is restricted in distribution between 380 m and the shale parting at 670 m. All occurrences of these sulfides are incorporated within calcite gangue. Commonly, the pyrrhotite grains are dispersed between calcite plates or along cleavage planes. The type 1 pyrrhotite assemblages comprise less than 1% of the total rock at any given depth but characteristically form large aggregates measuring up to 2 mm across. The effects of localized contact-metasomatism of pyrite are minimal. With this assemblage type 1 pyrrhotite constitutes 95%, chalcocite 3%, sphalerite 2%, gersdorffite <<1% of the sulfides.

The type 2 pyrrhotite assemblage first occurs at 460 m but the major influx occurs at 590 m to the bottom of the well. This assemblage is

phases identified by Moore (1980) (prehnite and tourmaline) are attributed to a predominantly Ca-Mg-Fe-Al-Si rich solution under prograde metamorphic conditions.

The predominance of calcite and sedimentary phyllosilicate sources for ions in the hydrothermal solution is supported by two additional observations. First, that the chemical composition of steam is high in methane, boric acids, ammonia, and carbon dioxide (White *et al.*, 1971; Ellis and Mahon, 1977). These species are characteristic of sedimentary sources (Nehring, 1981; Ellis and Mahon, 1977). Secondly, with the exception of a single report (Steiner, 1958), wairakite has not been observed in The Geysers (McNitt, 1961; Lambert, 1977; Moore, 1980). This is presumably due to the instability of zeolite in solutions with high CO_2 to H_2O ratios. In environments with moderate to high μCO_2 , greenschist assemblages form at relatively low temperatures (200°C), and zeolite facies minerals are excluded (Liou, 1971; Frost, 1980).

Figure 15. Distribution of opaque minerals vs depth in Geysers 2.

PY	Pyrite
MCI	Primary marcasite
CPY	Chalcopyrite
HM	Hematite
BN	Bornite
PO	Pyrrhotite
PS	Polished section

Sample Preparation

Representative cuttings of vein material, quartz and calcite were ground using 240 grit paper and polished with 5 μ alumina paste on silk. Prepared chips were analyzed on a heating/cooling stage mounted on a Nikon binocular microscope. Homogenization and freezing data were collected utilizing procedures described by Freckman (1978). The accuracy of the heating measurements are $\pm 2^{\circ}\text{C}$ (Freckman, 1978; this study) and $\pm .25^{\circ}\text{C}$ for freezing measurements (Freckman, 1978; Miller, 1979).

The chips proved to be difficult to work with due to (1) the small size of the chips; (2), the fine-grained nature of the vein material; (3) the propensity of the chips to shatter along cleavage planes and contacts between multiple veining events (discussed in a later section); and (4) thermal deformation incurred during homogenization.

Generally, the calcite and quartz chips contained abundant vacuoles yet relatively few were large enough to analyze. 85% of the measured fluid inclusions were less than 30 microns (averaging 12.5 to 20 microns) in length and vapor bubbles occupied only 7-15% of the inclusion area. The remaining inclusions ranged from 30 to 157 microns with an average length of 60 microns.

The homogenization temperatures were exceedingly high and exceedingly variable in different inclusions within a single chip. Heating to 50-60 $^{\circ}\text{C}$ above the homogenization temperatures caused the irreversible stretching and stress of the vacuole walls. Many leaked fluid, although none decrepitated. This deformation caused measured homogenization temperatures in inclusions allowed to cool to room temperatures to be irreproducible, and the tendency towards abnormally high measured homogenization temperatures

a diagenetic or regional metamorphic mineral. Furthermore, the sulfides seldom constitute more than 1/2% of the total sample at a given depth and gaps in the column, in which no sulfides are found, are common.

The opaque minerals are best-developed in the greenstone strata, taking into account the relative volume of material and the variety of phases. Sulfide and oxide deposition is restricted to open fractures and vugs and associated gangue material, calcite and minor quartz is minimal. The highest concentration of opaque minerals occurs between 900 and 1300 m where marcasite comprises up to 30% of the iron sulfide present.

Three assemblages are recognized in the greenstone strata. These are hematite+quartz, hematite+bornite and the dominant assemblage of pyrite+marcasite±chalcopyrite±pyrrhotite±sphalerite. The hematite-bearing assemblages are rare and are restricted to the upper 1100 m of the well. They occur at the same depths as the pyrite+marcasite assemblage, but are never observed to coexist nor even appear in the same rock chip. Pyrite forms massive veins, often brecciated, up to 1.5 mm. Isolated idiomorphic grains are rare, although densely packed subhedral to euhedral grains precipitated on probable fracture walls are not uncommon. Marcasite occurs as radiating prismatic or lamellar overgrowths on pyrite, optically continuous reaction rims replacing pyrite (especially along fractures) or as polygonal inclusions within pyrite aggregates. Chalcopyrite, pyrrhotite and sphalerite occur as late stage veinlets infilling fractures in brecciated pyrite veins.

Sulfide minerals in the metasedimentary rocks of Geysers 2 have similar crystalline habits to those in Geysers 1. In the upper wacke block

Figure 16. Calcite fluid inclusion homogenization temperatures
(uncorrected) from Geysers 1.

Range of temperatures (—————)

Modal mean temperatures ———+—————

The multiplicity of modal temperatures is due to the wide range of temperatures at each depth (up to 100°C), disparities between mean temperatures of different chips, and the apparent bimodal distribution of temperatures within individual chips. This can best be observed in Figures A-1 and A-2, where the temperature data from individual chips are differentiated. I interpret this distribution pattern to represent the superposition of multiple vein-filling events. The multiple modal mean temperatures displayed in Figures 16 and 17 are subjective divisions of the data to reflect changes in fluid temperature with time.

in the host rocks. No major contribution is required from a new magmatic source. Ca can be derived from pre-existing calcite as well as from plagioclase grains. Mg, Fe, Si and Al can be derived from volcanic chlorite, pumpellyite, volcanic glasses, ultramafic rocks (serpentinites) and sedimentary phyllosilicates. The sulfide constituents, S, An, Cu and Pb, can be leached from shaly material, phyllosilicates and carbonaceous material (Vaughan, 1976; Saxby, 1976). And finally, potassium can be derived from the Franciscan shale beds which exhibit appreciable potassium-feldspar concentrations at all depths as determined by X-ray analysis (Tables A-3 and A-6; Figures 6 and 10).

Disseminated pyrite precipitated directly from the reaction of the metal species dissolved in the thermal fluids with the carbonaceous material and organic-rich shaly material by the "thermal cracking" of organic matter catalyzed by clay minerals (Saxby, 1976; Bemer, 1970). Green epidote appears to replace pumpellyite mats in the greywacke and is consequently enriched in magnesium, iron and titanium in comparison to the fracture-filling yellow-green epidote (see Tables A-10 and A-11).

Thus the solutions that precipitated authigenic minerals could have been derived from the dissolution and decomposition of appropriate source materials (especially calcite) at depth in the presence of heat, water and carbon dioxide. These dissolved species precipitated minerals in fractures as a function of localized temperature, pressure, oxygen and sulfur fugacities, mole fraction CO_2 , and the availability of various ionic species according to source-rock type. Thus, all observed mineral phases in Geysers 1 and 2 (see Figures 11 and 12) in addition to the

bearing abnormally high vapor percentages (disregarding obviously necked examples) are absent. Co-existing water-filled and vapor-filled inclusions would be direct evidence of subsurface boiling (Roedder, 1979; Roedder et al., 1974). These inclusions appear to be normal hydrothermal inclusions formed under a water-dominated condition.

Solid inclusions are not uncommon and are found in the majority of the calcite chips. Stringers, veinlets and irregular masses of yellow-green chlorite are found in chips originating at or below 335 m that possess mean temperatures of 220°C or greater. Epidote is first observed at 610 m in a chip with a mean temperature of 250°C and is found in all chips at deeper depths. One chip, at 713 m and a mean temperature of 318°C, contained abundant dendritic (cruciform) growths of an unknown green mineral whose coloration strongly resembled diopside crystals encountered at 1220 m. Quartz fluid inclusion chips very rarely contained solid inclusions and the material was epidote.

Salinity measurements are sparse. Only four inclusions from a depth of 2000 ft (300 m) were sufficiently large to permit analysis. The calculated salinities are listed in Table 4. More than 20 freezing runs were attempted on chips representing several depths without success. Qualitatively, all inclusions displayed low salinity behavior (compared to personal experience of analyzing Salton Sea and Cerro Prieto fluid inclusions).

The polymodal distributions and extremely broad temperature spreads at several depths are significant features of the hydrothermal activity at The Geysers. Freckman (1978) and Roedder et al. (1974) reported temperature variations among primary inclusions of 30-50°C to be common.

FLUID INCLUSION GEOTHERMOMETRY

Introduction

Fluid inclusion geothermometry is a useful tool in the determination of prevailing temperatures and salinities of paleo-hydrothermal regimes. The literature is rich with fluid inclusion studies of ore deposits, especially those of Mississippi Valley-type deposits (Roedder, 1976). In the last ten years several studies of geothermal systems have utilized fluid inclusion geothermometry in conjunction with other temperature determination techniques. Roedder et al. (1974) observed that fluid inclusion temperatures correlated well with borehole temperatures at Broadlands. Freckman (1978) and Elders et al. (1978) determined that fluid inclusion temperatures concur with borehole temperatures and stable isotope temperatures at the Salton Sea and Cerro Prieto, Mexico, respectively.

Methodology

Briefly stated, the methodology is as follows. A fluid inclusion (or vacuole) is a small pocket of fluid (vapor or brine) trapped by growth irregularities in a crystal growing in a fluid medium (Roedder, 1979). Upon cooling, the fluid will contract, separating into liquid and vapor phases. If the vacuole is heated, under controlled conditions, the vapor bubble will disappear, indicating its homogenization temperature (Roedder, 1962). Additional correction factors for depth and salinity added to the homogenization temperature will yield the temperature of trapping (Roedder, 1963; Potter, 1977). The salinity of the fluid inclusion is determined by freezing the vacuole, reheating, and observing the melting temperature as the last piece of ice melts. The salinity is then mathematically calculated from the melting temperature (Potter et al., 1978).

The variations in Geysers 1 are 60-100°C. As described above, the chips are subject to brittle behavior during cleaning procedures or heating runs. Each of these individual fragments represented a limited thermal regime. A good example is the distribution of temperatures at 250 m (Figure 16). It is clear that this represents an aggregate of superimposed veining events.

Two distinctive thermal regimes are recorded. Homogenization temperatures above 700 m are all below the hydrostatic boiling curve for pure water (with the exception of the inclusions at 110 m). Above 700 m the main body of data range between 215 and 200°C with temperatures increasing downwards. This linear trend is significant in The Geysers steam field. In 1963, McNitt measured downhole steam temperatures utilizing a thermocouple. The wells located in the Big Geysers area sampled the shallow steam reservoir at depths between 100 and 300 m (Truesdell and White, 1973). All wells had pressures between 6 and 10 bars with an average of 8 bars and temperatures that ranged from 180 to 210°C with an average of 195°C. Thermal 7, at 300 m, had recorded temperatures of 210°C. In comparison, the calcite in Geysers 1 give fluid inclusion temperatures at 335 m of 210°C. It can be inferred that the bulk of the shallow calcite fluid inclusions formed in equilibrium with the steam cap at a descending boiling interface between the vapor and liquid phases.

Homogenization temperatures below 700 m either span the boiling curve or are above it. These are minimum values as no pressure corrections were applied to the filling temperatures. Adding a hydrostatic pressure factor would add only 3-5°C at these shallow depths (Potter, 1977) and it is apparent that unknown overburden pressures could have been

towards the end of analysis sessions. This problem was minimized by measuring all the inclusions in a chip in a single session and culling spurious high or low values. Only those inclusions which best fit the criteria for primary inclusions (Roedder, 1979) were selected for analysis.

Similarly, the freezing of the inclusions caused damage to the crystalline envelope. This effect is due to the small size and low salinities of the inclusions (Roedder, 1976). Several chips which were singled out for freezing before heating analyses, to prevent decrepitation of the large inclusions, subsequently yielded dubious homogenization temperatures. These data were not incorporated in the graphed figures but are noted in the table of salinities. Due to the low salinities of the entrapped fluids, only those inclusions larger than 50 microns were suitable for freezing studies.

Results for Geysers 1

Calcite

Approximately 70 chips of calcite vein material were prepared. Of these, only 17 chips representing nine depths contained measurable fluid inclusions. A total of 275 homogenization temperatures were measured (see Figure 16). Many depths display a bimodal or polymodal distribution of temperatures. This pattern is based on homogenization temperatures between different chips and also within single chips (see Figure A-1).

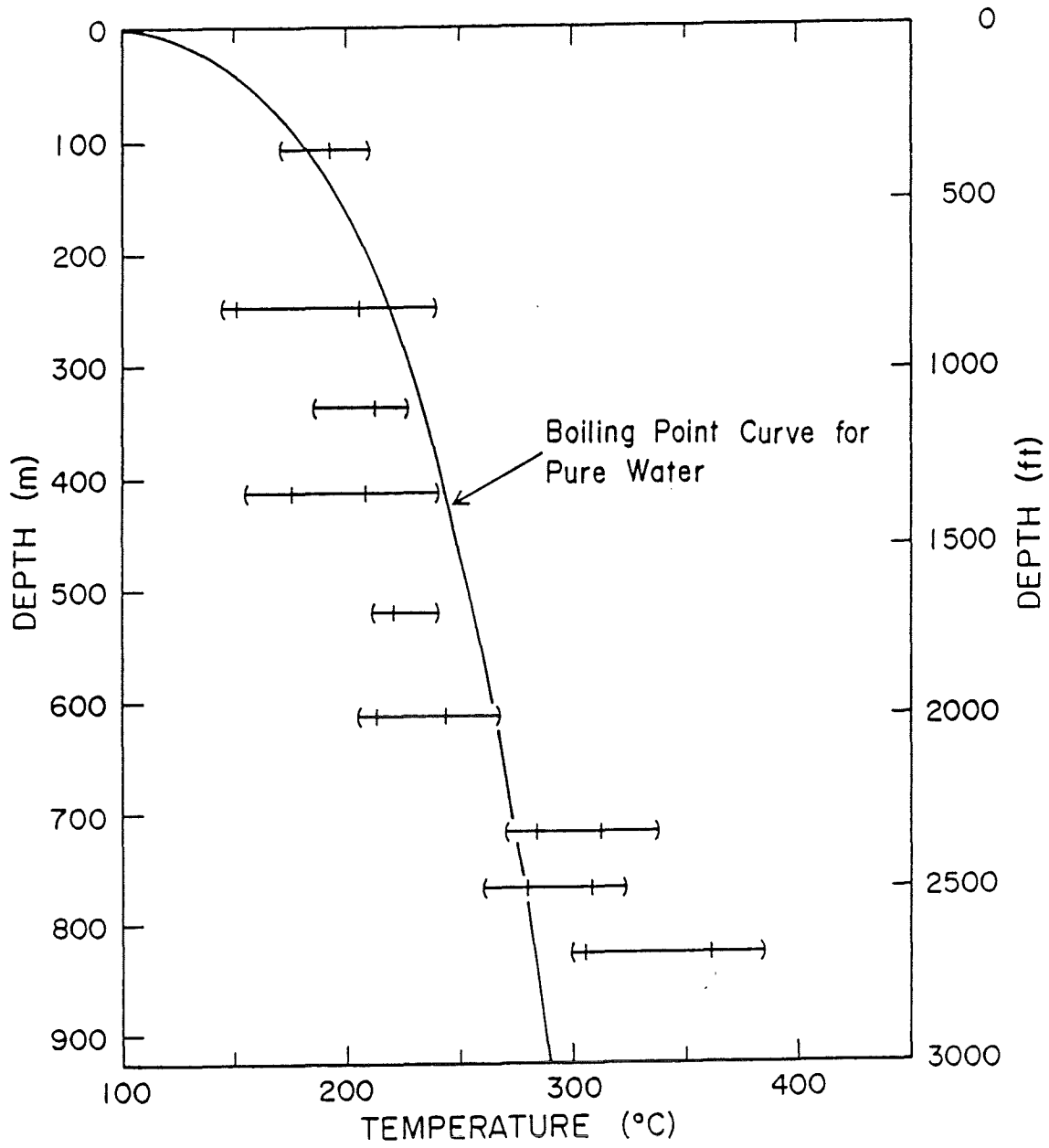
The inclusions display thin, shallow rectilinear to polygonal geometries typical of calcite. The vapor bubbles are relatively small, occupying an average of 7-15% of the vacuolar area. A slight increase in vapor bubble size (approaching 20%) is observed as a function of increasing temperatures, but vapor-dominated inclusions or inclusions

Figure 17. Quartz fluid inclusion homogenization temperatures (uncorrected) from Geysers 1. Note A and B represent measurements of inclusions from 840 m. A is massive vein material. B is quartz crystal material.

Range of temperatures (—————)

Modal mean temperatures ———+—————

The multiplicity of modal temperatures is due to the wide range of temperatures at each depth (up to 100°C), disparities between mean temperatures of different chips, and the apparent bimodal distribution of temperatures within individual chips. This can best be observed in Figures A-1 and A-2, where the temperature data from individual chips are differentiated. I interpret this distribution pattern to represent the superposition of multiple vein-filling events. The multiple modal mean temperatures displayed in Figures 16 and 17 are subjective divisions of the data to reflect changes in fluid temperature with time.



The mean quartz homogenization temperatures consistently plot above the boiling point curve for water at all depths. No fluid inclusions indicative of quartz in equilibrium with a steam phase were seen. However, the quartz data extend the apparent geopressurized environment up to a depth of 300 m, 400 m higher than the calcite data indicate.

Two types of quartz chips were analyzed from 840 m depth (see Figure 17). These were milky-white massive vein material (upper line) and two clear euhedral quartz crystals (lower line). The modal temperatures correspond well, indicating that either these phases crystallized from a single event or that they formed under similar temperature conditions. Unfortunately, only the salinities for the massive vein quartzes could be determined.

The size and clarity of the quartz chips were more conducive to successful freezing analysis than were the calcites. Fourteen salinities were calculated from four chips representing three depths (see Table 4). Salinities are distinctively low and decrease with depth. Salinity differences between 820 m (av = .55% NaCl equiv.) and 610 m (av = 1.17% NaCl equiv.) are twofold. This is further evidence for multiple vein events or stratification of water chemistries.

Results for Geysers 2

Fluid inclusion data from Geysers 2 is sparse. Seven calcite chips representing seven depths between 945 and 1830 m were analyzed (see Figure 18). Temperatures range from 120 to 300°C with a definite increase of temperature with depth. Few data plot between 180 and 205°C, which is the range of temperatures determined by Lambert (1977) to be characteristic

TABLE 4
Fluid Inclusion Salinities

<u>Mineral</u>	<u>Depth (ft)</u>	<u>T_M* (°C)</u>	<u>Wt% NaCl</u>	<u>T_H** (°C)</u>
Calcite	2000-20	-.59	1.028	ND
		-.59	1.028	
		-.49	.852	
Quartz	2000-20	-.71	1.23	309
		-.31	.54	
		-.64	1.13	
		-.77	1.34	
		-.72	1.25	
		-.54	.94	
		-1.28	2.22	
		-.54	.94	
		-.54	.94	
	2540-60	-.26	.45	298
		-.51	.90	
	2740-60 A	-.31	.54	299
		-.26	.45	
	2740-60 B	-.38	.67	293

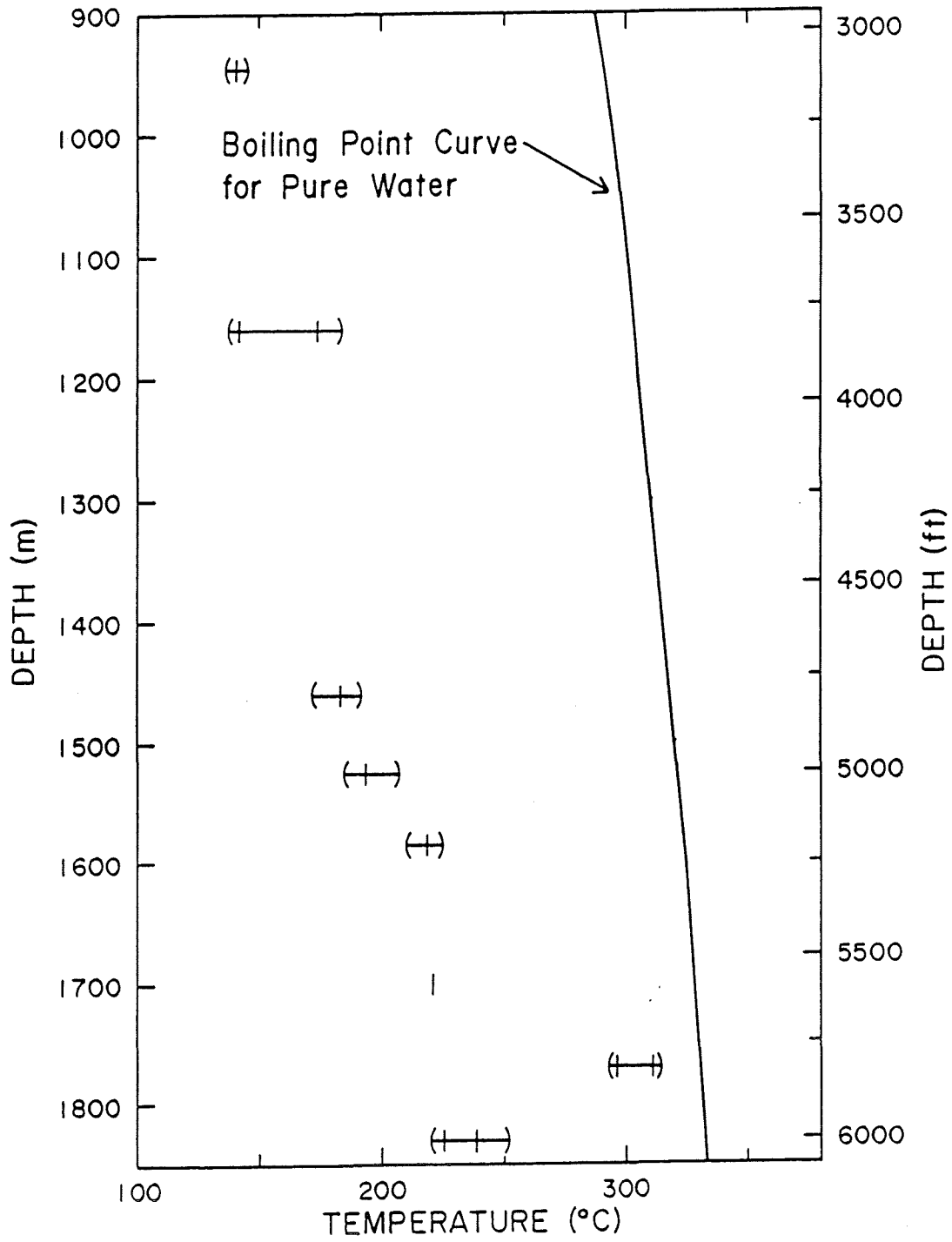
*T_M = Melting Temperature

**T_H = Homogenization Temperature

ND = Not determined due to vacuole
damage during freezing runs

2740-60 A = Milky-white massive vein quartz

2740-60 B = Clear euhedral quartz



present at the time of formation. The temperature of 315°C at 710 m implies a geopressured environment of 135 bars and pressures greater than 200 bars are necessary for the 360°C temperature observed at 820 m. To achieve the temperature of 315°C, without boiling, would require either a column of pure water of 1400 m, implying 690 m of erosion, or a fluid salinity of 25 wt % NaCl equivalent (Haas, 1971). Neither situation is feasible considering the local geology and that the observed salinities for quartz and calcite inclusions in this study are low. A more reasonable hypothesis is that the lithostatic overburden geopressed the fluid. Mechanisms that contribute toward a geopressed environment will be discussed in a subsequent section of this report.

*2. 1000
res. on 100
to 1000 m
calcites are
formed at 1000*

Quartz

3). Approximately 60 chips of quartz vein material and quartz crystals were prepared. Twelve chips representing five depths yielded 177 homogenization temperatures (see Figure 17).

The vacuole geometries are oblate spheroidal to irregular multi-lobed cavities. The percentages of vapor to fluid averaged 5 to 10% by volume (12 to 25% of apparent surface area). Vapor-dominated inclusions were not observed indicating water-dominated formation.

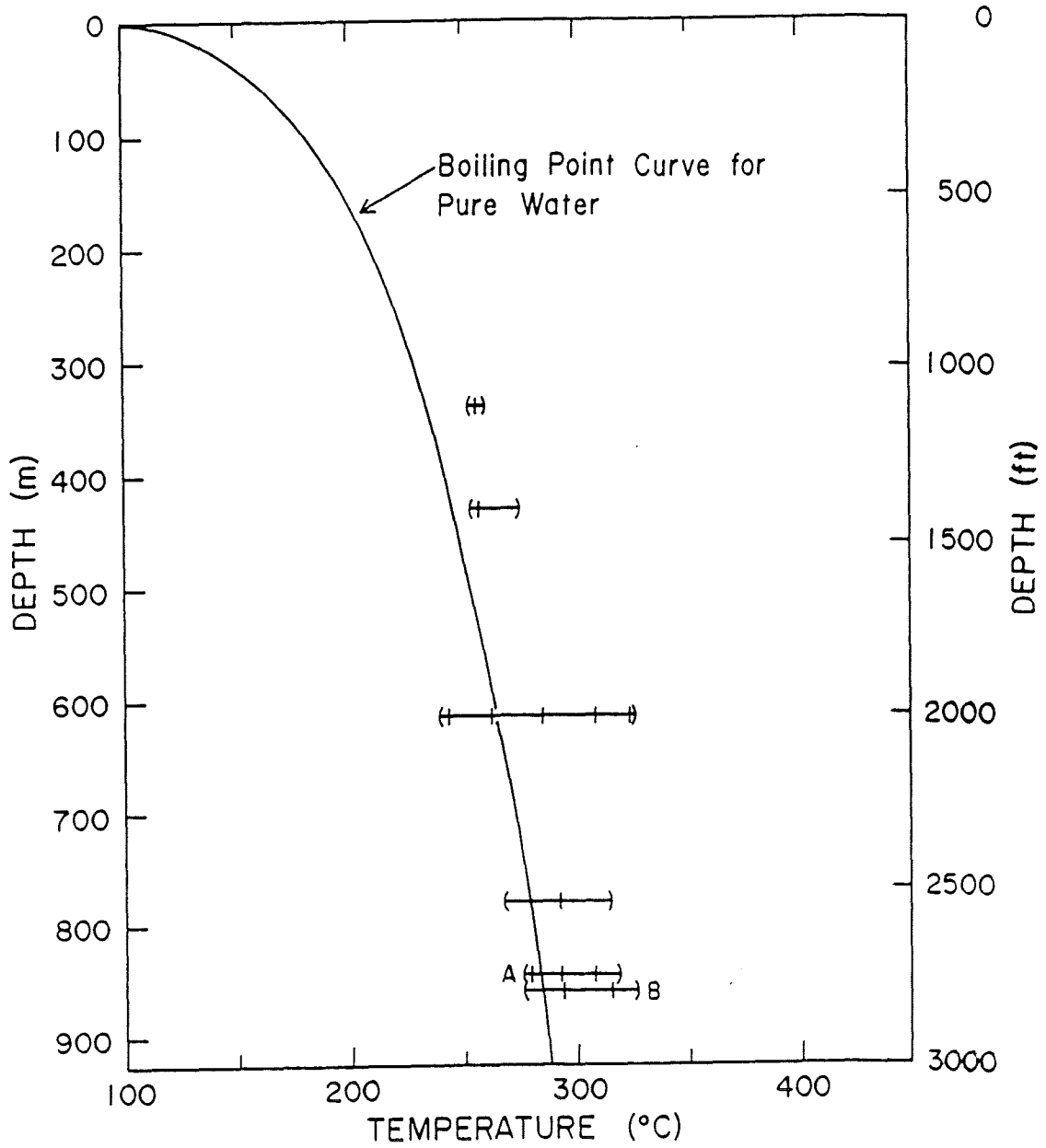
The variation of homogenization temperatures at a given depth display polymodal distributions similar to the calcites. However, the temperature range is relatively limited, exhibiting a spread of 30-50°C. The exception is the distribution at 610 m. Its spread approaches 100°C with values that resemble a composite of calcite temperatures from 610 and 715 m.

STABLE ISOTOPE GEOCHEMISTRY

Introduction

Hot water is a major agent of thermal metamorphism and the primary constituent of mineral forming fluids in hydrothermal systems. This is because water is an extremely effective solvent for most ionic solids of geologic interest. The isotopic geology of oxygen species, because oxygen is the dominant element in water and rock-forming minerals, displays systematic variations that reflect thermal and chemical reaction histories. Oxygen isotopic information can be obtained from the circulating water or steam in geothermal reservoirs, authigenic mineral phases recovered from cuttings and core, and whole rock analyses. Stable isotope analyses provide information about the source and direction of flow of the hydrothermal fluids, temperatures of formation of the mineral phases, volumetric evaluations of water-rock interaction and the equilibrium or disequilibrium relationships between mineral assemblages (O'Neil, 1979; Taylor, 1967).

The heavy isotopic species of oxygen and carbon, ^{18}O and ^{13}C respectively, are disparately distributed in naturally occurring phases on the earth's crust. $\delta^{18}\text{O}$ relationships in meteoric waters have been described by Craig (1963) and those in igneous rocks by Taylor (1969). $\delta^{13}\text{C}$ variations in various rock types and organic materials are summarized by Fritz (1976). Deviations, due to isotopic fractionation, from these pristine states are initiated by several types of chemical reactions and physical processes (Faure, 1977). Selected reactions which occur in geothermal systems are: isotopic exchange of an element between different phases (vapor-liquid; liquid-mineral) containing that element, evaporation



Since the fractionation factor is related to the equilibrium constant of the isotopic exchange reaction which is a function of temperature, measured isotopic ratios can be manipulated to calculate paleotemperature.

Two widely accepted oxygen isotopic geothermometers have been developed and tested in the 0-500°C temperature range. Δ Quartz-water is:

$$10^3 \ln \alpha = 2.78 (10^6 T^{-2}) - 2.89 \quad (\text{Clayton, O'Neil and Mayeda, 1972}).$$

Δ Calcite-water is:

$$10^3 \ln \alpha = 3.38 (10^6 T^{-2}) - 2.90 \quad (\text{O'Neil, Clayton and Mayeda, 1969}).$$

To apply these thermometers it is necessary to know the δ -value of the vein material and the δ -value of the depositional solution. The brine which deposited minerals is accessible for analysis in active geothermal fields such as the Salton Sea or Cerro Prieto. However, in the Geysers field, the hydrothermal fluid responsible for mineralization is not available and must be calculated by independent means. Alternately, if two oxygen bearing minerals were deposited from the same brine under equilibrium conditions, the difference between their $\delta^{18}\text{O}$ values would be approximately equivalent to α . Thus quartz and calcite can be utilized by the following equation:

$$\delta^{18}\text{O}_{\text{QUARTZ}} - \delta^{18}\text{O}_{\text{CALCITE}} = .6 (10^6 T^{-2}).$$

Previous Work

In the past 20 years, several authors have analyzed various surficial waters and steam samples at The Geysers. Craig (1963) and White, Barnes, and O'Neil (1973) reported meteoric waters near The Geysers to have $\delta^{18}\text{O}$ (SMOW) values that clustered closely between -7.0 and -8.0 ‰ and δD values of approximately -50 ‰. Steam $\delta^{18}\text{O}$ values were fractionated 6 ‰ to -2 ‰ although δD remained constant. Craig concluded that the present steam was originally of meteoric origin. $\delta^{13}\text{C}$ values for CO_2 in steam

Figure 18. Calcite fluid inclusion homogenization temperatures
(corrected for hydrostatic pressures) from Geysers 2.

Range of temperatures (————)

Modal mean temperatures ———+————

Limited core fragments from two Magma-Thermal wells gave quartz-calcite pair temperatures of 245° to 250°C and coupled with whole rock $\delta^{18}\text{O}$ analyses of the host wacke indicated extremely low water-rock ratios (.15 mass ratio) based on $\delta^{18}\text{O}$ of local meteoric waters.

Sample Preparation

Samples of silicate and carbonate vein material from selected depths were hand-picked for analysis. All samples were washed with distilled water to remove contaminants. The silicate material was then reacted with dilute HCl to eliminate carbonate debris.

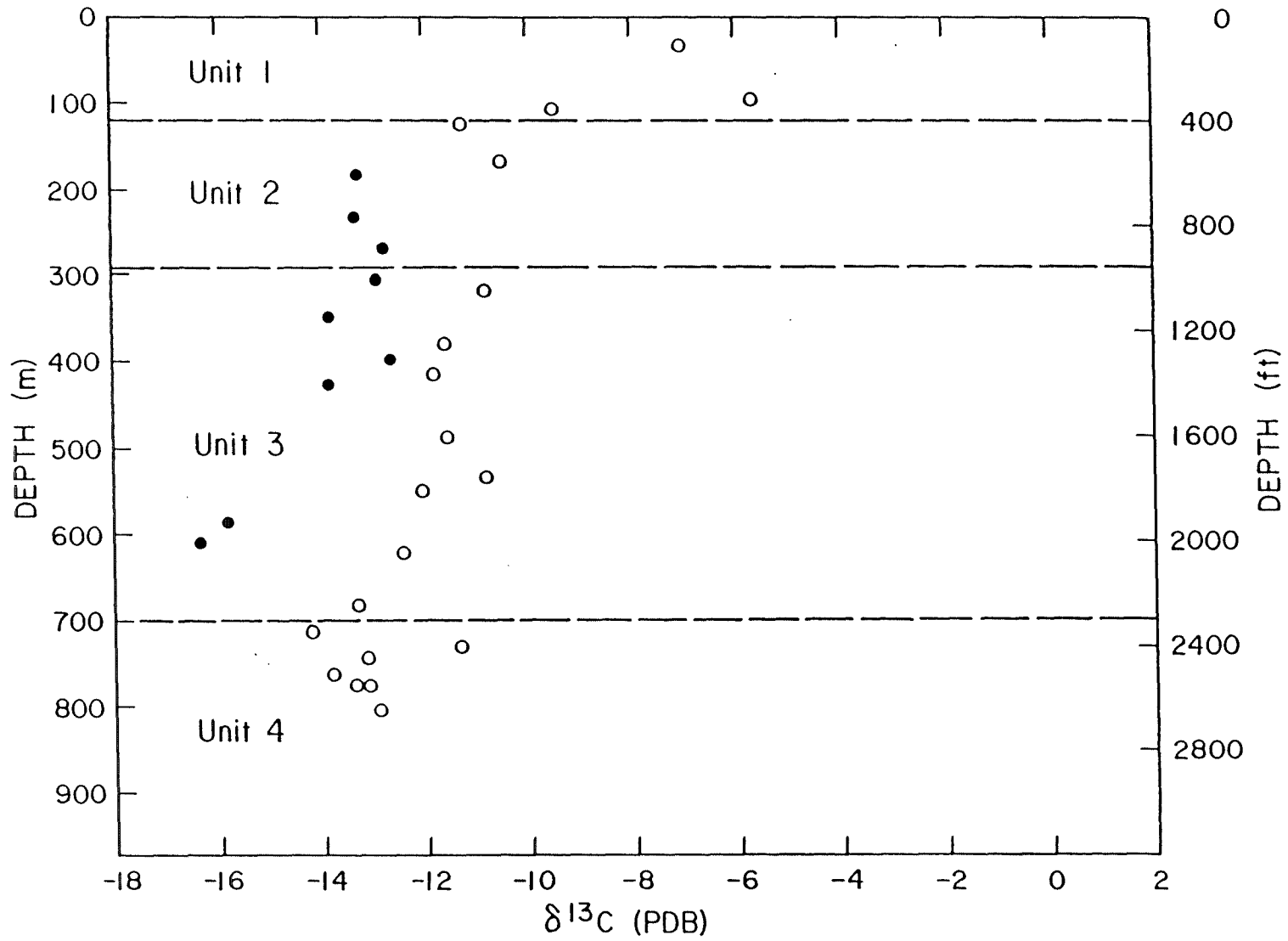
The calcite was converted to CO_2 gas by reaction with orthophosphoric acid (H_3PO_4) at 25°C for 12-15 hours (McCrea, 1950). The silicates were found into a coarse powder and reacted with bromine pentafluoride in nickel reaction tubes at 500-600°C to liberate O_2 gas (Clayton and Mayeda, 1963). The oxygen produced was converted into CO_2 by a carbon reduction process. The CO_2 gas, generated from either process, was analyzed on a double-focusing, double collecting isotope ratio mass spectrometer (Coplen, 1973).

Results of Present Study

Calcite

$\delta^{13}\text{C}$ - Measured $\delta^{13}\text{C}$ values versus depth for Geysers 1 carbonates are shown in Figure 19 and Geysers 2 values are shown in Figure 20. The overall variation of $\delta^{13}\text{C}$ in either well is extreme. Geysers 1 $\delta^{13}\text{C}$ values range from -6 to -16 ‰ while Geysers 2 $\delta^{13}\text{C}$ values range from +1 to -16 ‰. In both wells, there exists a general decrease in $\delta^{13}\text{C}$ with increasing depth.

of Franciscan metamorphism. This indicates that the chips are all hydrothermal in origin and not of Franciscan regional metamorphism.



and condensation, melting and crystallization, and diffusion due to concentration and temperature gradients.

In this study I have analyzed quartz and calcite vein material for $\delta^{18}\text{O}$ and $\delta^{13}\text{C}$ isotopic compositions. $\delta^{18}\text{O}$ is particularly useful as a geothermometer because calcite-water (O'Neil, Clayton and Mayeda, 1969) and quartz-water (Clayton, O'Neil and Mayeda, 1972) fractionation behaviors have been determined experimentally and theoretically (Bottinga *et al.*, 1973, 1975). $\delta^{18}\text{O}$ also serves to differentiate water sources, determine water-rock ratios, and indicate the degree of isotopic equilibrium. $\delta^{13}\text{C}$ acts as an indicator of sources in carbon for hydrothermal fluids.

Isotopic data are expressed in terms of the δ -value, which is the difference in absolute isotopic ratios between the sample and a standard as follows (Friedman and O'Neil, 1977):

$$\delta_x = \left(\frac{R_S - R_{\text{STD}}}{R_{\text{STD}}} \right) \times 1000$$

where R is the ratio of heavy to light isotopes ($^{18}\text{O}/^{16}\text{O}$, $^{13}\text{C}/^{12}\text{C}$, etc.) and STD is the internal standard in the mass spectrometer. The measured δ -value is then normalized to compare with internationally accepted reference standards. The standard for oxygen is SMOW (Standard Mean Ocean Water). Carbon is expressed in terms of PDB (PeeDee Belemnite).

The equilibrium fractionation factor between two phases (A, B) can be expressed as a ratio of heavy to light isotopes:

$$\alpha_{\text{A-B}} = \frac{R_A}{R_B} = \frac{1000 + \delta_A}{1000 + \delta_B} \quad (\text{Friedman and O'Neil, 1977})$$

This can be simplified to be expressed in terms of measured per mil values as follows:

$$\Delta_{\text{A-B}} = 10^3 \ln \alpha_{\text{A-B}} = \delta_A - \delta_B \quad (\text{Friedman and O'Neil, 1977})$$

Figure 11. Geothermal mineral zonation in Geysers 1.

1. The minerals mixed layer montmorillonite-illite and illite were formed during Franciscan metamorphism. The destruction of these minerals was due to geothermal metamorphism. See text.
2. Group I Sulfides: pyrite+sphalerite+chalcopyrite+galena.
3. Group II Sulfides: Minerals associated with the transition to steam (see text) marcasite+pyrrhotite+fahlore+gersdorffite+sphalerite+chalcopyrite+galena.

were reported to be -11 and -12 ‰ and -8 to -11 ‰ for HCO_3^- in hot springs.

Huebner (1981) conducted a $\delta^{13}\text{C}$ isotope study of steam and hot springs samples. He found that $\delta^{13}\text{C}$ of CO_2 in the steam varied from -15.9 to -19.9 ‰ and $\delta^{13}\text{C}$ of HCO_3^- in hot springs values (-9.3 to -11.6 ‰) similar to Craig's results (1963). He concluded that the $\delta^{13}\text{C}$ values were indicative of derivation from organic carbon and were too light to allow appreciable contributions from magmatic carbon sources.

Lambert (1977) conducted an intensive isotopic study of seven wells in The Big Geysers area using material supplied by Union Geothermal Co. He analyzed whole rock fragments as well as calcite and quartz vein material picked from well cuttings and core. He distinguished two generations of hydrothermal mineralization on the Lakoma Fame tract. These wells are situated about 5 km east of Geysers 1 and about 2.5 km south of Geysers 2.

The minerals of the upper zone were characterized by an extreme range of $\delta^{13}\text{C}$ values ranging from +1 to -15‰ and a narrow $\delta^{18}\text{O}$ range of +14 to +19 ‰ (Lambert, 1977). Quartz-calcite pairs yielded paleotemperatures of 170-206°C and calculated vein water $\delta^{18}\text{O}$ values of 5.5 to 7 ‰. This activity was interpreted as regional Franciscan metamorphism.

The lower zone was characterized by a relatively limited range of $\delta^{13}\text{C}$ values (-8 to -15 ‰) but a wide distribution of $\delta^{18}\text{O}$ values which ranged from +1 to +12 ‰. Quartz-calcite temperatures ranged from 160°C to 320°C. This zone, which coincided with the presence of steam entries, he aptly named the "active steam zone."

500 m the frequency of quartz, calcite and adularia veining increase substantially. At the base of lithic unit 3 the total volume of hydrothermal mineralization (including sulfides) approaches 20% of the total rock material.

Three calc-silicates are first encountered in close proximity to the interface between lithologic units 3 and 4. Sphene occurs at 550 m and persists throughout the well in trace amounts (<1%). The decrease in calcite coincides with the appearance of epidote. Green epidote occurs as porphyroblasts at 700 m and yellow green epidote veins at 760 m. The green epidote is abundant between 700 and 823 m where it comprises up to 2% of the total rock, but it decreases below 820 m. Yellow green epidote is dominant below 835 m.

An assemblage of diopside and tremolite suddenly occurs at 1220 m and pinch out by 1430 m. These minerals apparently replace the epidote as the yellow green epidote is present in only trace amounts, which could be contamination from the upper strata. Yellow green epidote reappears at 1430 m followed by tremolite at 1500 m.

A recrystallization trend in the clay minerals can be recognized. X-ray analyses of lawsonite-bearing Franciscan wackes from Panoche Pass contained interlayered illite and montmorillonite clays (1M on X-rays). Mixed layered clays in the wackes and shales of Geysers 1 disappear by 470 m (see Figure 5). The illite clay fraction subsequently becomes micaceous at approximately 1100 m. Below 1100 m, the major illite peaks on the powder patterns sharpen into a mica configuration but a pure muscovite (or biotite) does not form. These transitions occur within lithologic blocks and can be interpreted as thermally induced reactions

Figure 19. ^{13}C vs depth of calcites from Geysers 1.

- Low ^{13}C calcites
- High ^{13}C calcites

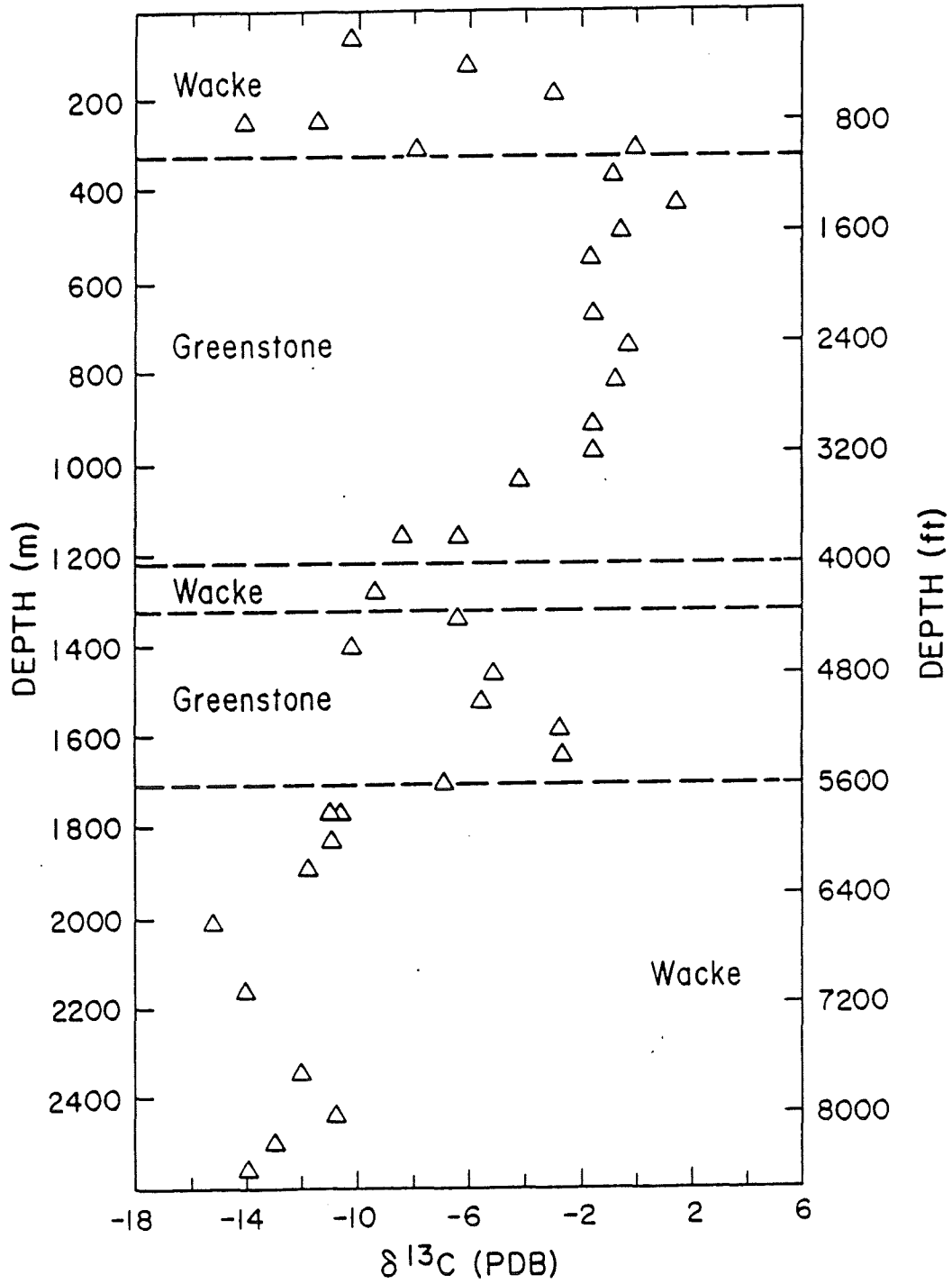
Unit 1, Unit 2, etc., are lithologic units.

Figure 12. Geothermal mineral zonation in Geysers 2. Mixed layer montmorillonite was formed during Franciscan metamorphism. The destruction of this clay was due to geothermal metamorphism.

Figure 20. ^{13}C vs depth of calcites from Geysers 2.

Wacke: sandstone and shale strata.

Greenstone: volcanic and micro-gabbro material.



A strong correlation between the measured $\delta^{13}\text{C}$ values and the lithology of the host rock is observed. This is best recorded in the samples from Geysers 2 (see Figure 20). Calcite vein material incorporated in greenstones have $\delta^{13}\text{C}$ values of +1 to -3 ‰. Calcite incorporated in shales and wackes have $\delta^{13}\text{C}$ values less than -9 ‰. Calcite samples derived from strata of mixed volcanics and wackes display a $\delta^{13}\text{C}$ range of -4 to -8 ‰. A symmetrical shift in $\delta^{13}\text{C}$ values can be observed between 1220 and 1495 m that corresponds with the transition from greenstone to wacke lithologies and back to greenstone (compare Figure 8 and Figure 20).

The carbon reservoir, therefore, was not uniform during the deposition of the calcite material. The carbon in the hydrothermal fluids was apparently leached directly from the local host rocks. This is indicative of interaction in a very low water-rock ratio environment. The greenstone $\delta^{13}\text{C}$ is normal for marine limestone (Shieh and Taylor, 1969) and was derived from primary carbonate deposited by sedimentary processes while the volcanics were exposed on the sea floor. The wacke $\delta^{13}\text{C}$ is within the range of marine biogenic carbon (Fritz, 1976) and was apparently derived from the interaction of the original connate waters and the carbonaceous material in the wackes during lithification and Franciscan metamorphism. Petrographic evidence for these carbon sources is plentiful. The volcanics contain abundant amygdules of calcite and aragonite and the wackes and shales contain abundant clasts of vitrinite. Further, the uniformity of the $\delta^{13}\text{C}$ within a single rock type compared with the heterogeneity of the $\delta^{18}\text{O}$ values (discussed in subsequent section), associated with the multiple generations of vein calcite, indicates that the recent

hydrothermal activity remobilized carbon originally deposited during the Franciscan metamorphism.

Two generations of calcites can be differentiated in Geysers 1, based on their different $\delta^{13}\text{C}$ values (see Figure 19). The "low $\delta^{13}\text{C}$ " calcites display a range of -13 to -16 ‰ and the "high $\delta^{13}\text{C}$ " calcites range from -6 to -14 ‰. Generally at any given depth, the low ^{13}C carbonates are 2 to 4 ‰ lighter. Both groups show a decrease in $\delta^{13}\text{C}$ with increasing depth. Additional evidence (see Figures 23 and 25) supporting this distinction and its significance will be discussed in a subsequent section.

$\delta^{18}\text{O}$ - Figure 21 is a plot of $\delta^{18}\text{O}$ versus depth of the calcites from Geysers 1 and Figure 22 presents similar data from the Geysers 2 well. Unlike the $\delta^{13}\text{C}$ distributions, which reflect similar carbon sources, the $\delta^{18}\text{O}$ trends of the two wells are radically different, implying dissimilar thermal histories. Geysers 1 calcites display a 9 ‰ variation but Geysers 2 calcites exhibit a 20 ‰ variation.

Geysers 1

The $\delta^{18}\text{O}$ values of the calcites range from +8 to +17 ‰. The "low $\delta^{13}\text{C}$ " carbonate samples have $\delta^{18}\text{O}$ values which are generally higher than the "high $\delta^{13}\text{C}$ " group. The $\delta^{18}\text{O}$ distribution for the "low $\delta^{13}\text{C}$ " samples is roughly linear, decreasing from 17 ‰ at 200 m to 10 ‰ at 600 m.

The "high $\delta^{13}\text{C}$ " carbonate samples are distributed in a continuous sinuous curve. The meandering trend of the "high ^{13}C " group shows a general decrease in $\delta^{18}\text{O}$ with depth interrupted by two prominent reversals at approximately 300 m (1 ‰) and 700 m (4 ‰). Each of these isotopic inversions is located at or near a boundary of lithologic units.

Figure 21. $\delta^{18}O$ vs depth of calcites from Geysers 1.



Low ^{13}C calcites



High ^{13}C calcites



Trend of high ^{13}C calcite

Unit 1, Unit 2, etc., are lithologic units.

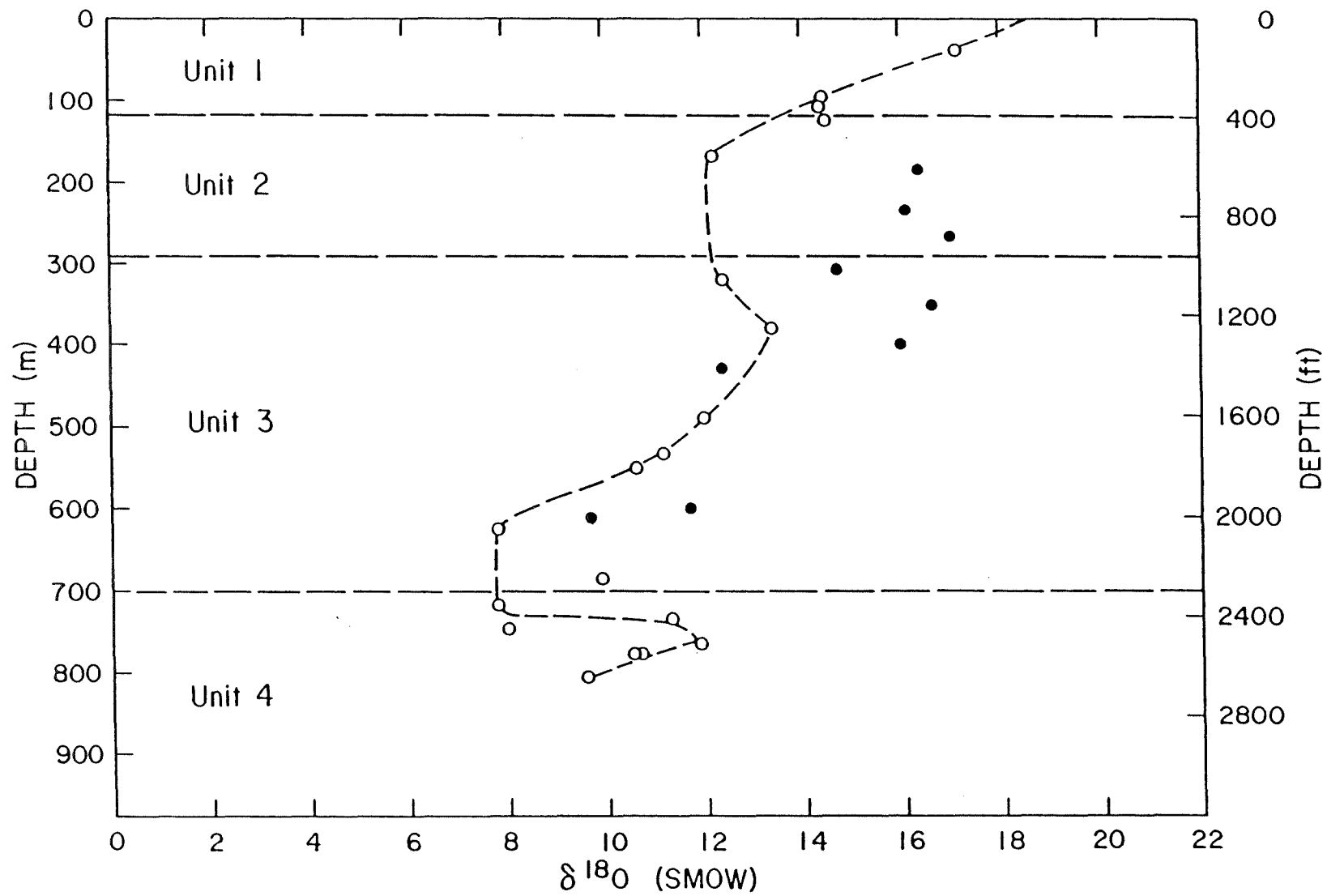


Figure 22. ^{18}O vs depth of calcites and quartzites from Geysers 2.



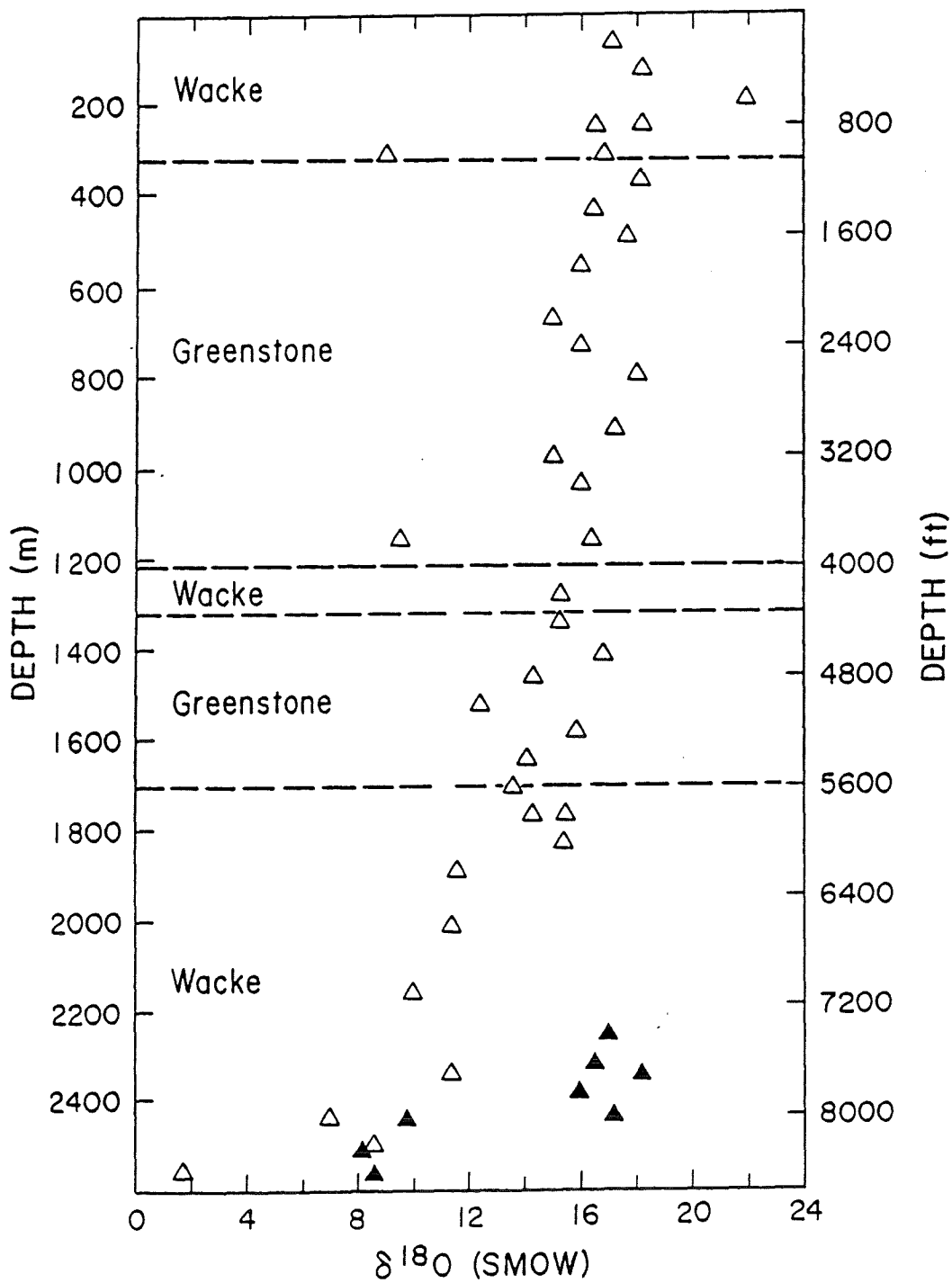
Calcite



Quartz

Wacke: sandstone and shale strata

Greenstone: volcanic and micro-gabbro material.



The upper inversion corresponds to the transition between units 2 and 3 and the lower inversion demarcates units 3 and 4 (see Figure 21).

Geysers 2

The $\delta^{18}\text{O}$ versus depth (Figure 22) trend for Geysers 2 exhibits a general decrease in $\delta^{18}\text{O}$ with increased depth characterized by small perturbations of 1 to 2 ‰ and a sharp $\delta^{18}\text{O}$ decrease of about 10 ‰ below 2440 m. There are two data points, at 300 m and 1160 m, which have $\delta^{18}\text{O}$ values of approximately 9 ‰ and corresponding $\delta^{13}\text{C}$ values of approximately -8 ‰ (see Figure 22). These two calcites must have a unique origin unrelated to the main body of the carbonate veins in this well.

The bulk of the data points (0 to 1800 m) range between 14 and 18 ‰. The small overall decrease in $\delta^{18}\text{O}$, 4 ‰ over 1800 m depth (compare with Geysers 1: 10 ‰ decrease in 700 m), is typical of the uniform ^{18}O reservoir of the Franciscan metamorphic event as described by Lambert (1977). The distribution of $\delta^{18}\text{O}$ values overlap his observed limits of Franciscan Event calcites (15-18 ‰). However, traces of hydrothermal activity, recorded by sulfide minerals and in fluid inclusions, is superimposed over the pre-existing fracture-fill mineralization and may account for the minor isotopic inversions. The sharp 10 ‰ $\delta^{18}\text{O}$ shift below 2440 m correlates with the appearance of epidote in the well.

^{13}C vs. ^{18}O - In a hydrothermal environment, the fractionation behavior of $\text{CaCO}_3\text{-CO}_2$ is inversely proportional to temperature. $\delta^{13}\text{C}$ and $\delta^{18}\text{O}$ will decrease with increased temperatures (Friedman and O'Neil, 1977). Therefore, a graph of ^{13}C versus ^{18}O will have a positive slope

(Shieh and Taylor, 1969). Figures 23 and 24 are $^{13}\text{C}/^{18}\text{O}$ graphs for Geysers 1 and Geysers 2, respectively.

It is evident from Figure 23 that the "high ^{13}C " and "low ^{18}O " calcites from Geysers 1 plot along two sub-parallel fractionation slopes, supporting the earlier suggestion that these carbonates were derived from dissimilar fluids. The difference in averaged $\delta^{13}\text{C}$ for any given $\delta^{18}\text{O}$ between the two groups is 4 ‰. The calcite data from Geysers 2 plots in a reversed L-shaped pattern that coincides with the calcite data from Lambert's (1977) study (see Figure 24). The base of this L-shape, however, does approximate a fractionation slope very similar to the slope of the "high ^{13}C " calcites in Figure 23.

When the data points are grouped according to the host rocks in which the vein materials were encountered (see Figure 25) three sub-parallel fractionation slopes can be recognized. Samples originating from the volcanic rocks and wacke (-shale) rocks plot in tightly clustered groupings. An intermediate group ("mixed") of calcites originating from volcanic rocks situated adjacent to wacke strata (i.e., greenstone-wacke thrust fault contacts or interbedded volcanoclastic wackes and shales) exhibits distinctive ^{13}C contamination. Comparing the two wells, it is evident that the "high ^{13}C " calcites from Geysers 1 and the "wacke" calcites of Geysers 2 are superimposed, and more significantly, all calcites derived from wackes in the seven wells studied by Lambert (1977) plot along this fractionation curve. It can be inferred that the ^{13}C reservoir for both the Franciscan metamorphic and geothermal hydrothermal carbonate mineralization of the sediments was derived from local organic material in the wacke and was not augmented by an igneous-volcanic ^{13}C

Figure 23. ^{13}C vs ^{18}O of calcites from Geysers 1.

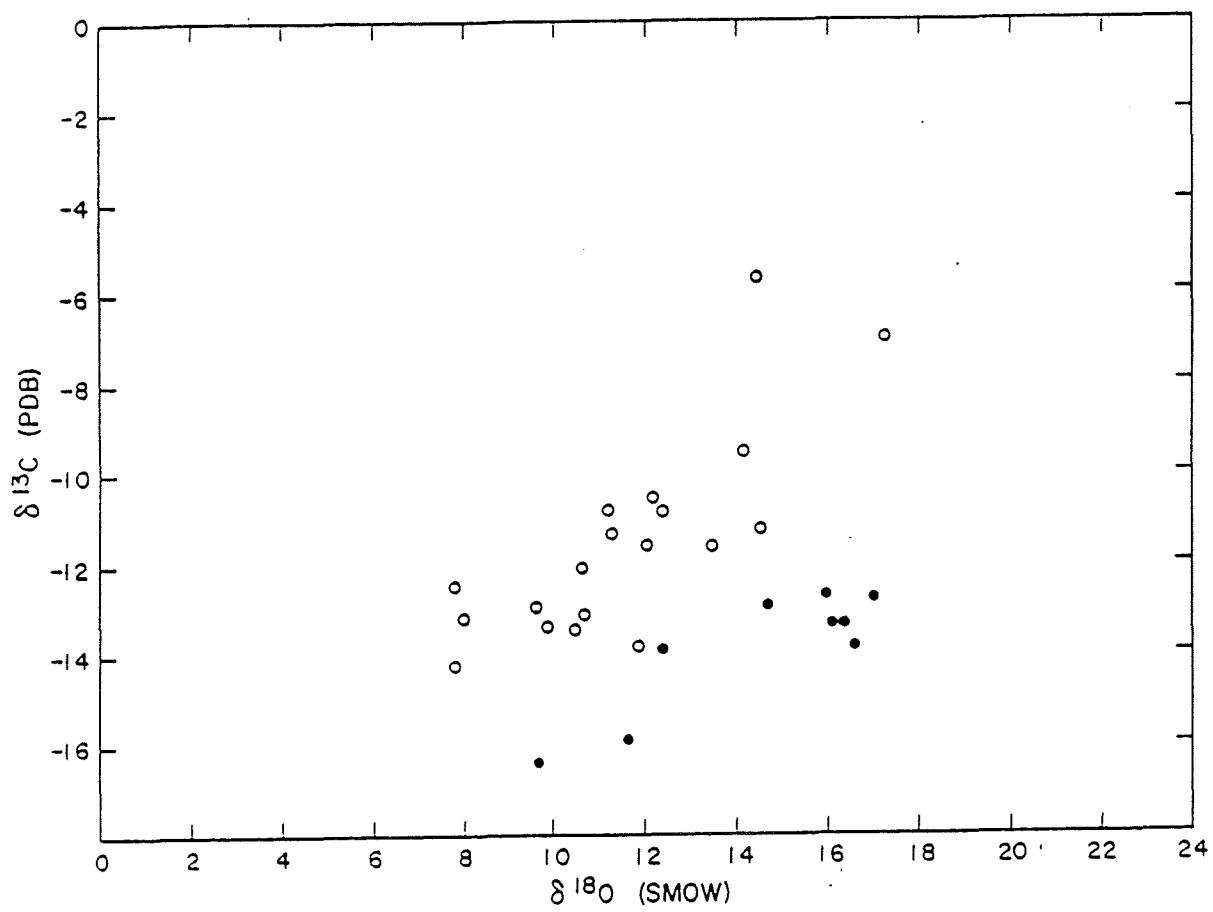


Figure 24. ^{13}C vs ^{18}O of calcites from Geysers 2.

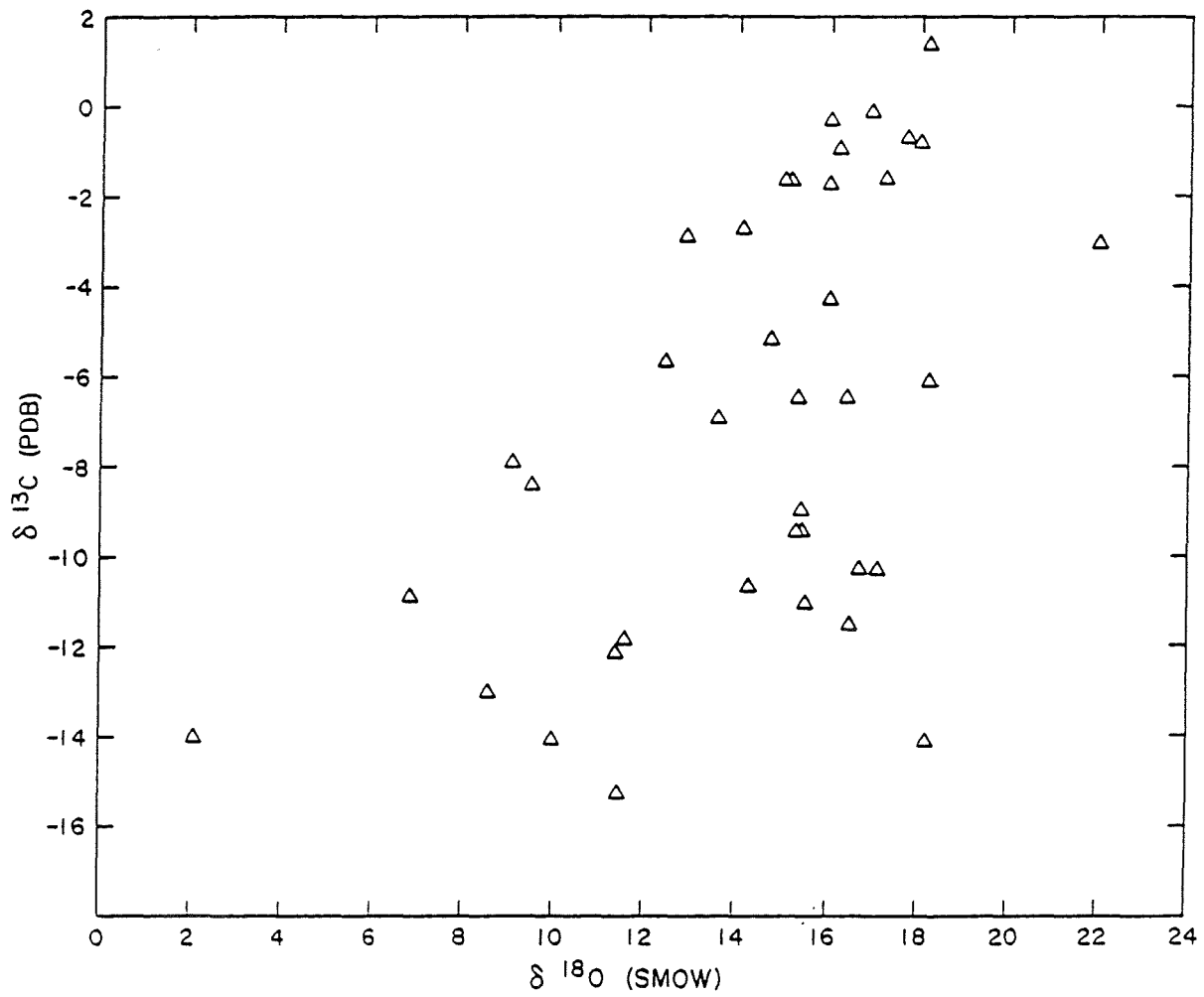
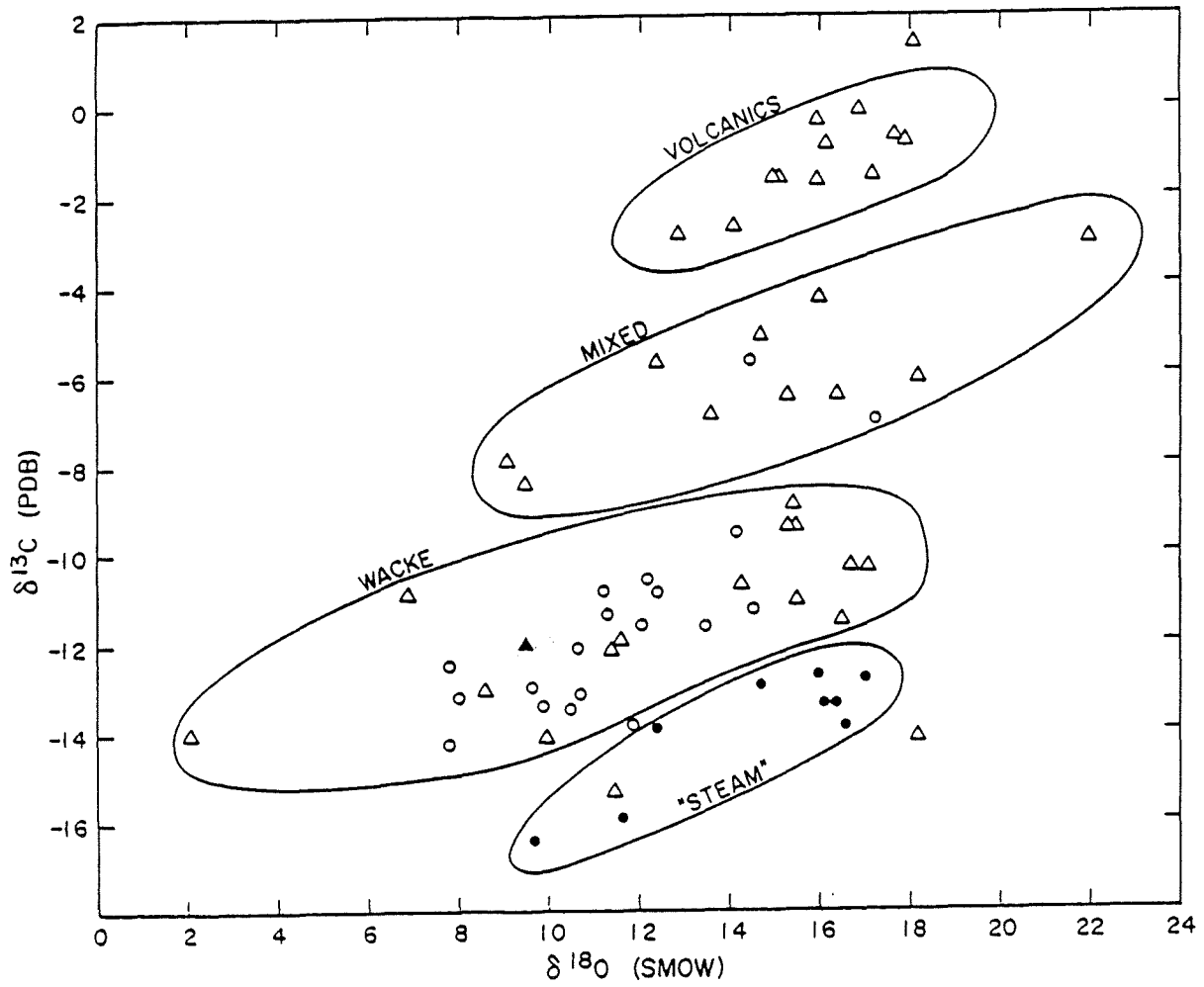


Figure 25. Composite ^{13}C vs ^{18}O .

- Low ^{13}C calcite, Geysers 1
- High ^{13}C calcite, Geysers 1
- △ Calcite, Geysers 2



source. Also, it is apparent that the recent geothermal activity dissolved and remobilized the carbon from calcite deposited during the Franciscan regional metamorphism. The characteristic "Franciscan" calcite $\delta^{18}\text{O}$ values of Lambert (1977) are not observed in Geysers 1 nor in the higher temperature epidote zone of Geysers 2.

The "low ^{13}C " calcite from Geysers 1, despite their occurrence in wacke host rocks and a presumably geothermal origin, plot outside the established wacke pattern and could not have been deposited from the dominant, hot water source.

Huebner (1981) conducted carbon isotope studies on CO_2 in steam samples from three wells in The Big Geysers area. These ^{13}C analyses ranged from -15.9 to -19.9 ‰. The two $\delta^{13}\text{C}$ data points near 600 m in Geysers 1 (see Figure 19) are -15.84 and -16.37 ‰ and fit within Heubner's range of steam isotope values. It can be inferred that the low ^{13}C calcites have equilibrated with steam condensate.

If we assume from the fluid inclusion data (see Figure 16 and text discussion) that steam was generated at temperatures between 210 and 200°C, the ^{13}C isotope fractionation between CO_2 (gas) and calcite is nearly zero (less than .5 ‰) (Friedman and O'Neil, 1977). Consequently, if the steam cooled to temperatures of 150 to 125°C (as indicated by the lower modal fluid inclusion temperatures at 250 m and 396 m depths on Figure 16) and condensed, the ^{13}C fractionation between calcite and CO_2 would be 3 ‰. This shift is observed in the isotope data (see Figure 19).

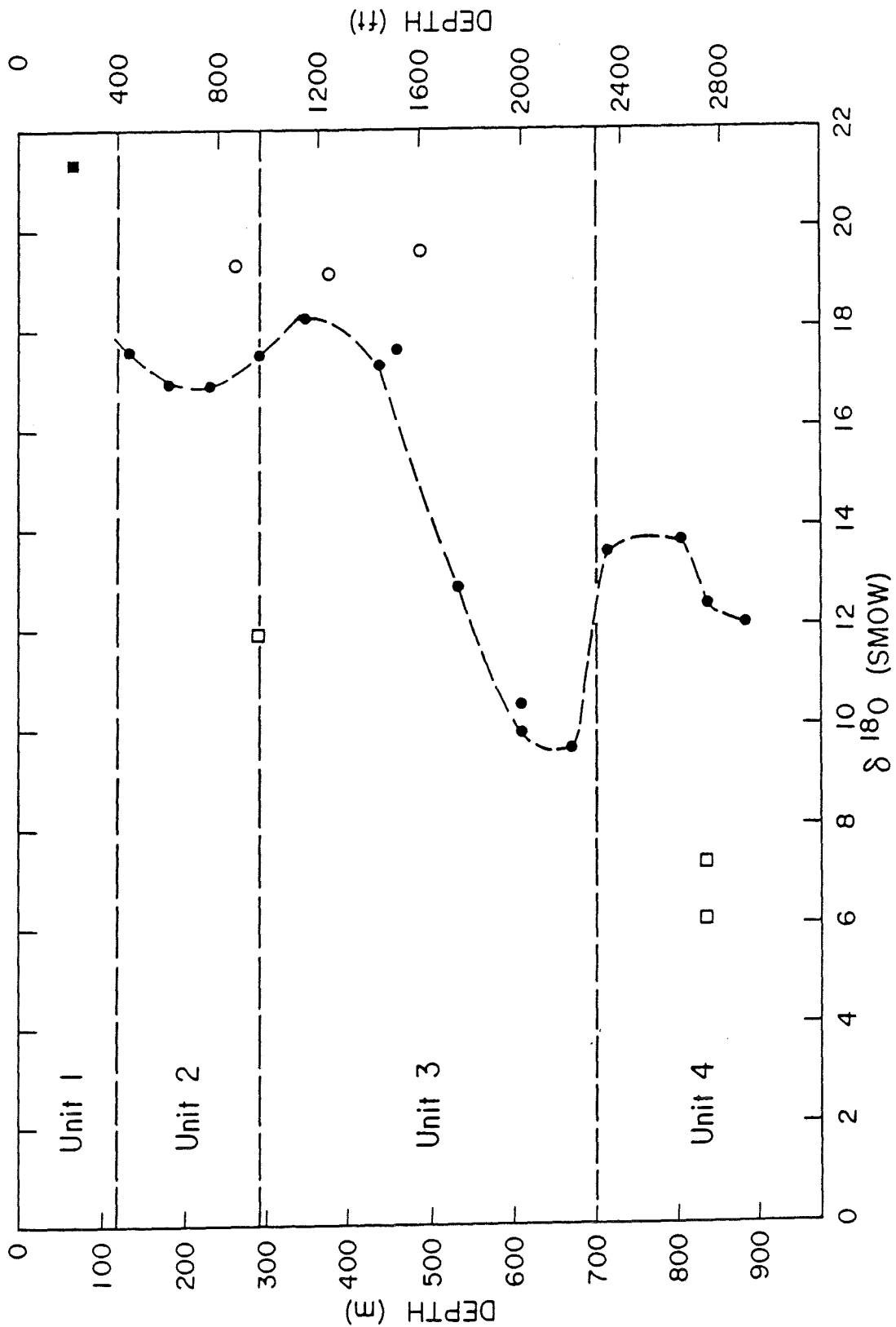
Quartz

$\delta^{18}\text{O}$ analyses of vein quartz and euhedral quartz crystal for Geysers 1 and Geysers 2 are plotted on Figures 26 and 22, respectively.

Figure 26. ^{18}O vs depth of quartz from Geysers 1.

- Chert
- Franciscan Event quartz
- High ^{18}O quartz
- Low ^{18}O quartz
- Trend of high ^{18}O quartz

Unit 1, Unit 2, etc., are lithologic units.



Three distinct $\delta^{18}\text{O}$ trends are recognized in Geysers 1. The majority of the analyzed quartz samples plot along a meandering path that mimics the trend of the high $\delta^{13}\text{C}$ calcite group (Figure 21). Isotope inversions of intensities similar to those observed in the calcite data are located at 300 m (1 ‰) and 700 m (4 ‰).

The remaining data points fall into two groups. Three analyses of samples originating between 250 and 500 m, are clustered about 19 ‰. These $\delta^{18}\text{O}$ values are very similar to measurements of vein quartz that Lambert (1977) attributed to the Franciscan metamorphism. Three data points for samples from 300 m and 835 m are 5 to 6 ‰ lighter than the major $\delta^{18}\text{O}$ trend at equivalent depths. The upper sample $\delta^{18}\text{O}$ is 12 ‰ and the lower samples 6.1 and 7.25 ‰. The 6.1 ‰ sample was composed of euhedral quartz crystals which are associated with pyrite-dominant base metal sulfides.

Two clusters of $\delta^{18}\text{O}$ values are observed in Geysers 2 (see Figure 22). One cluster ranges from 16 to 18 ‰ and lies slightly above 2440 m. The second cluster, situated below 2440 m, ranges from 8 to 10 ‰. This shift at 2440 m coincides with the appearance of hydrothermal epidote. The oxygen isotope shift of 9 ‰ is quite similar to the 10 ‰ $\delta^{18}\text{O}$ shift exhibited by the calcites at this depth. The higher $\delta^{18}\text{O}$ values are consistent with Franciscan metamorphic $\delta^{18}\text{O}$ values as established by Lambert (1977) and the lower $\delta^{18}\text{O}$ values represents recent geothermal activity.

Isotope Temperature and Water Calculations

Calculations of isotope exchange require either knowledge of the isotopic value for the original brine or of quartz-calcite pairs which

are in thermal and isotopic equilibrium. Neither of these conditions can be confidently established in The Geysers.

For Geysers 1, the similar trend between the "high $\delta^{18}\text{O}$ " quartz samples (Figure 26) and the $\delta^{18}\text{O}$ of the "high $\delta^{13}\text{C}$ " calcite group suggests that these samples were deposited under very similar P, T conditions. Between 400 and 1400 m, calculated quartz-calcite temperatures range from 57 to 92°C (± 10), but between 1600 and 2400 m temperatures range from 174 to 308°C (± 20). Only the temperatures originating between 1600 and 2400 m are substantiated by fluid inclusion homogenization data. The apparent disequilibrium within a single reservoir event is not unexpected as a uniform isotopic composition of the reservoir fluid is unlikely in a fracture system characterized by low water-rock ratios. Representative calculations for Geysers 2 are not possible due to the paucity of data.

It is possible to calculate the $\delta^{18}\text{O}$ of the geothermal waters from the measured $\delta^{18}\text{O}$ quartz and calcite data assuming they equilibrated at the corresponding fluid inclusion temperatures. Table 5 lists the calculated $\delta^{18}\text{O}$ values and the temperatures utilized in their derivation. The calculated waters, associated with the "high $\delta^{18}\text{O}$ " quartz (Figure 26) and "high $\delta^{13}\text{C}$ " calcites (Figure 21) groups are clearly stratified with respect to depth. The calculated $\delta^{18}\text{O}_{\text{H}_2\text{O}}$ values above 610 m average +3.8 ‰. At 610 m the calculated $\delta^{18}\text{O}_{\text{H}_2\text{O}}$ drops to +1.0 ‰ then increases, with increasing depth, to +4.6 ‰. The calculated water associated with the "low $\delta^{18}\text{O}$ " quartz group are isotopically lighter having negative $\delta^{18}\text{O}$ values ranging from -2.5 ‰ to -1.0 ‰.

The local meteoric water in The Geysers area has a $\delta^{18}\text{O}$ value of -8 ‰ (Craig, 1963; Lambert, 1977). The "low $\delta^{18}\text{O}$ " quartzes exhibit a stronger meteoric signature while the "high $\delta^{18}\text{O}$ " quartz and "high $\delta^{13}\text{C}$ "

TABLE 5

Calculated Water δO^{18}

Depth	$T_{F.I.}^*$ (°C)	T_{Q-C}^{**} (°C)	$O^{18}_{H_2O}-Q^+$ (‰ SMOW)	$O^{18}_{H_2O}-C^{++}$ (‰ SMOW)	Average (‰ SMOW)
I - High ^{18}O quartz, high ^{13}C calcite trends					
340-60	196			4.4	
1100-20	212			3.5	3.8 ‰
1360-80	208			4.3	
1800-20		248	3.3	3.3	-----
2000-20	248			.9	.9 ‰
		258	.8	.8	-----
	307'		2.8		
2200-20		308	2.4	2.4	2.5 ‰
2340-60	299'			2.2	
2400-20		248	4.0	4.0	-----
2500-20	295'			4.8	4.6 ‰
2540-60	293		6.1		
2700-20	304			4.2	
2740-60	294'		4.8		
II - Low ^{18}O quartz trend					
2740-60	315		-1.4		
	298		-.8		
960-80	252		-2.5		

* F.I. = fluid inclusion

** Q-C = quartz-calcite isotope calculation

+ Calculated water O^{18} based on quartz isotopes++ Calculated water O^{18} based on calcite isotopes

calcite groups have calculated waters that are indicative of extremely low water to rock ratios. Lambert (1977) calculated a water-rock oxygen atom ratio of .27 (mass ratio of .15) for The Geysers based on data from well T7. The high values of the calculated waters from the "high $\delta^{13}\text{C}$ " calcite and "high $\delta^{18}\text{O}$ " quartz groups are very similar to the T7 data ($\delta^{18}\text{O}_{\text{H}_2\text{O}}$ of +3 ‰) and may be representative of similar water-rock ratios.

Interpretation of Isotope Data

Stable isotope geochemistry is useful to distinguish the generations of hydrothermal veining through time and the principal zones of fluid flow in The Geysers. The $\delta^{18}\text{O}$ isotope data in the wells can be first divided into distinctive trends or groupings which represent veining from the Franciscan metamorphism and subsequent geothermal activity. The distribution of geothermal veining occurs in distinct zones whereas the Franciscan veining appears to have been uniformly pervasive throughout the well bores.

The $\delta^{18}\text{O}$ values in Geysers 2 can be differentiated into two paired cogenetic calcite and quartz trends. These two suites of data can be identified as hydrothermal events of Franciscan metamorphic and geothermal origins. The data from Geysers 1 can also be characterized as metamorphic or geothermal in origin. The geothermal activity, however, is more complex as it is composed of two groupings of quartz $\delta^{18}\text{O}$ values and two groupings of calcite $\delta^{18}\text{O}$ that represent a minimum of three periods of deposition.

The Franciscan quartz and calcite are insufficiently sampled in this study to allow comprehensive evaluation. The quartz and calcite $\delta^{18}\text{O}$ data from Geysers 1 and Geysers 2 replicate the results of Lambert (1977)

which were based on studies of nine wells, including some that had not undergone recent hydrothermal alteration. Lambert calculated an original water $\delta^{18}\text{O}$ composition of 5 to 6 ‰ (dependent on temperature) which was connate in character (Lambert, 1977; Craig, 1963). The metamorphic deformation during the Cretaceous and Tertiary periods served to thermally and mechanically remove available pore waters. It can therefore be assumed that the source waters for the geothermal activity were meteoric.

The geothermal activity is complex due to the variations in the superimposed isotopic chemistries. It is possible to pair several groups of the disparate quartz and calcite data within or between the wells, using similarities in their isotopic ratios and corresponding authigenic mineralization. The geothermal calcite and quartz vein materials from Geysers 2 appear to be cogenetic due to the correlative behavior of their $\delta^{18}\text{O}$ values at 2400 m (see Figure 22 and supporting text). The "low $\delta^{18}\text{O}$ " quartz group in Geysers 1 corresponds to the geothermal quartz in Geysers 2; they have $\delta^{18}\text{O}$ values of 6 to 9 ‰ and have associated pyrite and pyrite-field base metal sulfide mineralization. The calculated water $\delta^{18}\text{O}$ values interpreted from Geysers 1 quartz samples are negative, ranging from -.8 to -2.5 ‰. These values are indicative of a strong meteoric influence.

The "high $\delta^{18}\text{O}$ " quartz and the "high ^{13}C " calcite groups of Geysers 2 have similar $\delta^{18}\text{O}$ trends and can therefore be attributed to a single period of deposition. The calculated water $\delta^{18}\text{O}$ compositions for this depositional event are highly stratified and range from +.8 to +5 ‰. These values are intermediate between the connate waters of the Franciscan event and the meteoric geothermal mineralization, and are indicative of greater water

to rock contact. Three "high $\delta^{13}\text{C}$ " calcite samples contained pyrrhotite (see Table A-13). However, it is difficult to attribute this generation of intermediate $\delta^{18}\text{O}$ mineralization solely to pyrrhotite-bearing fluids. The pyrrhotite-bearing quartz and calcite veins are minor compared to the large amount of deposition of pyrite in Geysers 1. The intermediate $\delta^{18}\text{O}$ quartz is dominant in Geysers 1, as are occurrences of pyrite. It is reasonable to assume that the chemical transition to a low sulfur fugacity fluid is a minor, late-stage development of the fluids which deposited the intermediate $\delta^{18}\text{O}$ quartz and calcites.

The progression from meteoric to higher $\delta^{18}\text{O}$ fluid compositions is difficult to evaluate in space and time. The higher $\delta^{18}\text{O}$ fluids have destroyed all evidence of Franciscan and low $\delta^{18}\text{O}$ calcite, just as the geothermal calcite replaced Franciscan calcite in Geysers 2, indicating a change in thermal and/or chemical equilibrium. Yet the mineral assemblages associated with these different geothermal fluid compositions are identical (pyrite, adularia, yellow-green epidote, garnet - compare Figures 11 and 12) and the prevailing temperatures of formation of the different $\delta^{18}\text{O}$ quartz mineral phases are identical (see Figure 17 at 835).

The last generation of mineral deposition is represented by the "low $\delta^{13}\text{C}$ " calcites of Geysers 1. Its derivation from steam condensate has been suggested (see Figures 19 and 25 and supporting text). The linear distribution of "low $\delta^{13}\text{C}$ " calcite (see Figure 21), superimposed over the sinuous trend of the "high $\delta^{13}\text{C}$ " calcites, suggests late stage deposition post-dating the water-dominated reservoir. Thus a chronologic sequence of mineral deposition has been established. The initial geothermal fluids

had meteoric $\delta^{18}\text{O}$ and were characterized by a high f_{S_2} . These were displaced by fluids with a heavier $\delta^{18}\text{O}$ composition which display a transition from high f_{S_2} to low f_{S_2} chemistries. Finally, the water-dominated reservoir was replaced by a vapor-dominated one. Fault contacts between imbricated thrust sheets have been delineated for both wells in this report. A strong correlation exists between these thrust contacts and the geothermal $\delta^{18}\text{O}$ isotope patterns in Geysers 1 and Geysers 2 (see Figure 27).

In Geysers 2, geothermal low values of $\delta^{18}\text{O}$ values for calcite vein material (see Figure 22) occur at 300 and 1200 m. These samples correspond to a wacke-greenstone boundary that is assumed to be a thrust fault contact. The $\delta^{18}\text{O}$ shift in quartz vein material at 2400 m from Franciscan to geothermal values also corresponds to a sharp lithology change in wacke blocks that is also probably a fault contact.

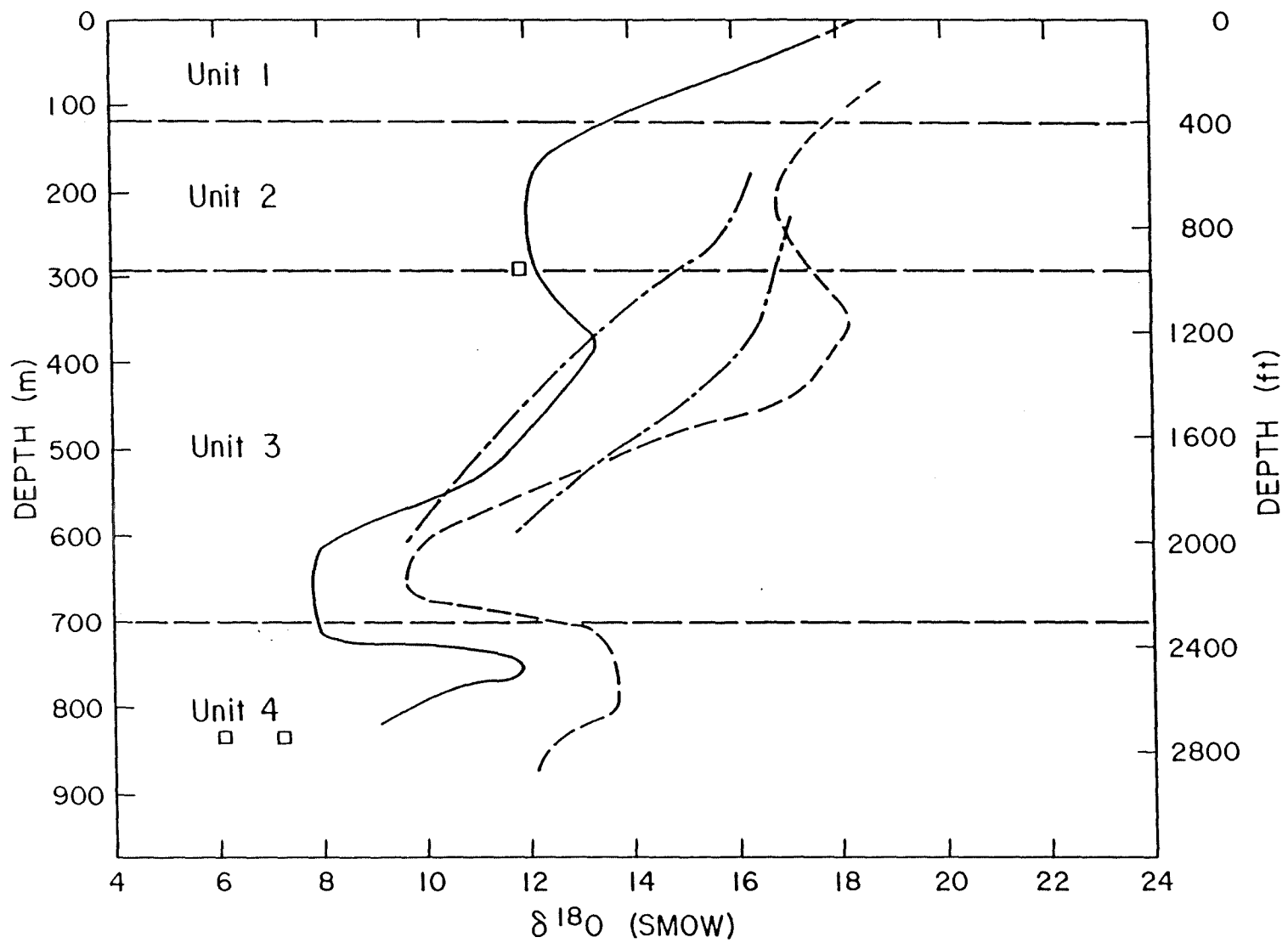
A strong correlation exists between the $\delta^{18}\text{O}$ minima of the "high ^{13}C " calcites and "high ^{18}O " quartzes in Geysers 1 at 200 m and 600 m and thrust fault contacts (see Figure 27). These depths are also zones of intense authigenic mineralization. As described earlier, quartz, calcite, sulfides and adularia comprise 3 to 4% of the total rock (by volume) at 200 m and 10% of the total rock between 550-650 m. A third minimum is present at 800-850 m which corresponds to the occurrence of base metal sulfides and euhedral vug quartz. This suggests the existence of another fracture system at this depth.

The sharp isotopic maxima which flank the minima at 600-650 m cannot result from simple temperature effects. The fluid inclusion homogenization temperatures (see Figures 16 and 17) and correlated quartz-calcite

Figure 27. Composite of ^{18}O trends vs depth of the Big Geysers
Event - Geysers 1.

— — — — —	High ^{18}O quartz
—————	High ^{13}C calcite
- - - - -	Low ^{13}C calcite
□	Low ^{18}O quartz

Unit 1, Unit 2, etc., are lithologic units.



temperatures below 600 m do not vary more than 20°C and are insufficient (see Table 5) to induce an isotope shift of 4 ‰. Stratigraphic control over fluctuations in fluid chemistries are improbable in an interconnected fracture system. The lithology cannot explain these isotope reversals, nor can liquid to vapor fractionation of water at these temperatures (Friedman and O'Neil, 1977).

A similar pattern of paired minima and maxima of the mineral oxygen isotopic data is also observed in the Salton Sea geothermal field (Kendall, 1976). Low $\delta^{18}\text{O}$ values in the Salton Sea field are associated with sandstone aquifers characterized by high permeabilities and high concentrations of precipitated minerals. An analogy of such highly permeable zones can be applied to the mineralized fault zones in The Geysers.

In a system of low water to rock ratio, the hydrothermal fluids will tend to show a strong shift of $\delta^{18}\text{O}$ as they approach isotopic equilibrium with their surrounding host rocks. The stratified values of the calculated water $\delta^{18}\text{O}$ values (see Table 5) can be attributed to the effects of relative permeability. Fluid flow through the minor fractures in the greywacke within thrust sheets would be sluggish. Because the surface area to volume ratio is greater in these veins, resulting in protracted contact with the wall rocks, more oxygen exchange would occur, producing high fluid $\delta^{18}\text{O}$ compositions. Fluid flow through the larger fractures in the fault zone would be higher but the surface area to vein volume would be lower, resulting in less oxygen shift in the fluid, hence lower $\delta^{18}\text{O}$.

It has been shown that the source of carbon for all hydrothermal activity is isotopically light and has been derived from the reservoir rocks. The $\delta^{13}\text{C}$ distribution (see Figure 25) is controlled by the inherent

$\delta^{13}\text{C}$ sources in the wall rocks. All geothermal hydrothermal veining (with the exception of the steam derived calcites) exhibits this lithological dependency. This indicates that the primary carbon source for the recent hydrothermal activity was the pre-existing Franciscan calcites or original sedimentary material and, more importantly, that vertical mixing of aqueous solutions was minimal. The intermediate $\delta^{13}\text{C}$ of the "mixed lithology" calcite group is observed only within 100 m of greenstone-wacke thrust contacts. This distance correlates well with the clearly defined 50-100 m zones of high fluid flow adjacent to thrust faults in Geysers 1.

Several generalizations about the nature of the geothermal reservoir can be derived from the isotope data: (1) the primary fluid conduits within the system are associated with thrust faults, not vertical tectonic faults; (2) the thrust fault conduits are dense networks (stockworks) of interconnected veins and veinlets in zones 50-100 m wide; (3) the thrust fault zones not only act as conduits for lateral flow, but also as semi-permeable membranes to vertical flow in the minor fractures that pervade the greywacke blocks; and (4) the volume of water circulated through the intra-slab fractures is comparatively low, although an intrinsic chemical and pressure equilibrium is maintained with the fault zones.

INTERPRETATION AND ASSIMILATION OF DATA

Synthesis of Hydrothermal Processes

Two superimposed generations of hydrothermal mineralization are recognized in Geysers 1 and 2. Each reservoir event is characterized by distinct mineral assemblages and stable isotopic compositions. The earliest such event was contemporaneous with the low temperature - high pressure regional metamorphism of the Franciscan Formation during the late Cretaceous and early Tertiary periods. This will be labeled the "Franciscan Event." The second event which will be called "The Geysers Event," represents more recent hydrothermal activity, presumably related to the Clear Lake volcanism. The transition from a water-dominated, geothermal system to the present vapor-dominated system of The Geysers Event will be differentiated into three distinct stages in the following discussion.

The minerals formed during the Franciscan Event were phengite, pumpellyite, lawsonite, albite, chlorite, quartz, calcite, ankerite, ferrierite, and an unknown zeolite which are found in the greenstones and meta-sedimentary rocks. An assemblage of interlayered chlorite, clays and vermiculite pseudomorphous after antigorite, talc, dolomite and magnesite, is observed in the ultramafic serpentinite rocks. In the Franciscan Event, quartz and calcite veining was deposited in a temperature range of 175-206°C, from a connate solution with calculated water $\delta^{18}\text{O}$ isotope values of 5.5 to 6.5 ‰ (Lambert, 1977). The X_{CO_2} of the fluid was low (Ernst, 1972).

The three stages of The Geysers Event are distinguished by the twin criteria of distinctive quartz and calcite $\delta^{18}\text{O}$ values and the apparent sulfur fugacity of the hydrothermal solution. Stage 1 of the water-

dominated system is characterized by a high sulfur fugacity and low meteoric $\delta^{18}\text{O}$ values, stage 2 by a high sulfur fugacity and high $\delta^{18}\text{O}$ values, stage 3 by a lower sulfur fugacity and high $\delta^{18}\text{O}$ values of the geothermal waters. Minerals associated with each successive stage of development are superimposed upon those of the earlier events.

The assemblage of authigenic minerals characterized by high sulfur fugacities (stages 1 and 2) are the dominant geothermal mineralogy in Geysers 1 and the only geothermal mineral suite in Geysers 2. The assemblage is composed of pyrite, base metal sulfides in equilibrium with pyrite, massive quartz veins, quartz crystals, calcite, adularia, sphene, green epidote, yellow-green epidote, andradite, tremolite and diopside. Clay mineral recrystallization associated with this deposition involves the disappearance of mixed-layered clays and the transition of illite to micaceous structures. This assemblage represents continuous prograde metamorphism from greenschist to greenschist-epidote to hornfels (Winkler, 1979; Miyashiro, 1973).

The observed mineral phases and zonation in The Geysers is remarkably analogous to the present day mineralization at the Broadlands Geothermal Field in New Zealand. Each system has similar host rocks (greywacke) and recent silicic volcanism (rhyolites and dacites). The two mineral assemblages share the following characteristics: (1) the absence of zeolites; (2) epidote compositions that are low in iron; and (3) well-developed sulfide deposition dominated by pyrite and base metal sulfides, including unique sphalerite crystallization. The most important relationship is the absence of wairakite which indicates a high X_{CO_2} (see discussion on ionic species).

Applying the Broadlands model and utilizing chemical data from Ellis and Mahon (1977) and Browne (1971), the original geothermal fluids can be inferred to have the following chemical parameters:

- (1) Low salinity (Broadlands is 2-4%).
- (2) High CO_2 concentration of .1 m (Broadlands is .15 m).
- (3) High S_2 concentration of .001 m (Broadlands is .003 m).
- (4) Low metal to sulfur ratio (Broadlands is .1).
- (5) pH range of 6-8 (Broadlands pH averages 8 from well discharge and has an estimated downhole pH of 6).

Estimates of the prevailing f_{S_2} and f_{O_2} conditions during the sphalerite deposition can be derived from the data on Figure 15. At approximately 300°C , the log f_{S_2} ranges from -10 to -11 (Barton and Skinner, 1979) and the log f_{O_2} is less than -32 (Holland, 1959).

Initially, under conditions of 300°C , f_{S_2} of 10^{-10} to 10^{-11} and f_{O_2} of less than 10^{-32} , the fluid migrated from the pyrite stability field (deposition of pyrite+sphalerite+quartz) to the pyrrhotite stability field (deposition of type 2 pyrrhotite+quartz) and subsequently, decreases in temperature, f_{S_2} , f_{O_2} and fluid chemistry (deposition of type 1 pyrrhotite+calcite) occurred. This process could only occur in the residual waters of a boiling fluid.

Normally, boiling will induce the precipitation of pyrite because the loss of H_2 is exceedingly more rapid than the loss of H_2S , driving the $\text{H}_2/\text{H}_2\text{S}$ ratio down (Ellis and Browne, 1970). This is observed in the Broadlands geothermal field where pyrrhotite is rare and it precipitates only from steam condensate. This process does not operate in The Geysers because the pyrrhotite depositing fluids also precipitates base metal

phases which would not form from steam condensate but will form from a boiling system which concentrates the heavy metals in a more saline residual liquid. Three explanations are possible: (1) the presence of abundant organic matter stabilized the pyrrhotite phase (Ellis and Browne, 1970; Ellis and Mahon, 1977); (2) if the Broadlands analogy is applied, the pH of the fluid was 7 to 8 and the rapid increase in pH at the onset of boiling (Ellis and Mahon, 1977), without affecting the f_{O_2} and f_{S_2} of the solution, moved the fluid chemistry into the pyrrhotite stability field (Barton and Skinner, 1979); or (3) the fluid did initially precipitate pyrite and the evidence is preserved in the high volume of pyrite material deposited between 500 and 650 m (the column "Py+Qtz" on Figure 13). It is my feeling that the last explanation or a combination of the latter two explanations is correct.

The mineral assemblage associated with the low sulfur fugacity (stage 3) occurs only in Geysers 1. It consists of quartz, calcite, adularia, pyrrhotite and base metal sulfides in equilibrium with pyrrhotite at depths greater than 360 m. The stratigraphic range of the low f_{S_2} mineral assemblage coincides with steam phase-dependent calcite veining identified by fluid inclusion and isotope data and steam entries.

Pyrrhotite is a metastable iron sulfide that usually occurs only in environments of high temperatures and pressures (Ramdohr, 1969; Hurlbut, 1971). It is a minor iron sulfide phase in several described geothermal systems. In the Salton Sea field, it is precipitated from brines in the deeper portions of the reservoir (Skinner et al., 1967; McKibben, 1979) and in Broadlands pyrrhotite precipitates from hydrothermal solutions derived from condensed steam (Browne and Ellis, 1970) at relatively shallow depths.

The pyrrhotite in Geysers 1 has formed under complex fluctuating thermal and chemical conditions. It is observed in two forms. Type 1 pyrrhotite is associated with calcite gangue and is restricted to strata above 700 m. Type 2 pyrrhotite is associated with quartz gangue and is dominant below 600 m. It occurs abundantly in distinct zones that are characterized by mineralogical evidence for boiling (500-780 m) or the presence of steam (1200-1400 m). And finally, a zone of pyrite destruction corresponds to the strata of maximum pyrrhotite deposition (550-760 m). Pyrite dissolution is prominent, although replacement by pyrrhotite is rare.

Subsurface boiling appears to be the intrinsic prerequisite for the chemical variations which stabilized pyrrhotite as the primary iron sulfide phase. Boiling of a water characterized by a pyrite-normal sulfur fugacity will result in a residual liquid with a higher pH, lower f_{CO_2} , f_{S_2} and low f_{O_2} due to the loss of acidic gases such as CO_2 and H_2S (Ellis and Mahon, 1977). The separation of just 2% steam will reduce the sulfur content by 50% (Ellis and Mahon, 1977). These conditions will favor the formation of pyrrhotite (Garrels and Christ, 1969; Helgeson, 1969). A side effect of this chemical reaction is the destruction of pyrite under these same acid-reduction conditions (Garrels and Christ, 1969). These phenomena are observed.

Sulfur and oxygen fugacity estimates for the pyrrhotite types can be calculated from the probe data and associated fluid inclusion temperature data (see Figure 15). Type 2 pyrrhotite has a $\log f_{\text{S}_2}$ of -10 to -11 (Barton and Skinner, 1979) and a $\log f_{\text{O}_2}$ of less than -32 (Holland, 1959). Type 1 pyrrhotite has a $\log f_{\text{S}_2}$ of -12 to -13 (Barton and Skinner, 1979) and a $\log f_{\text{O}_2}$ of less than -36 (Barton and Skinner, 1979).

Incorporating the f_{S_2} and f_{O_2} data from the sphalerite analyses, a sequential transformation of the fluid chemistry is noted.

This process would require the complete separation of the steam phase from the liquid to avoid retrograde reactions. Evidence exists to support the total separation of steam. The upper 100 m of the borehole and surface deposits in the Sulphur Banks area exhibit mineral assemblages characteristic of acid conditions. Surface manifestations of acid springs, fumaroles, acid leaching of outcrop greywacke and greenstone, cinnabar and sulfate minerals are abundant (McNitt, 1961; Garrison, 1972; Allen and Day, 1927). The upper 100 m of strata in Geysers 1 is characterized by an assemblage of primary marcasite and coexisting quartz+calcite+adularia. These mineralogies form under high acid conditions (Ramdohr, 1969; Hoagland and Elders, 1978).

The preceding observations describe the accumulation of acids and volatiles in the upper stratigraphic sections of Geysers 1. Two lines of evidence are indicative of a residual liquid persisting at depth. The presence of pyrrhotite and base metal sulfides, as discussed earlier, is characteristic of the concentration of residual fluid components and a more alkaline environment. And finally, the increased pH of reservoir fluids accompanied by the loss of HCO_3 in the water as CO_2 goes into steam (caused by vaporization in the production zone) in Wairakei Geothermal Field, New Zealand, induced the precipitation of calcite as the fluid became oversaturated with respect to calcite (Ellis and Mahon, 1977). This reaction may explain the dominance of type 1 pyrrhotite+calcite veining between 550 and 650 m (see Figure 13).

The last interpretive discussion in this section will be concerned with the pressure-temperature environment of these mineral assemblages.

The inferred thermal gradient of the pyrite-bearing assemblage in Geysers 1 is extremely steep, dominated by temperatures above the hydrostatic boiling curve. Quartz fluid inclusion data include paleotemperatures of 250°C at 300 m, 325°C at 600 m, and 315°C at 835 m (see Figure 16). Calcite fluid inclusion temperatures are 315°C at 715 m and 355°C at 823 m (see Figure 17). The vein mineral zonation appears to be prograde and progresses from quartz+calcite at shallow depths to quartz+epidote+andradite at 975 m, and finally to quartz+diopside+tremolite+micaceous illite at 1250 m.

The assemblage of epidote+diopside+amphibole is characteristic of temperatures between 320 to 350°C, as indicated by well-documented geothermal systems such as Cerro Prieto (Elders *et al.*, 1978) and the Salton Sea (Kendall, 1976). Andradite garnet stability indicates a temperature range of 300 to 400°C in regional metamorphic environments (Coombs *et al.*, 1977) and andradite garnet in the Salton Sea field corresponds to a temperature of 360°C (McDowell and Elders, 1980). A thermal gradient estimated from these petrologic data and available fluid inclusion temperatures would lie 40°C above hydrostatic boiling for pure water.

There are only two conditions which would permit the geothermal liquid to exist at these temperatures: high salinities (~ 25 wt % NaCl; Haas, 1971) or greater than hydrostatic overburden pressures. Evidence for the existence of concentrated brine solutions is absent as all calculated salinities were low, under 2 wt % NaCl equivalent (see Table 4). Such high pressures cannot be conveniently attributed to a hydrostatic water column as this would require the removal of 690 m of rock material since the emplacement of the veins which give 315°C fluid inclusion temperatures

observed between 700 and 800 m depth in Geysers 1. This leaves a geopressed environment as the only viable option.

A recognized permeability barrier to isolate the fluid at greater than hydrostatic pressure is not apparent (McLaughlin and Stanley, 1976; McLaughlin, 1978) in the Big Geysers area. Serpentinite bodies do act as barriers in other areas of the field, such as the Lakoma Fame track (Lambert, 1977) and the Castle Rock Springs area (McLaughlin and Stanley, 1976). The greenstone (lithologic unit 1) could conceivably have acted as a localized cap, except that this block is now extensively fractured. The known shallow steam reservoir now extends under areas which have no such greenstone cap.

It is likely that the hydrothermal fluids were generated at greater than hydrostatic pressures at depth and subsequently ascended adiabatically. These fluids would migrate along the thrust faults, which were zones of relative weakness, by a combination of hydraulic fracturing, decarbonation, and dissolution of pre-existing mineralized veins. When the initial hot ascending fluids depressurized in proximity to the surface, the conduits would become self-sealed by the precipitation of authigenic minerals (an "incrustation seal"; Facca and Tonani, 1968), preserving geopressed conditions for the fluids below. Several lines of evidence support this. Firstly, pre-existing Franciscan calcite is absent from the isotope record in the geothermal zones of Geysers 1 and Geysers 2. Secondly, the apparent incrustation seal in Geysers 1 is composed not of calcite or anhydrite, as suggested by Facca and Tonani (1968), but of quartz+calcite+adularia, indicative of the precipitation of boiling fluids in a cold environment (Hoagland and Elders, 1978). Thirdly, the mineral

assemblages within the thrust fault zones (pyrite at 200 m, quartz fluid inclusion temperatures at 600 m and diopside and tremolite at 1250 m) are hotter by 10 to 20°C than the surrounding intra-slab mineralization.

The transition of the water-dominated into a vapor-dominated system is recorded by the pyrrhotite mineralization at depth, associated with the pyrite+marcasite mineralization higher in the well bore, and acid leaching and fumaroles at the surface. It has been shown that the pyrrhotite assemblages formed under the same high pressure - superheated conditions as the pyrite assemblages. This indicates that the vaporization process, at least in the early stages, was due to decompression of the reservoir fluids. This interpretation runs counter to the present hydrostatic/under-hydrostatic pressured models based on steam reservoir studies (Truesdell and White, 1973). A thorough discussion of a reservoir model is the topic of the next section.

Lastly, the physical and chemical conditions of deposition of Geysers 2 must be considered. The bulk of the geothermal minerals in the well bore and the stable isotope chemistries are similar to the stage 1 pyrite assemblages of Geysers 1. However, the distribution of geothermal mineralization differs between Geysers 1 and 2. Geysers 1 shows evidence of high paleo-temperatures (above boiling) at relatively shallow depths and intense mineralization in well-defined zones adjacent to thrust faults. This pattern is characteristic of a hydrothermal discharge system (Elders et al., 1980). Geothermal mineralization in Geysers 2 is sparse throughout the well until a depth of 2400 m is attained. The predominance of calcite veining, the wide range of fluid inclusion homogenization temperatures (100 to 300°C below boiling), the paucity of

sulfides and the persistence of Franciscan calcite in the upper 2400 m of this well indicate a limited influx of thermal waters.

The two sulfide assemblages of pyrite+marcasite±base metal sulfides and bornite+hematite are characteristic of acidic and fluctuating oxidation conditions. The assemblage of bornite+pyrite+hematite can form if the pH of the fluid is less than 7, the $\log f_{S_2}$ is -15 to -10 and the $\log f_{O_2}$ is -30 to -40 at the temperatures of 100-200°C which are indicated by fluid inclusion temperatures (see Figure 18) (Barton and Skinner, 1979; Holland, 1959), but the pyrite+base metal sulfide would be unstable and would form only at lower f_{S_2} and f_{O_2} at these temperatures. These variations in chemical environments occur in ore deposits in which ascending and descending fluids occupy the same fracture system (Ramdohr, 1969). The brecciated textures and mineral assemblages observed in the greenstone strata (600 to 1600 m on Figure 14) can also be attributed to the interaction of hot thermal fluids and cold meteoric waters (Toulmin and Clark, 1967). These relationships infer that periodic pulses of high temperature discharge did occur but the fracture system in Geysers 2 was generally saturated by cooler descending meteoric waters.

In Geysers 2, a steep thermal gradient is recorded in the minerals below 2400 m (quartz+adularia+epidote+andradite appear and calcite disappears) and $\delta^{18}O$ values for quartz and calcite decrease rapidly. This pattern of telescoping mineral zones and sudden isotope shifts is observed in recharge zones in Cerro Prieto (Elders *et al.*, 1980). Although a direct comparison between the fracture system of The Geysers and the sandstone aquifers of Cerro Prieto cannot be assumed, the evidence implies recharge. McLaughlin (1977) also proposed that the Cobb Mountain vent area provides recharge to the geothermal system.

Presentation of a Reservoir Model

The following discussion will present a model describing the Geysers reservoir during its water-dominated stage and the chemical and physical transitions of the reservoir fluid during the transition to a vapor-dominated system. The interpretation will be based on the mineral assemblage, fluid inclusion geothermometry and isotope geochemistry of the two wells.

The following observations must be accounted for:

- (1) The stable isotope shift from meteoric to "rock-dominated" signatures.
- (2) The transition of the mineral-depositing fluids from pyrite (high f_{S_2}) to pyrrhotite (low f_{S_2}) precipitation.
- (3) The restriction of the pyrrhotite+calcite assemblage and calcite veining interpreted to be derived from steam condensate to a zone above 610 m, although pyrrhotite distribution is more widespread (especially below 1200 m).
- (4) Geopressured-superheated fluid temperatures as interpreted from fluid inclusion data.
- (5) The present steam reservoir is uniformly under-pressured with respect to hydrostatic conditions, and water entries, with the exception of steam condensate, have not been encountered.

I suggest that the geothermal fluids were conductively heated at depth by the magma chamber beneath The Geysers (McLaughlin, 1977; Iyer *et al.*, 1979; Isherwood, 1976; Chapman, 1975). These geothermal fluids ascended adiabatically through vertical fractures and subsequently migrated

laterally along the steeply dipping thrust fault zones toward the surface. The fluids occupied an interconnected lattice work of fractures throughout the reservoir wackes and this convective circulation carried dissolved solids derived from pre-existing Franciscan carbonate veins. These early geothermal fluids exhibited a pyrite-normal sulfur fugacity and low $\delta^{18}\text{O}$ quartz isotope chemistries. I have called this the "meteoric stage."

Vein material from Geysers 2 and the Lakoma Fame area (Lambert, 1977), sites which are immediately adjacent to Cobb Mountain, exhibit mineral assemblages and calculated $\delta^{18}\text{O}_{\text{H}_2\text{O}}$ which have the meteoric signatures of this "meteoric stage."

The intrusion of volcanic material during the Cobb Mountain volcanism must have generated localized fracturing which allowed the interaction of meteoric water and the heat source. This is significant for three reasons. Firstly, the fractures permitted significant volumes of meteoric waters to permeate through the system, resulting in the low $\delta^{18}\text{O}$ values. Secondly, hydrostatic pressures were prevalent through the open fractures, as evidenced by the fluid inclusion data. Thirdly, the tourmaline deposition reported by Moore (1980) was probably induced by volcanic-derived boron and high temperatures.

The vein materials from well bores Geysers 1 and Thermal 7 (Lambert, 1977), which are located in The Big Geysers area several kilometers west of Cobb Mountain, were deposited under different physical and chemical conditions. The material exhibits calculated $\delta^{18}\text{O}_{\text{H}_2\text{O}}$ values which are indicative of greater water-rock interaction, fluid inclusion temperatures which are indicative of a geopressured environment and a mineralogy characteristic of subsurface boiling. The transition of the water-

dominated system to a vapor-dominated reservoir appears to have been a progressive process as interpreted from Geysers 1. Three stages can be delineated based on observed isotopic and f_{S_2} modifications of the reservoir fluids through time.

The initial hydrothermal activity is similar to the meteoric stage already described. The $\delta^{18}O$ of the quartz crystals associated with the sphalerite grains at 840 m (see Figure 26) bears a strong meteoric signature. The fluid inclusion temperatures of these crystals (see Figure 17) are greater than hydrostatic boiling. It can be concluded that these fluids were geopressed although the cause(s) of the geopressing is (are) unknown. I suggest that the fluids originated at depth under temperatures and pressures greater than hydrostatic and migrated upwards through the thrust fault zones. If this flow occurred not in open fractures but by hydraulic fracturing and the thermal destruction and replacement of the pre-existing Franciscan veins (particularly calcite), then the geopressed conditions could be maintained. In addition to the lithostatic pressure of the rock column, other factors might be hydraulic pressures due to convection or the addition of volatiles, particularly CO_2 (Ellis and Mahon, 1977).

This hydrothermal activity built an incrustation seal at the outer margins of the reservoir where depressurization and boiling occurred. This barrier effectively limited the meteoric recharge into the system, prevented further discharge to the surface and permitted the high geopressed fluid temperatures to develop locally. Continued convective movement below the seal through the fracture network increased the $\delta^{18}O$ composition of the fluids due to considerable wall rock interaction (low

water-rock ratio). I have called this the "sealed-circulation stage" (see Figure 28).

The final step, the vaporization process of the reservoir fluids, is more complex than suggested by White et al. (1971) although the principal mechanism they suggested did operate. A steam cap developed at the crest of the reservoir when steam discharge through fractures (generated by the geopressured conditions in the incrustation seal) exceeded the system's ability to replenish itself by natural recharge (White et al., 1971; Truesdell and White, 1973). This depressurization resulted in a boiling front that did not affect the fractured reservoir uniformly but descended in graduated steps as each successive thrust fault zone was encountered. I have called this the "stepped boiling stage" (see Figure 28).

The rapid changes in pressure induced the precipitation of a mineral barrier at the upper boundary of each successive brecciated fault zone. The extensive pyrite concentrations at 200 m and 600 m coincide with the upper limit of the stable isotope minima which have been shown to be indicative of high flow regimes. Drastic changes in f_{CO_2} , f_{O_2} , f_{S_2} and pH due to boiling induced the mineralogical changes (pyrite to pyrrhotite) in the residual fluids. The depressurization process assured the absolute separation of the steam from the residual fluids, resulting in the supersaturation of calcite and the precipitation of pyrrhotite and base metal sulfides.

The temporary incrustation seal had two effects. Firstly, the fluids below the seal were insulated and able to maintain their high temperatures and overpressures. Secondly, the waters above the seal were trapped in an

isolated basin-like reservoir and subject to cooling, boiling and vaporization, establishing a steam-static condition.

The prevailing temperatures in the entrapped waters had to decline on depressurization due to vapor loss on boiling, forming new steam-static pressure conditions with depth. This cooling is evidenced by the polymodal distribution in quartz and calcite fluid inclusion temperatures (see quartz data at 600 m on Figure 17). The water table in the fracture network gradually descended as the water boiled at the steam-water interface. The evidence for this process is the systematic temperature trend of liquid-dominated calcite fluid inclusions ranging between 200 to 215°C originating at depths from 250 to 610 m (see Figure 16).

It is significant that all evidence for a vapor-saturated reservoir - low $\delta^{13}\text{C}$ calcites derived from steam condensate and steam-equilibrated calcite - is restricted to a zone above 610 m in Geysers 1. Mineralogical evidence for subsurface boiling at elevated temperatures - pyrite dissolution, type 2 pyrrhotite, and coeval calcite+quartz+adularia - is, however, present below 610 m. This implies that a convecting liquid-saturated reservoir persisted below the incrustation seal at 600 m. This fluid was in thermal and barometric disequilibrium with the shallower vapor-dominated reservoir. Later, boiling occurred at near hydrostatic conditions (see Figures 16 and 17).

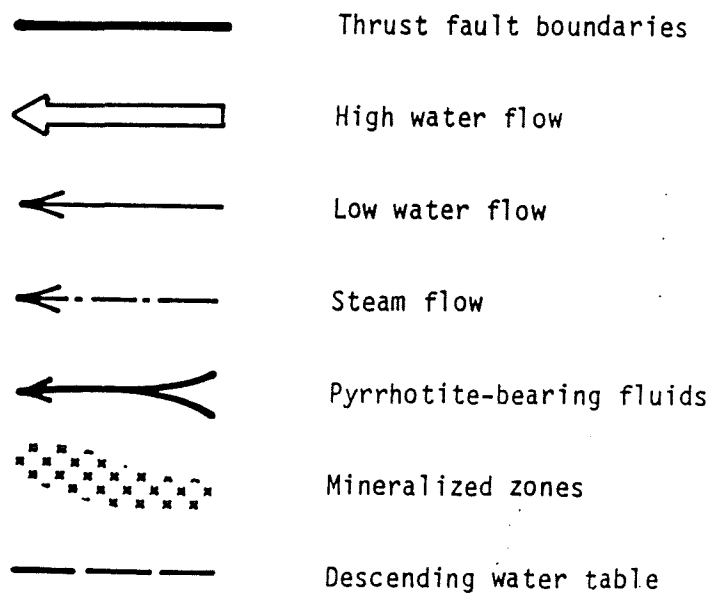
A consequence of the rapidly changing barometric conditions in the shallow boiling reservoir is the generation of fractures due to the build-up of a significant pressure gradient across the incrustation seal. Textural and mineralogical evidence suggests that these mineral seals were periodically breached by hydraulic fracturing. The mineralized

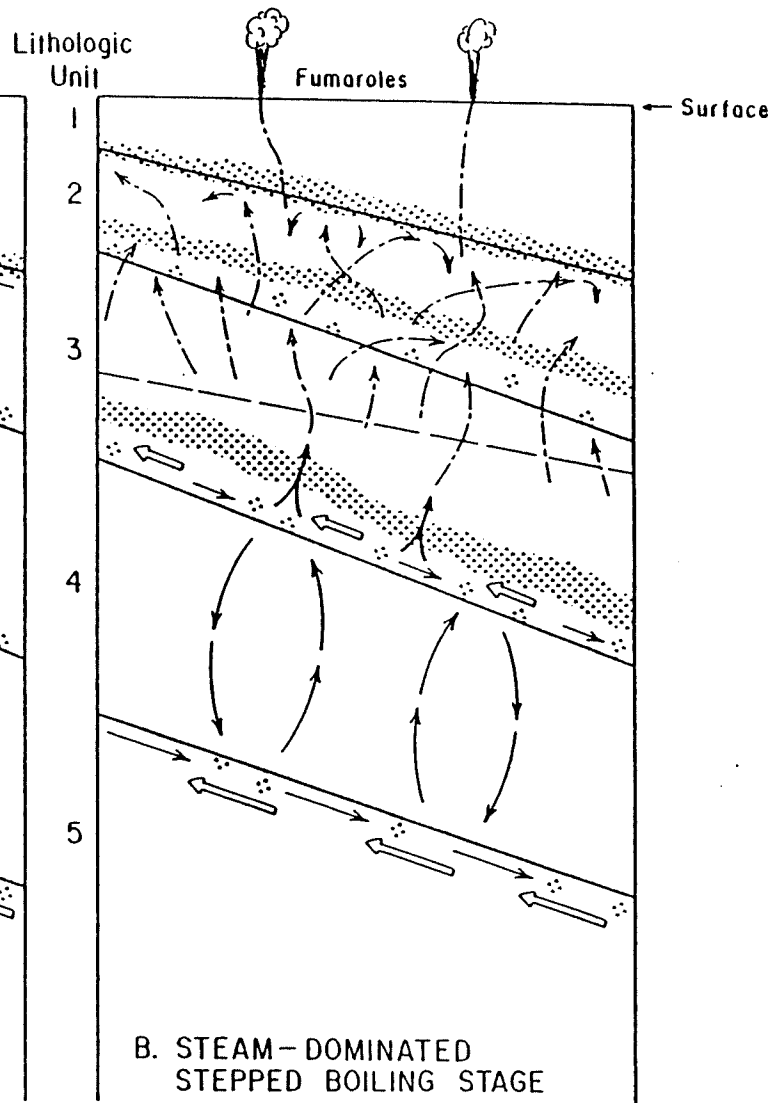
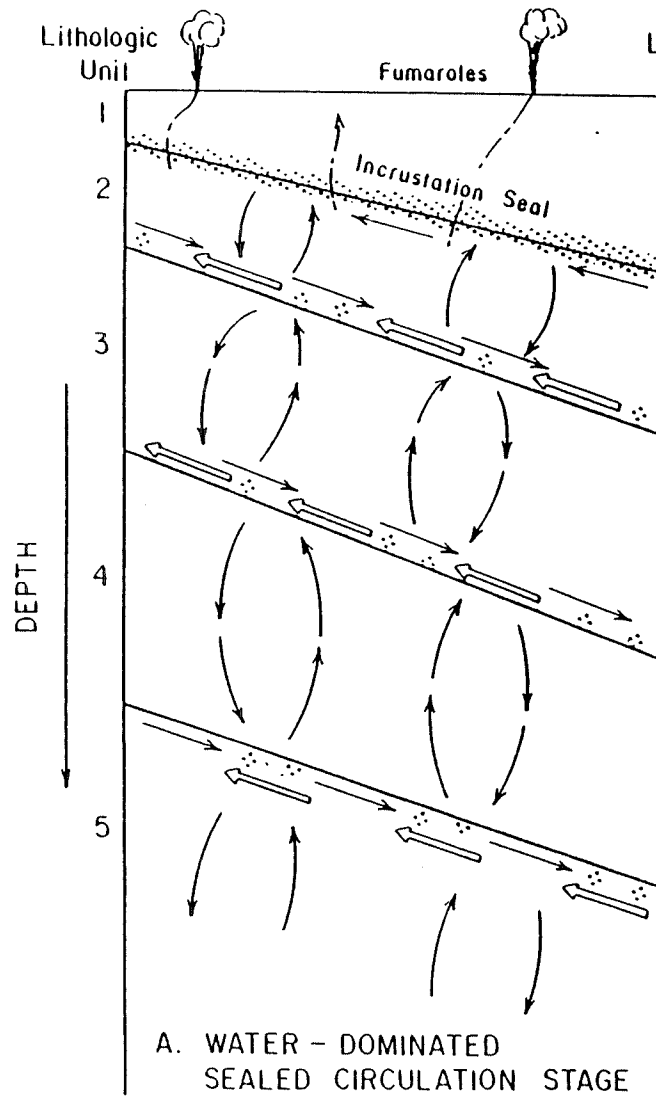
barrier at 200 to 250 m was destroyed, allowing the vaporization of fluids in lithologic unit 3 (see Figure 28). Evidence of brecciation and replacement of massive pyrite veins by marcasite in this zone is appreciable. The mineral seal at 600 m was disrupted by similar episodes of hydraulic fracturing and vein deposition by pyrrhotite-bearing fluids. Superheated fluids which penetrated the seal were flashed into steam in the low pressure region and their residual liquids precipitated quartz and calcite veins (see Figure 28).

The most important controlling factor in the vaporization/decompression reduction of the reservoir fluids is the creation of open fractures to allow expansion of the steam phase while maintaining mass and enthalpy balances. The most obvious mechanism is hydraulic fracturing across the barometric gradient. This method operates on a local scale, but whether or not it is the primary source of fracture generation is open to debate. Another candidate is the catastrophic release of over-pressure due to tectonic activity triggering phreatic eruptions. The Geysers area is a seismically active region and earthquakes have been observed to intensify fumarolic activity in many geothermal areas (i.e., Yellowstone Park, Cerro Prieto). This second mechanism may be a significant factor in the history of the steam reservoir.

Intermittent tectonic movement may explain many curious observations. Production wells in The Geysers have penetrated to a depth of 3,000 m without encountering hot water (Lipman *et al.*, 1978). Steam temperatures and pressures in the deep production wells are consistently vapor static, or less, and steam enthalpies have remained constant, corresponding to the maximum enthalpy for pure water (Truesdell and White, 1972). The measured

Figure 28. Schematic diagram of reservoir model showing sealed circulation and stepped boiling stages.





steam temperature and well-head pressures of Geysers 1, 196°C and 19.4 kg/cm², respectively (Union Geothermal, written communication, 1979) plot on the maximum enthalpy curve (White et al., 1971). This evidence indicates the presence of a pure steam phase at depth. Furthermore, a brine-steam interface is unlikely as steam temperatures and enthalpies (as at Lardarello) should increase with increasing water salinities (Truesdell and White, 1972). This temperature and enthalpy behavior however, is consistent with a decompression model of a geopressed low salinity fluid. Vaporization of a fluid greater than 240°C results in a steam phase characterized by an enthalpy on the maximum enthalpy curve (White et al., 1971).

The distribution of calcite vein material indicative of steam accumulation (isotope and fluid inclusion evidence) in Geysers 1 is restricted to a zone between 200 and 610 m. Below 610 m the occurrences of pyrrhotite, the only mineralogical evidence for the transition of water to steam, are localized to a distinct aureole about what is now the primary steam entries but was once a zone of high fluid flow, as evidenced by the concentrations of diopside, tremolite, sphalerite and chalcopyrite. It can be inferred that the vaporization process was slow and steady above 610 m allowing the development of a mineralized barrier and a well-defined descending water table.

A progressive stepped boiling mechanism or the Truesdell and White descending water table model would predict the continuous deposition of steam associated calcite veins plus pyrrhotite. Below 610 m, however, no evidence for vaporization is preserved except for the minor localized type 2 pyrrhotite deposition. This absence indicates a rapid large

scale vaporization process without a vapor-static equilibrated descending water table. The steam entries in Geysers 1 do correspond to the fractures once occupied by water. Minor, insignificant entries correspond to minor intra-slab fractures and the major production pressured steam entries correspond to the primary flow channels of a thrust fault zone.

Thus, one possible working hypothesis for the history of Geysers 1, and possibly the steam field as a whole, is that at one time the steam zone was restricted to a shallow zone in the Big Geysers - Big Sulphur Creek area induced by natural attrition of circulating fluids and the stepped boiling of a geopressured system. Subsequently, a succession of tectonic events catastrophically released steam and pressures at increasing depths, driving the existing water table downward and allowing the expansion of vaporized fluids into pre-existing fractures and ultimately to the surface.

The model described in this paper is based on observations collected from the study of only two wells. Two wells are not sufficient to characterize the hydrothermal activity of an entire reservoir, especially when the geothermal system is as large and as complex as The Geysers. Additional wells must be studied to substantiate or revise the mechanisms suggested here. The Geysers steam field is composed of five major steam concentrations (Dick Thomas, oral communication, 1981). Each localized steam reservoir may be characterized by unique subsurface structural geometries and authigenic mineral assemblages (McLaughlin and Stanley, 1976; Moore, 1980). More research is necessary to characterize the reservoir rocks in all areas of The Geysers in order to optimize the exploitation of all available energy resources.

REFERENCES

- Anderson, C. A., 1936, Volcanic history of the Clear Lake area, California; Geol. Soc. Am. Bull., 47, pp. 629-664.
- Bailey, E. H., 1946, Quicksilver deposits of the western Mayacmas district, Sonoma County, California; Calif. Jour. of Min. and Geol., 42, no. 3, pp. 199-230.
- Bailey, E. H., Irwin, H. P. and Jones, D. L., 1964, Franciscan and related rocks and their significance in the geology of western California; Calif. Div. Mines and Geol. Bull., 183, 177 p.
- Barton, P. B. and Skinner, B. J., 1979, Sulfide Mineral Stability, from Geochemistry of Hydrothermal Ore Deposits, 2nd ed., Barnes (ed.), John Wiley and Sons, New York.
- Blake, M. C., Jr., Irwin, W. P. and Coleman, R. G., 1967, Upside-down metamorphic zonation, blueschist facies, along a regional thrust in California and Oregon; U.S.G.S. Prof. Paper 575-C, pp. C1-C9.
- Browne, P. R. L., 1969, Sulfide mineralization in a Broadlands geothermal drill hole, Taupo Volcanic Zone, New Zealand; Econ. Geol., 64, pp. 156-159.
- Browne, P. R. L., 1971, Mineralisation in the Broadlands Geothermal Field, Taupo Volcanic Zone, New Zealand; Soc. Mining Geol., Japan, Spec. Issue 2, pp. 64-75.
- Browne, P. R. L., 1978, Hydrothermal alteration in active geothermal fields; Ann. Rev. Earth Planet. Sci., 6, pp. 229-250.
- Browne, P. R. L. and Ellis, A. J., 1970, The Ohaki-Broadlands hydrothermal area, New Zealand: Mineralogy and related chemistry; Am. Jour. Sci., 269, pp. 97-131.

- Browne, P. R. L. and Lovering, J. F., 1973, Composition of sphalerites from the Broadlands Geothermal Field and their significance to sphalerite geothermometry and geobarometry, *Econ. Geol.*, 68, pp. 381-387.
- Browne, P. R. L., Roedder, E. and Antoni, W., 1976, Comparison of past and present geothermal waters, from a study of fluid inclusions, Broadlands Field, New Zealand; *Proc. Int'l. Symp. on Water-Rock Interaction, Czechoslovakia, 1974*.
- Chapman, R. H., 1975, Geophysical study of the Clear Lake region, California; *Calif. Div. of Mines and Geol., spec. rept. 116*, 23 p.
- Clayton, R. N., O'Neil, J. R. and Mayeda, T. K., 1972, Oxygen isotopic exchange between quartz and water; *Jour. Geophys. Res.*, 77, no. 17, pp. 3057-3067.
- Coombs, D. S., Kawachi, Y., Houghton, B. F., Hyden, G., Pringle, J. J. and Williams, J. G., 1977, Andradite and andradite-grossular solid solutions in very low-grade regionally metamorphosed rocks in southern New Zealand; *Contrib. Mineral. Petrol.*, 63, pp. 229-246.
- Coplen, T. B., 1973, A double-focusing, double-collecting mass spectrometer for light stable isotope ratio analysis; *Int. J. Mass Spectrom. Ion Phys.*, 11, pp. 37-40.
- Craig, H., 1963, The isotopic geochemistry of water and carbon in geothermal areas; in Nuclear Geology in Geothermal Areas, E. Torgiorgi (ed.), Conference Spoleto, Consiglio Nazionale Delle Ricerche, Laboratorio di Geologia Nucleare - Pisa.
- Craig, J. R. and Scott, S. D., 1974, Sulfide phase equilibria; from *Sulfide Mineralogy, Min. Soc. Am. Short Course Notes*, pp. CS1-CS110.

- Dickinson, W. R., 1970, Interpreting detrital modes of graywacke and arkose; *Jour. Sed. Pet.*, 40, no. 2, pp. 695-707.
- Donnelly, J. M., Hearn, B. C. and Goff, F. E., 1977, The Clear Lake volcanics, California: Geology and Field Trip Guide; from Field Trip Guide to the Geysers-Clear Lake Area, Cordilleran Section of the Geological Society of America.
- Ehni, W. J., 1981, Summary of 1980 geothermal drilling; western United States; *Geothermal Energy*, 9, no. 9, pp. 4-15.
- Elders, W. A., Hoagland, J. R., Olson, E. R., McDowell, S. D. and Collier, P., 1978, A comprehensive study of samples from geothermal reservoirs: Petrology and light stable isotope geochemistry of twenty-three wells in the Cerro Prieto geothermal field, Baja California, Mexico; *Univ. Calif., Riverside/Inst. of Geophys. and Planet. Phys. rept.* 78/26, 264 p.
- Elders, W. A., Hoagland, J. R. and Williams, A. E., 1980, Hydrothermal alteration as an indicator of temperature and flow regime in the Cerro Prieto geothermal field of Baja California; *Geother. Res. Council*, 4, pp. 121-125.
- Ellis, A. J. and Mahon, W. A. J., 1977, Chemistry and Geothermal Systems, Academic Press, New York.
- Ernst, W. G., 1971, Petrologic reconnaissance of Franciscan metagraywackes from the Diablo Range, central California Coast Ranges; *Jour. Petrol.*, 12, pp. 413-437.
- Ernst, W. G., 1972, CO₂-poor composition of the fluid attending Franciscan and Sanbagawa low-grade metamorphism; *Geochim. Cosmochim. Acta*, 36, pp. 497-504.

- Facca, G. and Tonani, F., 1967, The self-sealing geothermal field, Bull. Volcan., 30, pp. 271-273.
- Freckman, J. T., 1978, Fluid inclusion and oxygen isotope geothermometry of rock samples from Sinclair #4 and Elmore #1 boreholes, Salton Sea Geothermal Field, Imperial Valley, California, U.S.A.; Master's thesis, Univ. of Calif., Riverside/Inst. Geophys. and Planet. Phys. rept. 78/5, 76 p.
- Friedman, I. and O'Neil, J. R., 1977, Compilation of stable isotope fractionation factors of geochemical interest; U.S.G.S. Prof. Paper 440-KK.
- Fritz, P., 1976, Oxygen and carbon isotopes in ore deposits in sedimentary rocks; from Handbook of Strata-bound and Stratiform Ore Deposits, K. H. Wolf (ed.), pp. 191-217, Elsevier-Scientific Publishing Co., Amsterdam.
- Garrels, R. M. and Christ, C. L., 1965, Solutions, Minerals and Equilibria; Freeman, Cooper and Co., San Francisco.
- Garrison, L. E., 1972, Geothermal steam in The Geysers-Clear Lake region, California; Geol. Soc. Am. Bull., 83, pp. 1449-1468.
- Glass, W. A., 1977, 1977 drilling methods and costs at The Geysers, in Geothermal: State of the Art; Geotherm. Res. Council Trans., 1, pp. 103-104.
- Haas, J. L., Jr., 1971, The effect of salinity on the maximum thermal gradient of a hydrothermal system at hydrostatic pressure; Econ. Geol., 66, pp. 940-946.
- Hearn, B. C., Jr., Donnelly, J. M. and Goff, F. E., 1976a, Geology and geochronology of the Clear Lake volcanics, California; Proc. 2nd U.N. Symp. on the Develop. and Use of Geothermal Resources, 1, p. 423.

- Hearn, B. C., Jr., Donnelly, J. M. and Goff, F. E., 1976b, Preliminary geologic map of the Clear Lake volcanic field, Lake County, California; U.S.G.S. Open File Rept. 75-391.
- Helgeson, H. C., 1969, Thermodynamics of hydrothermal systems at elevated temperatures and pressures; *Am. Jour. Sci.*, 267, pp. 729-804.
- Hoagland, J. R. and Elders, W. A., 1978, Hydrothermal mineralogy and isotopic geochemistry in the Cerro Prieto Geothermal Field, Mexico. I. Hydrothermal mineral zonation, *Geother. Res. Council Trans.*, 2, pp. 283-286.
- Holland, H. D., 1959, Some applications of thermochemical data to problems of ore deposits. I. Stability relations among the oxides, sulfides, sulfates, and carbonates of ore and gangue metals; *Econ. Geol.*, 54, p. 184.
- Huebner, M., 1981, Carbon-13 isotope values for CO₂ and dissolved carbon species from selected springs and wells in the Clear Lake-Geysers region; from U.S.G.S. Prof. Paper 1141.
- Hurlbut, C. S., Jr., 1971, Dana's Manual of Mineralogy, John Wiley and Sons, New York.
- Isherwood, W. F., 1976, Gravity and magnetic studies of the Geysers-Clear Lake geothermal region, California, U.S.A.; *Proc. 2nd U.N. Symp. on the Develop. and Use of Geothermal Resources*, 2, pp. 1065-1073.
- Iyer, H. M., Oppenheimer, D. H. and Hitchcock, T., 1979, Abnormal P-wave delays in The Geysers-Clear Lake geothermal area, California; *Science*, 204, pp. 495-497.
- Kendall, C., 1976, Petrology and stable isotope geochemistry of three wells in the Buttes area of the Salton Sea geothermal field, Imperial

- Valley, California, U.S.A.; Master's thesis, Univ. Calif., Riverside/
Inst. Geophys. and Planet. Phys. rept. 76/17, 227 p.
- Lambert, S. J., 1976, Stable isotope studies of some active hydrothermal systems; unpublished Dissertation, California Inst. of Technology.
- Liou, J. C., 1971, P-T stabilities of laumontite, wairakite, lawsonite, and related minerals in the system $\text{CaAl}_2\text{Si}_2\text{O}_8\text{-SiO}_2\text{-H}_2\text{O}$; J. Petrol., 12, part 2, pp. 379-411.
- Lipman, S. C., Strobel, C. J. and Gulati, M. S., 1978, Reservoir performance of The Geysers field; Geothermics, 7, pp. 209-219.
- McDonald, J. A., 1967, Metamorphism and its effects on sulphide assemblages; Min. Dep., 2, pp. 200-220.
- McDowell, S. and Elders, W. A., 1980, Authigenic layer silicate minerals in borehole Elmore 1, Salton Sea Geothermal Field, California, U.S.A.; Contrib. Mineral. Petrol., 74, pp. 293-310.
- McKibben, M. A., 1979, Ore minerals in the Salton Sea geothermal system, Imperial Valley, California, U.S.A.; Master's thesis, Univ. Calif., Riverside/Inst. Geophys. and Planet. Phys. rept. 79/17, 99 p.
- McLaughlin, R. J., 1974, Preliminary geologic map of The Geysers steam field and vicinity, Sonoma County, California; U.S.G.S. Open File Map 74-238.
- McLaughlin, R. J., 1977, The Franciscan assemblage and Great Valley sequence in The Geysers-Clear Lake region of northern California; in Field Trip Guide to The Geysers-Clear Lake Area from Cordilleran Section of the Geological Society of America, pp. 3-24.
- McLaughlin, R. J., 1978, Preliminary geologic map and structural sections of the central Mayacmas Mountains and The Geysers steam field, Sonoma,

- Lake and Mendocino Counties, California; U.S.G.S. Open File Rept. 78-389.
- McLaughlin, R. J. and Stanley, W. D., 1976, Pre-Tertiary geology and structural control of geothermal resources, The Geysers steam field, California; Proc. 2nd U.N. Symp. on the Develop. and Use of Geothermal Resources, 1, pp. 475-485.
- McNitt, J. R., 1961, Geology of The Geysers thermal area, California; Proc. U.N. Conf. on New Sources of Energy, Geothermal Energy, 2, 1, Rome.
- McNitt, J. R., 1968, Geology of the Kelseyville quadrangle, Sonoma, Lake and Mendocino Counties, California; Calif. Div. Mines and Geol., Map Sheet no. 9.
- Miyashiro, A., 1973, Metamorphism and Metamorphic Belts, Halsted Press, New York.
- Moore, D., 1980, Hydrothermal alteration minerals of The Geysers steam field, California, and their potential use in exploration; Stanford Geothermal Workshop.
- Nehring, N., 1981, Gases from springs and wells in the Clear Lake-Geysers area of northern California; from U.S.G.S. Prof. Paper 1141.
- Potter, R. W., II, Pressure corrections for fluid inclusion homogenization temperatures based on the volumetric properties of the steam NaCl-H₂O; Hour. Res. U.S.G.S., 5, no. 5, pp. 603-607.
- Ramdohr, P., 1969, The Ore Minerals and Their Intergrowths, Pergamon Press, Oxford.
- Roedder, E., 1963, Studies of fluid inclusions II: Freezing data and their interpretations; Econ. Geol., 58, no. 2, pp. 167-211.

- Roedder, E., 1972, Composition of fluid inclusions; U.S.G.S. Prof. Paper 440-JJ.
- Roedder, E., 1976, Fluid inclusion evidence on the genesis of ores in sedimentary and volcanic rocks; from Handbook...Ore Deposits, Wolf (ed.), Elsevier Publishing Co., pp. 67-110.
- Roedder, E., 1979, Fluid inclusions as samples of ore fluids; from Geochemistry of Hydrothermal Ore Deposits; 2nd ed., H. Barnes (ed.), pp. 684-737.
- Schriener, A., Jr. and Suemnicht, G., 1980, Subsurface intrusive rocks at The Geysers geothermal area, California; U.S.G.S. Open File Rept.
- Shieh, Y. N. and Taylor, H. P., Jr., 1969, Oxygen and carbon isotope studies of contact metamorphism of carbonate rocks; Jour. Pet., 10, pt. 2, pp. 307-331.
- Steiner, A., 1958, Occurrence of wairakite at The Geysers, California; Am. Mineral., 43, p. 781.
- Swanson, S. E. and Schiffman, P., 1979, Textural evolution and metamorphism of pillow basalts from the Franciscan complex, western Marin County, California; Contrib. Mineral. Petrol., 69, pp. 291-299.
- Toulmin, P. and Clark S., Jr., 1967, Thermal aspects of ore formations; in Geochemistry of Hydrothermal Ore Deposits, H. Barnes (ed.), John Wiley and Sons, New York.
- Truesdell, A. H. and Nathenson, M., 1978, Downhole measurements and fluid chemistry of a castle rock steam well, The Geysers, Lake County, California; 4th Workshop on Geothermal Reservoir Engineering, pp. 96-105.

- Truesdell, A. H. and White, D. E., 1973, Production of superheated steam from vapor-dominated geothermal reservoirs; *Geothermics*, 2, no. 3-4, pp. 154-173.
- Vonsen, M., 1946, Minerals at "The Geysers," Sonoma County, California; *Calif. Jour. Mines and Geol.*, 42, pp. 287-293.
- Weres, O. Tsao, K. and Wood, B., 1977, Resource, technology and environment at The Geysers; Lawrence Berkeley Laboratory rept. LBL-5231.
- White, D. E., Muffler, L. J. P. and Truesdell, A. H., 1971, Vapor-dominated hydrothermal systems compared with hot-water systems; *Econ. Geol.*, 66, pp. 75-97.
- Winkler, H. G. F., 1979, Petrogenesis of Metamorphic Rocks (5th ed.), Springer-Verlag, New York.
- Wise, W. S., Nokleberg, W. J. and Kokinos, M., 1969, Clinoptilolite and ferrierite from Agoura, California; *Am. Min.*, 54, pp. 887-893.
- Wise, W. S. and Tschernich, R. W., 1976, Chemical composition of ferrierite; *Am. Min.*, 61, pp. 60-66.

APPENDIX

TABLE A-1

Samples Used in XRD Standardization

<u>Rock Type</u>	<u>Textural Grade*</u>	<u>Source Location</u>
Meta-greywacke (lawsonite)	1	UCR #2977**
Meta-greywacke (lawsonite+jadeite)	2	UCR #2978
Meta-greywacke (lawsonite+jadeite+ glaucophane)	2.5	UCR #2979
Blueschist (lawsonite+jadeite+ glaucophane)	3	UCR #2987
Greenstone (lawsonite+jadeite)	1.5	UCR #2972
fs ₁ meta-greywacke [†]	1	T11N R9W Sec 25
fs ₁ argillite	1	T11N R9W Sec 25
fs ₂ meta-greywacke	2	T11N R8W Sec 19
fs ₂ argillite	1.5	T11N R8W Sec 7

* Blake *et al.*, 1964.

** UCR Panóche Pass collection

† McLaughlin, 1974 and 1978.

Table A-2
XRD mineralogy of
Geysers 1 sandstones

SAMPLE NO.	DEPT	QUAR	PLAG	ALKA	MICA	ILLI	IMIX	2MIX	MONT	CILO	CALC	DOLO	ARAG	MAIR	LAUM	PUMP	LWSO	PYRI	HEMA	ILME	MAGN	EPID	PREH	AMPH	AUGI	
001D	210.0	30.0	29.6	6.8	-	8.9	2.2	-	-	19.4	1.2	-	-	-	-	-	-	1.9	-	-	-	-	-	-	-	
003D	400.0	46.1	21.1	6.0	-	9.9	4.0	-	-	10.8	0.5	-	-	-	-	-	-	1.7	-	-	-	-	-	-	-	
004D	500.0	42.6	29.1	8.4	-	7.9	-	-	-	11.9	-	-	-	-	-	-	-	1.7	-	-	-	-	-	-	-	
005D	600.0	44.6	23.3	5.1	-	8.5	1.7	-	-	12.9	3.1	-	-	-	-	-	-	0.7	-	-	-	-	-	-	-	
006D	760.0	41.2	25.7	5.3	-	7.0	3.5	-	-	13.4	2.3	-	-	-	-	-	-	1.5	-	-	-	-	-	-	-	
007D	860.0	38.4	15.2	7.5	-	9.3	9.3	-	-	10.6	1.6	-	-	-	-	-	-	-	-	-	-	-	-	-	-	
008D	1000.0	43.7	23.2	6.0	-	8.2	4.9	-	-	12.5	2.6	-	-	-	-	-	-	-	-	-	-	-	-	-	-	
009D	1100.0	42.1	24.1	6.6	-	9.1	5.4	-	-	12.8	1.0	-	-	-	-	-	-	-	-	-	-	-	-	-	-	
010D	1200.0	42.2	24.6	6.6	-	9.2	2.3	-	-	13.8	2.4	-	-	-	-	-	-	-	-	-	-	-	-	-	-	
011D	1300.0	43.4	21.6	5.3	-	10.4	7.0	-	-	12.3	-	-	-	-	-	-	-	-	-	-	-	-	-	-	-	
012D	1400.0	42.4	25.4	4.8	-	9.5	3.2	-	-	12.1	2.5	-	-	-	-	-	-	-	-	-	-	-	-	-	-	
013D	1500.0	40.8	26.0	4.7	-	9.8	3.9	-	-	13.8	1.0	-	-	-	-	-	-	-	-	-	-	-	-	-	-	
014D	1600.0	41.1	22.1	5.4	-	10.7	-	-	-	13.6	3.3	-	-	-	-	-	-	-	-	-	-	-	-	-	-	
015D	1700.0	43.6	23.6	5.0	-	8.2	-	-	-	14.5	1.1	-	-	-	-	-	-	3.7	-	-	-	-	-	-	-	
016D	1820.0	42.1	23.6	5.8	-	11.4	-	-	-	12.4	1.5	-	-	-	-	-	-	4.3	-	-	-	-	-	-	-	
017D	1920.0	47.7	23.6	6.0	-	11.8	-	-	-	7.5	1	-	-	-	-	-	-	3.2	-	-	-	-	-	-	-	
018D	2000.0	39.9	19.1	4.2	-	24.2	-	-	-	10.4	2.3	-	-	-	-	-	-	3.3	-	-	-	-	-	-	-	
019D	2100.0	45.0	27.0	7.6	-	8.4	-	-	-	10.3	1.7	-	-	-	-	-	-	-	-	-	-	-	-	-	-	
020D	2200.0	47.7	23.1	6.8	-	9.3	-	-	-	13.2	1	-	-	-	-	-	-	-	-	-	-	-	-	-	-	
021D	2300.0	46.9	23.4	7.1	-	9.8	-	-	-	10.7	2.1	-	-	-	-	-	-	-	-	-	-	-	-	-	-	
022D	2400.0	47.8	21.4	8.0	-	10.9	-	-	-	11.9	1	-	-	-	-	-	-	-	-	-	-	-	-	-	-	
023D	2500.0	43.2	27.3	6.0	-	12.3	-	-	-	11.2	1.1	-	-	-	-	-	-	-	-	-	-	-	-	-	-	
024D	2600.0	39.4	29.3	6.4	-	10.6	-	-	-	14.4	-	-	-	-	-	-	-	-	-	-	-	-	-	-	-	
025D	2700.0	45.6	27.2	8.6	-	7.1	-	-	-	9.0	1.5	-	-	-	-	-	-	-	-	-	-	-	-	-	-	
026D	2800.0	43.5	26.5	6.9	-	8.5	-	-	-	9.3	-	-	-	-	-	-	-	-	-	-	-	-	-	-	-	
027D	2900.0	46.3	26.8	5.4	-	8.9	-	-	-	8.5	-	-	-	-	-	-	-	-	-	-	-	5.2	-	-	-	
																						4.1	-	-	-	-

Table A-3
 XRD mineralogy of
 Geysers 1 shales

SAMPLE NO.	DEPT	QUAR	PLAG	ALKA	MICA	ILLI	IMIX	2MIX	MONT	CHLO	CALC	DOLO	ARAG	HAIR	LAUM	PUMP	LNSO	PYRI	HEMA	ILME	MAGN	EPID	PREH	AMPH	AUGI
0280	400 0	30.1	11.7	4.4	-	14.4	9.6	-	-	19.7	-	-	-	-	-	-	-	2.0	-	-	-	-	-	-	-
0290	600 0	44.0	13.1	3.3	-	10.8	6.4	-	-	19.1	2.1	-	-	-	-	-	-	2.2	-	-	-	-	-	-	-
29 5	860 0	26.9	4.4	4.0	-	26.3	6.6	-	-	30.5	-	-	-	-	-	-	-	1.4	-	-	-	-	-	-	-
0300	1100 0	38.2	10.0	4.1	-	20.3	6.8	-	-	19.7	-	-	-	-	-	-	-	0.9	-	-	-	-	-	-	-
0310	1300 0	39.0	8.0	2.7	-	20.3	4.5	-	-	22.1	2.4	-	-	-	-	-	-	0.9	-	-	-	-	-	-	-
0320	1700 0	31.1	10.0	3.9	-	25.0	-	-	-	26.4	-	-	-	-	-	-	-	2.7	-	-	-	-	-	-	-
0330	1900 0	26.4	15.0	6.6	-	24.6	-	-	-	20.9	-	-	-	-	-	-	-	5.7	-	-	-	-	-	-	-
0340	2100 0	34.5	12.0	5.5	-	27.1	-	-	-	14.0	2.4	-	-	-	-	-	-	3.8	-	-	-	-	-	-	-
0350	2200 0	33.1	10.4	6.3	-	26.0	-	-	-	24.1	-	-	-	-	-	-	-	-	-	-	-	-	-	-	-
0360	2500 0	29.1	16.1	9.2	-	21.1	-	-	-	23.0	1.6	-	-	-	-	-	-	-	-	-	-	-	-	-	-
0370	2600 0	26.3	18.0	8.0	-	23.2	-	-	-	23.7	-	-	-	-	-	-	-	-	-	-	-	-	-	-	-

Table A-4
XRD mineralogy of
Geysers 1 air drilled cuttings

SAMPL NO.	DEPT	QUAR	PLAG	ALKA	NICA	ILLI	IMIX	2MIX	MOHT	CHLO	CALC	DOLO	ARAG	MAIR	LAUN	PUMP	LHSO	PYRI	HEMA	ILME	MAGN	EPID	PREH	AMPH	AUGI
0380	3000	48.8	21.1	10.3	-	6.8	-	-	-	11.1	1.8	-	-	-	-	-	-	-	-	-	-	-	-	-	-
0390	3100	47.8	20.2	7.9	-	9.7	-	-	-	10.6	0.9	-	-	-	-	-	-	-	-	-	-	-	-	-	-
0400	3200	48.1	22.9	7.8	-	6.5	-	-	-	8.8	-	-	-	-	-	-	-	-	-	-	-	3.0	-	-	-
0410	3300	44.8	25.5	11.7	-	6.4	-	-	-	8.7	-	-	-	-	-	-	-	-	-	-	-	5.9	-	-	-
0420	3400	50.8	24.8	10.7	-	2.9	-	-	-	8.0	-	-	-	-	-	-	-	-	-	-	-	2.9	-	-	-
0430	3500	47.8	21.1	15.4	-	3.2	-	-	-	6.9	-	-	-	-	-	-	-	-	-	-	-	2.7	-	-	-
0440	3600	49.5	28.5	11.1	-	3.1	-	-	-	5.0	-	-	-	-	-	-	-	-	-	-	-	5.8	-	-	-
0450	3700	49.0	25.7	10.6	-	6.8	-	-	-	6.3	-	-	-	-	-	-	-	-	-	-	-	2.8	-	-	-
0460	3800	47.3	25.3	11.6	-	3.2	-	-	-	6.9	-	-	-	-	-	-	-	-	-	-	-	2.6	-	-	-
0470	3920	49.4	24.6	10.6	-	5.8	-	-	-	9.6	-	-	-	-	-	-	-	-	-	-	-	5.8	-	-	-
0480	4000	50.3	18.1	11.5	-	6.3	-	-	-	12.0	-	-	-	-	-	-	-	-	-	-	-	-	-	-	-
0490	4100	47.8	21.4	9.7	-	6.4	-	-	-	7.0	-	-	-	-	-	-	-	-	-	-	-	-	-	-	1.8
0500	4200	44.5	20.4	11.1	-	9.2	-	-	-	10.0	-	-	-	-	-	-	-	-	-	-	-	5.8	-	-	1.8
0510	4300	45.0	18.9	11.7	-	7.7	-	-	-	12.7	-	-	-	-	-	-	-	-	-	-	-	-	-	1.4	3.4
0520	4400	46.2	18.8	10.7	-	7.1	-	-	-	11.6	-	-	-	-	-	-	-	-	-	-	-	-	-	1.8	2.2
0530	4500	43.4	20.3	12.3	-	10.2	-	-	-	13.8	-	-	-	-	-	-	-	-	-	-	-	-	-	1.6	4.0
0540	4600	48.3	23.3	9.9	-	6.6	-	-	-	7.1	-	-	-	-	-	-	-	-	-	-	-	-	-	-	-
0550	4700	50.8	21.1	11.9	-	5.6	-	-	-	10.7	-	-	-	-	-	-	-	-	-	-	-	-	-	3.0	1.8
0560	4800	49.3	20.3	9.9	-	9.8	-	-	-	10.7	-	-	-	-	-	-	-	-	-	-	-	-	-	-	-
0570	4900	50.6	21.9	12.8	-	7.0	-	-	-	7.7	-	-	-	-	-	-	-	-	-	-	-	-	-	-	-
0580	5000	45.0	25.4	11.6	-	7.6	-	-	-	10.4	-	-	-	-	-	-	-	-	-	-	-	-	-	-	-
0590	5100	50.1	23.2	12.7	-	-	-	-	-	7.6	-	-	-	-	-	-	-	-	-	-	-	-	-	-	-
0600	5200	47.1	22.6	12.9	-	-	-	-	-	11.6	-	-	-	-	-	-	-	-	-	-	-	6.3	-	-	-
0610	5300	38.1	24.4	11.1	-	11.0	-	-	-	12.0	-	-	-	-	-	-	-	-	-	-	-	-	-	5.8	-
																								3.3	-

Table A-6
XRD mineralogy of
Geysers 2 shales

SAMPLE NO.	DEPT	QUAR	PLAG	ALKA	MICA	ILLI	IMIX	ZMIX	MONT	CHLO	VERM	CALC	HATR	LAUM	PUMP	LWSO	PYRI	HEMA	ILME	MAGH	EPID	PREH	AMPH	AUGI	JADE	GLAU
31	320.0	28.0	8.2	5.1	-	6.2	-	-	32.3	15.1	5.0	-	-	-	-	-	-	-	-	-	-	-	-	-	-	-
32	400.0	31.1	20.3	10.3	-	11.3	2.8	-	-	20.1	3.2	0.8	-	-	-	-	-	-	-	-	-	-	-	-	-	-
33	520.0	35.6	17.8	9.6	-	11.9	2.0	-	-	18.4	4.7	-	-	-	-	-	-	-	-	-	-	-	-	-	-	-
34	800.0	28.7	12.0	6.0	-	17.8	1.6	-	-	25.8	5.9	1.1	-	-	-	-	1.2	-	-	-	-	-	-	-	-	-
35	900.0	19.5	15.8	7.1	-	24.9	2.8	-	-	29.0	-	-	-	-	-	-	0.9	-	-	-	-	-	-	-	-	-
36	4200.0	29.9	17.9	6.2	-	15.6	3.9	-	-	25.7	-	0.9	-	-	-	-	-	-	-	-	-	-	-	-	-	-
37	4300.0	22.4	20.9	11.5	-	14.6	2.2	-	-	27.6	-	-	-	-	-	-	0.8	-	-	-	-	-	-	-	-	-
38	5600.0	25.1	16.7	6.9	-	18.7	2.2	-	-	28.7	-	-	-	-	-	-	-	-	-	-	-	-	-	-	-	-
39	5700.0	29.9	18.2	4.3	-	19.8	3.1	-	-	31.0	-	1.7	-	-	-	-	-	-	-	-	-	1.8	-	-	-	-
40	5800.0	26.9	15.7	6.6	-	16.8	2.0	-	-	30.7	-	-	-	-	-	-	-	-	-	-	-	-	-	-	-	-
41	5900.0	21.8	15.7	7.2	-	22.6	3.7	-	-	28.4	-	0.7	-	-	-	-	-	-	-	-	-	1.3	-	-	-	-
42	6000.0	22.1	18.8	6.7	-	20.8	3.5	-	-	26.3	-	-	-	-	-	-	-	-	-	-	-	-	-	-	-	-
43	6100.0	34.4	18.2	4.8	-	10.5	2.6	-	-	28.9	-	0.5	-	-	-	-	-	-	-	-	-	1.8	-	-	-	-
44	6200.0	31.1	14.9	5.1	-	9.5	0.4	-	-	39.0	-	-	-	-	-	-	-	-	-	-	-	-	-	-	-	-
45	6300.0	23.6	15.5	4.4	-	19.9	3.0	-	-	33.6	-	-	-	-	-	-	-	-	-	-	-	-	-	-	-	-
46	6420.0	25.7	21.0	7.7	-	15.6	2.2	-	-	27.9	-	-	-	-	-	-	-	-	-	-	-	-	-	-	-	-
47	6500.0	30.2	15.2	9.1	-	13.1	2.2	-	-	29.4	-	0.9	-	-	-	-	-	-	-	-	-	-	-	-	-	-
48	6800.0	35.9	26.6	4.9	-	14.6	2.8	-	-	7.5	-	0.8	-	-	-	-	-	-	-	-	-	-	-	-	-	-
49	7000.0	65.7	11.6	4.7	-	8.6	1.1	-	-	8.1	-	0.7	-	-	-	-	-	-	-	-	-	6.8	-	-	-	-
50	7100.0	32.3	17.2	7.4	-	18.4	-	-	-	22.4	-	0.9	-	-	-	-	1.7	-	-	-	-	-	-	-	-	-
51	7200.0	33.5	24.3	8.2	-	14.3	-	-	-	16.8	-	-	-	-	-	-	1.4	-	-	-	-	-	-	-	-	-
52	7300.0	29.2	16.4	7.4	-	26.7	4.6	-	-	13.3	-	2.2	-	-	-	-	-	-	-	-	-	2.9	-	-	-	-
53	7700.0	27.7	25.2	8.0	-	16.1	2.2	-	-	19.8	-	1.0	-	-	-	-	2.0	-	-	-	-	-	-	-	-	-
54	7800.0	34.1	23.3	11.2	-	13.1	2.5	-	-	14.3	-	1.4	-	-	-	-	-	-	-	-	-	-	-	-	-	-
55	7900.0	36.8	18.3	6.7	-	13.2	1.7	-	-	20.8	-	2.5	-	-	-	-	-	-	-	-	-	-	-	-	-	-
56	8120.0	38.0	22.0	6.4	-	14.7	-	-	-	17.9	-	0.9	-	-	-	-	-	-	-	-	-	-	-	-	-	-
57	8400.0	34.0	19.7	11.9	-	11.1	-	-	-	23.3	-	-	-	-	-	-	-	-	-	-	-	-	-	-	-	-
58	8500.0	27.4	22.1	13.2	-	11.9	-	-	-	23.4	-	-	-	-	-	-	-	-	-	-	-	-	-	-	-	-
59	8900.0	27.5	20.9	11.8	-	13.0	-	-	-	27.1	-	-	-	-	-	-	1.9	-	-	-	-	-	-	-	-	-
60	9000.0	44.4	23.7	8.2	-	14.6	-	-	-	9.2	-	-	-	-	-	-	-	-	-	-	-	-	-	-	-	-
61	9100.0	29.3	24.9	14.2	-	22.2	-	-	-	9.6	-	-	-	-	-	-	-	-	-	-	-	-	-	-	-	-
62	9200.0	31.5	24.1	11.0	-	24.8	-	-	-	8.6	-	-	-	-	-	-	-	-	-	-	-	-	-	-	-	-

TABLE A-7
Plagioclase

	1. Wt. % Oxides	2.
Al ₂ O ₃	19.70	19.46
SiO ₂	69.39	69.28
Na ₂ O	11.77	8.38*
K ₂ O	.10	.10
CaO	.13	.18
FeO		.09
Total	101.09	97.46
Structural formula based on 8 (O)		
Si	2.996	3.054
Al	1.003	1.012
Na	.985	.717
K	.005	.006
Ca	.006	.009
Fe		.003
Mol. % Ab	98.86	98.03

Analysis: 1 and 2. Geysers 1, 762-768 m.

*Na₂O loss on analysis.

TABLE A-8

White mica (phengite)

	1. Wt. % Oxides	2.	3.
Na ₂ O	.48	.18	1.19
MgO	5.51	1.76	1.17
Al ₂ O ₃	23.81	27.23	29.82
SiO ₂	46.62	54.71	47.76
K ₂ O	7.79	9.40	9.29
CaO			.10
TiO ₂		.08	.51
MnO	.09		.07
FeO	9.01	1.67	4.52
Cl	.07		.12
H ₂ O	6.57	4.85	5.49
Total	99.95	99.88	100.04

Analysis: 1 to 3. Geysers 1, 762-768 m.

TABLE A-9

Pumpellyite*

	1. Wt. % Oxides	2.	3.	4.	5.	6.
Na ₂ O	.60	.43	.04			
MgO	1.63	1.77	3.05	8.01	8.28	6.98
Al ₂ O ₃	26.57	26.01	21.65	20.83	22.14	22.40
SiO ₂	44.79	40.55	44.72	33.14	31.35	31.29
K ₂ O	2.82	2.51	1.86			
CaO	12.82	15.84	11.28	11.10	9.74	14.69
TiO ₂	.04	.05	.08			
MnO	.12	.18	.20	.25	.26	.26
FeO	4.43	6.65	9.49	18.02	18.91	13.22
Cl	.20	.09	.05			
H ₂ O	6.23	5.96	7.45	8.65	9.31	11.05
Total	100.25	100.04	99.90	100.00	99.93	99.89

- Analysis:
1. Geysers 1, 762-768 m. Green acicular growths in plagioclase (see plag. anal. 1).
 2. Geysers 1, 762-768 m. Brown acicular growths in plagioclase (see plag. anal. 2).
 3. Geysers 1, 762-768 m. Fibrous mat in matrix.
 4. Geysers 1, 823-829 m. Unknown bladed "pumpellyite" probed 12/80.
 5. Geysers 1, 823-829 m. Unknown bladed "pumpellyite" probed 12/80.
 6. Geysers 1, 823-829 m. Unknown bladed "pumpellyite" probed 1/81.

*Analyses represent bulk composition of fine-grained multi-mineral intergrowths in which pumpellyite is the dominant phase.

TABLE A-10
Green Epidote

	1. Wt. % Oxide	2.	3.	4.	5.
Al ₂ O ₃	24.18	24.50	24.17	24.96	23.65
SiO ₂	38.48	38.50	38.50	38.17	37.81
CaO	23.10	21.61	20.04	22.36	24.13
FeO	11.26	11.86	10.69	10.67	12.06
MnO	.15	.12	.20	.13	.27
MgO	.19	.87	.47		
TiO ₂	.14	.12	.07	.07	.08
H ₂ O	2.41	2.33	3.93	3.43	2.01
Total	99.91	99.86	99.28	99.83	100.01
Structural Formula based on 13 (O,OH)					
Si	3.03	3.02	3.05	3.03	2.97
Al	2.24	2.27	2.26	2.34	2.10
Fe	.74	.78	.71	.71	.79
Mn	.01	.01	.01	.01	.02
Mg	.23	.10	.06		
Ti	.01	.01	.01	.01	.01
Pistacite %	24.84	25.48	23.89	23.28	26.57

Analysis: 1 and 2. Geysers 1, 762-768 m.

3 and 4. Geysers 1, 823-829 m.

5. Geysers 1, 872-878 m.

TABLE A-11

Yellow green epidote

	1.	2.	3.	4.	5.	6.	7.
Wt. % Oxides							
Al ₂ O ₃	26.31	27.70	25.88	26.73	25.42	25.93	25.76
SiO ₂	38.13	38.28	38.73	37.05	38.58	37.96	37.74
CaO	23.82	24.08	24.19	22.99	24.03	23.79	23.65
FeO	9.19	7.21	9.02	10.84	10.09	9.64	11.10
MnO	.19	.18	.32	.13	.13	.16	.11
MgO				.26			
TiO ₂							
H ₂ O	2.37	2.43	1.78	1.96	1.71	2.38	1.46
Total	100.01	99.88	99.92	99.96	99.96	99.80	99.82
Structural formula based on 13 (0,OH)							
Si	2.98	2.97	3.01	2.88	3.00	3.00	2.94
Al	2.42	2.54	2.37	2.45	2.33	2.39	2.36
Ca	1.99	2.00	2.01	1.92	2.00	1.99	1.97
Fe	.60	.47	.59	.71	.66	.63	.72
Mn	.01	.01	.02	.01	.01	.01	.01
Mg				.03			
Ti							
Pistacite %	19.73	15.57	19.83	22.35	21.99	20.86	23.42

Analysis: 1 to 4. Geysers 1, 872-878 m.

5 to 7. Geysers 2, 2774-2780 m.

TABLE A-12

Andradite

	Wt. % Oxide
SiO ₂	36.20
CaO	34.30
FeO	28.09
MnO	.23
TiO ₂	.18
H ₂ O	1.07
Total	99.89

Structural formula based on 12 (O)

Si	3.18
Ca	3.23
Fe	2.06
Mn	.02
Ti	.01

Analysis: Geysers 2, 2774-2780 m.

TABLE A-13

Ferrierite

	1. Wt. % Oxides	2.
Al ₂ O ₃	11.74	13.19
SiO ₂	68.80	65.02
MgO	3.00	3.00
K ₂ O	.14	1.48
CaO	.55	1.05
Na ₂ O	.06	.21
BaO	2.46	2.54
FeO	.03	.12
SrO	--	.40
Total	86.76	87.01
Structural formula based on 72 (O,OH)		
Si	30.10	28.99
Al	6.06	6.93
Fe	.01	.04
Mg	1.96	1.99
Ca	.26	.50
Sr		.10
Ba	.42	.45
Na	.05	.18
K	.08	.84

Analysis: 1. Geysers 2, 183-189 m.

2. Barium-bearing ferrierite from Wise and Tschernich, 1976.

TABLE A-14

Pyrrhotite

	1.	2.	3.	4.	5.	6.	7.
	Wt. %						
Fe	60.32	60.83	60.88	60.34	61.71	59.92	60.01
S	37.53	38.51	38.03	37.99	38.12	38.21	38.83
Ni	.05	.06	.06	.15	.15	.17	.11
Cu	.06	.09	.04	.05	.04	.07	.07
Zn			.03	.04	.07	.05	
Co	.06	.04	.04	.10	.07	.06	.09
Total	98.02	99.53	99.08	99.01	100.16	98.48	99.11
	Atomic %						
Fe	47.80	47.41	47.70	47.52	47.96	47.13	46.83
S	51.80	52.28	51.90	52.11	51.61	52.35	52.77
Ni	.04	.04	.04	.11	.11	.12	.08
Cu	.04	.06	.03	.04	.03	.05	.05
Zn			.02	.04	.05	.04	
Co	.05	.03	.03	.08	.05	.04	.07
						47.36	

Analysis: 1 to 3. Geysers 1, 598-604 m. Type 1 pyrrhotite.

4 to 7. Geysers 1, 598-604 m. Type 2 pyrrhotite.

TABLE A-15
Chalcopyrite

	1.	2.
	Wt. %	
Fe	31.87	31.83
S	33.40	34.53
Ni	.03	.03
Cu	31.28	30.96
Zn	.39	.62
Co	.04	.08
Total	97.01	98.35
	Atomic %	
Fe	26.92	26.54
S	49.13	50.14
Ni	.02	.03
Cu	23.22	22.69
Zn	.29	.44
Co	.03	.06

Analysis: 1 and 2. Geysers 1, 598-604 m.

TABLE A-16

Sphalerite

	1.	2.	3.	4.	5.	6.	7.	8.
	Wt. %							
Zn	54.33	54.10	54.60	52.33	61.29	61.55	60.56	59.65
S	32.76	33.21	32.71	33.00	33.37	33.69	33.95	33.04
Fe	11.29	11.04	11.23	12.83	5.22	5.53	5.68	5.76
Cd	.05	.17	.14	.19	.55	.50	.31	.43
Cu	.17	.18	.12	.63	.16	.13	.03	.27
Mn	.14	.20	.18	.15	.12	.12	.10	.16
Co					.10	.02	.05	.05
Ni					.05	.04		
Total	98.76	98.90	98.98	98.80	100.87	101.58	100.80	99.30
	Atomic %							
Zn	40.19	39.87	40.40	38.51	44.92	44.68	44.19	44.25
S	49.41	49.90	49.34	49.51	49.86	49.86	50.50	49.98
Fe	9.78	9.52	9.73	11.05	4.48	4.69	4.85	5.00
Cd	.02	.07	.06	.08	.24	.21	.13	.19
Cu	.13	.14	.09	.47	.12	.10	.02	.20
Mn	.13	.18	.15	.13	.10	.10	.08	.14
Co					.08	.02	.04	.04
Ni					.04	.03		
Fe/Zn								

Analysis: 1 to 3. Geysers 1, 598-604 m. Associated with Type 1 pyrrhotite.

4. Geysers 1, 598-604 m. Associated with Type 2 pyrrhotite.

5 and 6. Geysers 1, 841-847 m. Grain 1 with exsolved chalcopyrite.

7 and 8. Geysers 1, 841-847 m. Grain 2 with exsolved chalcopyrite.

TABLE A-17

Geysers 1 carbonates

<u>Depth</u>	<u>Description</u>	$\delta^{13}\text{C}$ <u>PDB</u>	$\delta^{18}\text{O}$ <u>SMOW</u>
110-120	vein w/greenstone	-7.01	17.14
300-20	vein w/greenstone	-5.64	14.42
340-60	vein w/wacke	-9.47	14.18
400-20	vein w/shale	-11.23	14.53
540-60	vein; vein w/wacke	-10.47	12.21
600-20	vein w/wacke	-13.31	16.36
760-80	vein w/wacke	-13.36	16.10
860-80	vein w/wacke	-12.77	17.00
1000-20	vein w/wacke	-12.90	14.72
1040-60	vein w/wacke	-10.80	12.41
1140-60	vein w/wacke	-13.83	16.57
1240-60	vein w/wacke	-11.60	13.45
1300-20	vein w/wacke	-12.66	15.95
1400-20	vein w/wacke; vein	-13.85	12.37
1600-20	vein w/wacke + trace pyrrhotite	-11.56	12.04
1740-60	vein w/wacke	-10.78	11.08
1800-20	vein w/wacke + trace pyrrhotite	-12.05	10.62
1920-40	vein w/shale	-15.84	11.66
2000-20	vein; vein w/wacke	-16.37	9.67
2040-60	vein w/shale	-12.45	7.78
2240-60	vein w/shale	-13.35	9.87
2340-60	vein; vein w/wacke	-14.20	7.78
2400-20	vein; vein w/shale	-11.31	11.33
2440-60	vein + trace pyrrhotite	-13.16	7.98
2500-20	vein	-13.81	11.91
2540-60 A	vein; vein w/wacke	-13.10	10.67
2540-60 B	vein	-13.40	10.55
2640-60	vein w/shale	-12.93	9.63

TABLE A-18

Geysers 1 silicates

<u>Depth</u>	<u>Description</u>	δ^{18} <u>SMOW</u>
210-20	chert	21.43
440-60	vein	17.57
600-20	vein	16.94
760-80	vein	16.90
860-80	vein	19.93
960-80 A	vein	11.88
960-80 B	vein	17.52
1140-60	vein	18.24
1240-60	vein	19.16
1440-60	vein from wacke	17.28
1500-20	vein	17.58
1600-20	vein from wacke	19.56
1740-60	vein from wacke	12.83
2000-20 A	vein	9.91
2000-20 B	vein	10.46
2200-20	vein	9.56
2340-60	vein from wacke	13.54
2640-60	vein from shale	13.75
2740-60 A	vein	21.43
2740-60 B	vein	7.13
2740-60 C	euohedral crystals	6.06
2900-20	vein from wacke	12.04

TABLE A-19

Geysers 2 carbonates

<u>Depth</u>	<u>Description</u>	$\delta^{13}\text{C}$ PDB	$\delta^{18}\text{O}$ SMOW
210-20	vein w/chert	-10.31	17.11
400-20	vein (bladed crystals)	-6.07	18.20
600-20	vein w/wacke	-2.97	21.98
800-20 A	vein	-11.46	16.46
800-20 B	vein	-14.09	18.21
1000-20 A	vein, vein w/greenstone	-.07	16.83
1000-20 B	vein w/greenstone	-7.92	9.04
1200-20	vein w/greenstone	-.90	16.16
1400-20	vein w/greenstone	1.39	18.15
1600-20	vein	-.66	17.65
1800-20	vein w/greenstone	-1.69	15.95
2200-20	vein w/greenstone; vein	-1.61	15.01
2420-40	vein w/greenstone	-.32	15.97
2600-20	vein	-.78	17.97
3000-20	vein w/greenstone	-1.61	17.17
3200-20	vein; vein w/greenstone	-1.59	15.08
3400-20	vein; vein w/greenstone, chert	-4.24	15.98
3800-20 A	vein (milky white)	-6.42	16.38
3800-20 B	vein (clear)	-8.40	9.51
4200-20	vein	-9.40	15.33
4400-20	vein w/greenstone	-6.23	15.31
4620-40	vein w/wacke	-10.26	16.72
4800-20	vein w/greenstone	-5.14	14.70
5000-20	vein	-5.66	12.40
5200-20	vein w/greenstone	-2.84	12.86
5400-20	vein (bladed crystals)	-2.68	14.07
5600-20	vein	-6.91	13.61
5800-20 A	vein	-10.63	14.28
5800-20 B	vein w/shale	-11.02	15.52
6000-20	vein	-10.94	15.42
6200-20	vein w/shale	-11.84	11.61

TABLE A-19 (continued)

<u>Depth</u>	<u>Description</u>	<u>δ^{13} PDB</u>	<u>δ^{18} SMOW</u>
6600-20	vein w/shale	-15.22	11.42
7100-20	vein	-14.05	9.98
7700-20	veinw/wacke	-12.12	11.36
8000-20	vein	-10.84	6.93
8200-20	vein; vein w/wacke	-12.99	8.58
8400-20	vein w/wacke	-14.00	2.08

TABLE A-20
Geysers 2 silicates

<u>Depth</u>	<u>Description</u>	δ^{18} <u>SMOW</u>
7400-20	vein	16.96
7600-20	vein	16.34
7700-20	vein	18.22
7820-40	vein	15.95
8000-20 A	vein	17.17
8000-20 B	euohedral crystals	9.73
8200-20	vein	8.11
8400-20	vein	8.33

Figure A-1. Distribution of individual calcite fluid inclusion homogenization temperature data versus depth from Geysers 1.



Each of these symbols represent data from single chips.

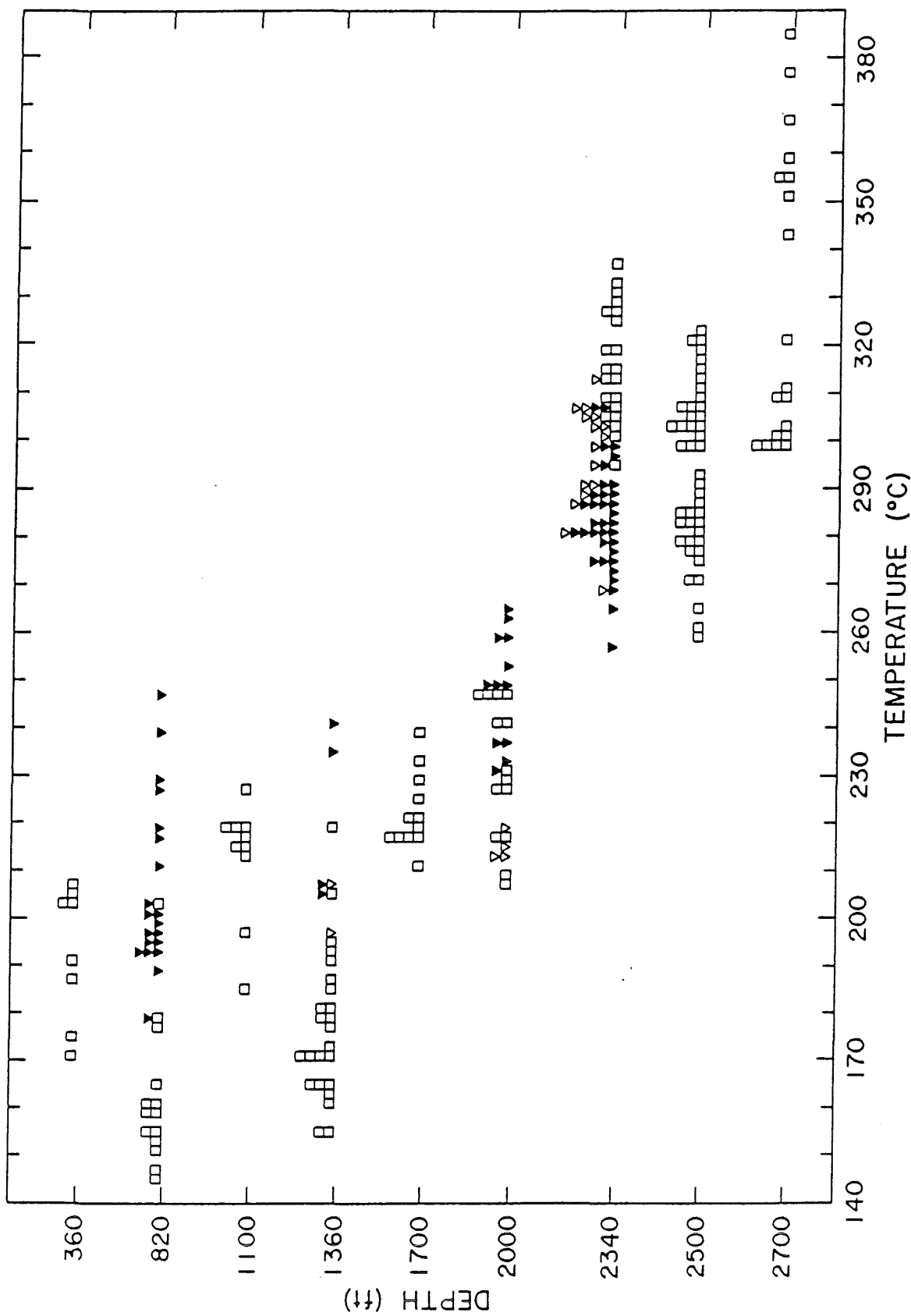


Figure A-2. Distribution of individual quartz fluid inclusion temperature data versus depth from Geysers 1.

□ ■ ▽ ▼ Each of these symbols represent data from single chips.

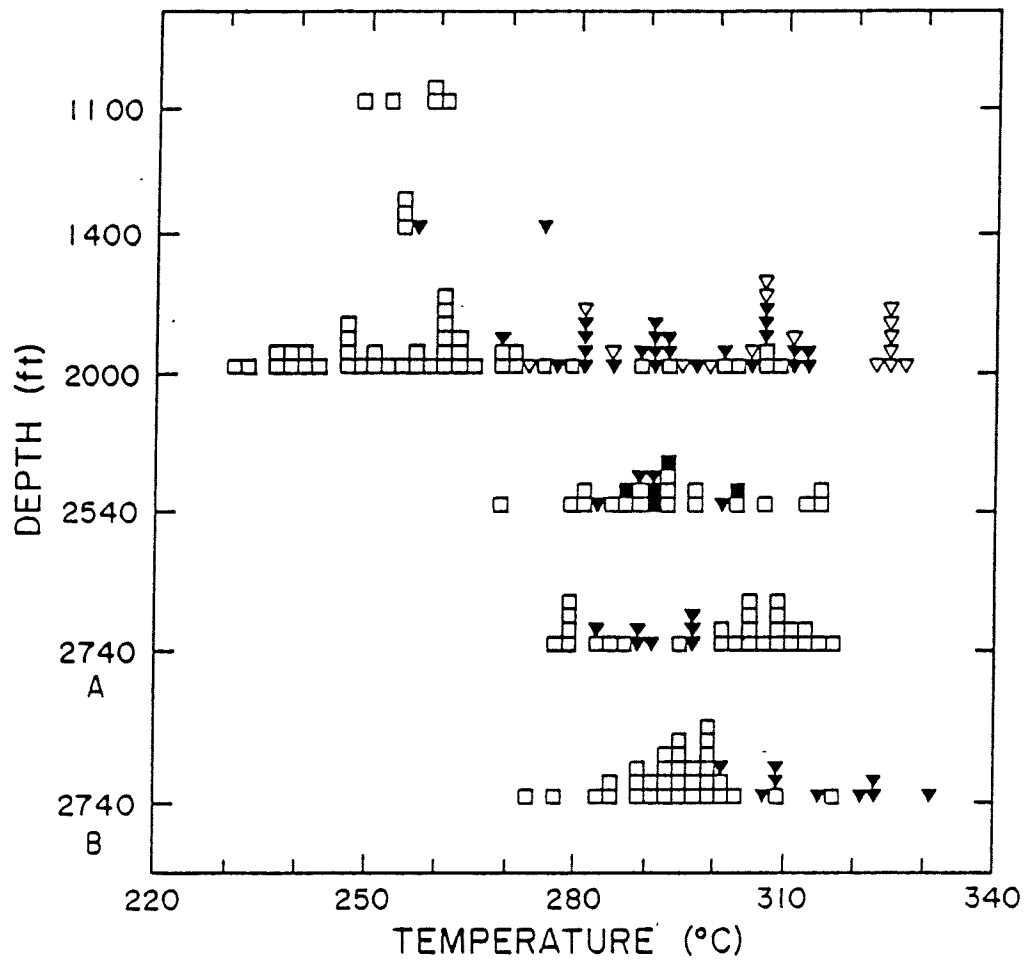


Figure A-3. Distribution of individual calcite fluid inclusion homogenization temperature data versus depth from Geysers 2.



Each of these symbols represent data from single chips.

